Automated Tool Path Generation Using the Steepest Directed Isocusp Method for 3-Axis CNC Machining of Sculptured Parts

by

Paul Ashley Wenger

BASc., University of Calgary, 1999

A Thesis Submitted in Partial Fulfillment of the
Requirements for the Degree of

MASTER OF APPLIED SCIENCE

in the Department of Mechanical Engineering

We accept this thesis as conforming
to the required standard

[redacted]

Dr. Geoffrey W. Vickers, Supervisor (Department of Mechanical Engineering)

[redacted]

Dr. Zuomin Dong, Supervisor (Department of Mechanical Engineering)

[redacted]

Dr. Andrew Rowe, Departmental Member (Department of Mechanical Engineering)

[redacted]

Dr. Hausi A. Müller, External Examiner (Department of Computer Science)

Supervisors: Dr. Geoffrey W. Vickers and Dr. Zuomin Dong

ABSTRACT

Sculptured surfaces are widely used in aeronautical, automotive, electronics, and other manufacturing industries. Three-axis computer numerically controlled (CNC) mills are commonly used to mill these surfaces and their respective mold and die tooling. Research on tool path planning for sculptured surfaces using end-mills for 3-axis CNC milling have focused on five methods of tool path generation: isoparametric, surface-plane intersection, isocusp, steepest directed tree, and steepest directed isocusp (SDIC) method.

The purpose of this thesis is to examine and quantify the benefits of using the SDIC tool path generation method for a series of basic primitive shapes as well as freeform concave and convex surfaces. These basic primitive shapes are chosen to show the effect of angle of inclination and steepest path placement on SDIC tool path length.

An algorithm is presented which generates the SDIC tool path for general convex and concave sculptured surfaces. The results of the SDIC method are presented and compared with conventional tool path generation methods for these surfaces.

Examiners:

[redacted]

Dr. Geoffrey W. Vickers, Co-Supervisor (Department of Mechanical Engineering)

[redacted]

Dr. Zuomin Dong, Co-Supervisor (Department of Mechanical Engineering)

[redacted]

Dr. Andrew Rowe, Departmental Member (Department of Mechanical Engineering)

[redacted]

Dr. Hausi A. Müller, External Examiner (Department of Computer Science)

TABLE OF CONTENTS

LIST OF FIGURES

ACKNOWLEDGMENTS

Special thanks to my supervisors, Dr. Geoffrey W. Vickers and Dr. Zuomin Dong. I really appreciate their guidance and support during the preparation of this thesis. I would also like to thank to Dr. Zehong Chen for his foundational work in proving the efficiency of the steepest directed isocusp toolpath, and for his assistance in getting this research rolling.

The heavens declare the glory of God, the skies proclaim the works of his hands.
Day after day they pour forth speech, night after night the display knowledge.
There is no speech or language where their voice is not heard.
Their voice goes out into all the earth,
their words to the ends of the world.
Psalm 19-1-4

CHAPTER 1 INTRODUCTION

1.1. Background

Sculptured surfaces are widely used in aeronautical, automotive, electronics, and other manufacturing industries. Three-axis computer numerically controlled (CNC) mills are commonly used to mill these surfaces and their respective mold and die tooling. A series of simple command codes generate numerical instructions to the machine tool controller, which guides the tool along a *tool path* to machine the sculptured surface. Tool paths are the locus of cutter contact points where the cutting tool makes contact with the *design surface*. The design surface refers to the actual surface created by the designer using a CAD system.

Sculptured surface machining is carried out in two stages: rough machining (which maximizes the material removal rate to approximate the finished surface from the original stock) and finish machining (which machines the final surface by removing the excess material left by rough machining).

Tool path length is the total distance the tool travels along the tool path. By minimizing overall *tool path length* machining time is minimized, producing savings in tool wear, scheduling, CNC mill operation costs, and operator time. Generating efficient tool paths for finish machining of sculptured surfaces is the focus of this research.

Cost effectiveness in finish machining is maximized by producing a satisfactory *manufactured surface* in a minimum of machining time. *Manufactured surfaces* are surfaces created as a result of the milling process, within the *tolerance surface* of the design surface. The tolerance surface is the surface generated by offsetting the design surface by a specified tolerance value as shown in Figure 1.1.

Generating a tool path that produces a manufactured surface within specified tolerance while maximizing machining efficiency remains a major technical challenge. Typically gains made in improving surface finish quality are offset by decreased machining efficiency caused by *redundant machining*. Redundant machining is the process of removing material between the design surface and the tolerance surface, material within the tolerance offset volume.

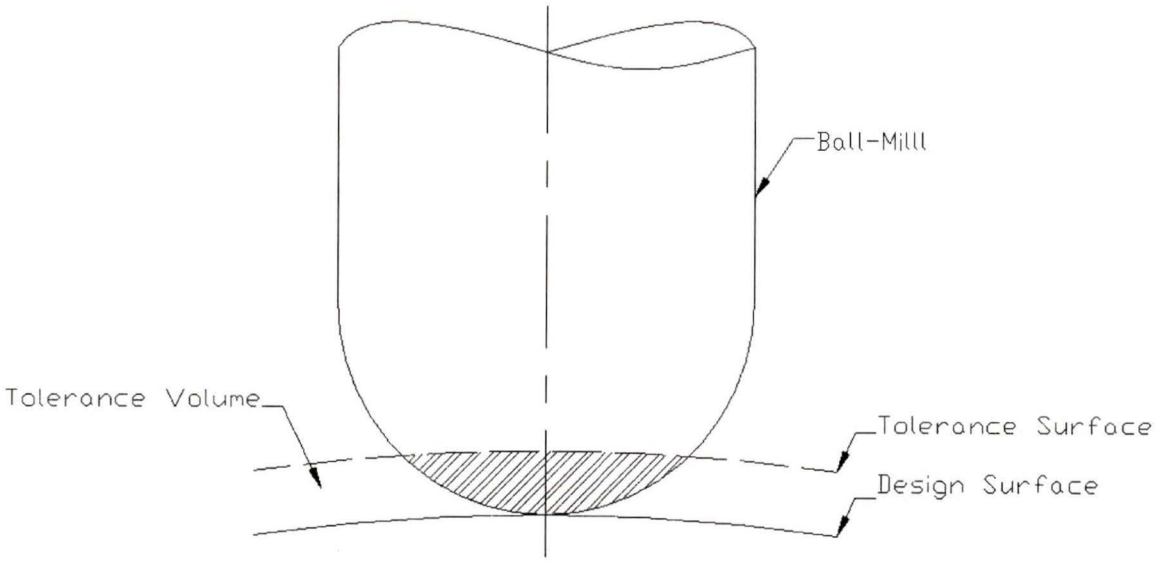

Figure 1.1 Tolerance Volume

1.2. Related Work

Current research on tool path planning for sculptured surfaces using end-mills for 3-axis CNC milling have focused on five methods of tool path generation:

1) Isoparametric,
2) Surface Plane Intersection,
3) Isocusp,
4) Steepest Directed Tree, and
5) Steepest Directed Isocusp.

1.2.1. Isoparametric Machining

Sculptured surfaces can be represented by parametric surfaces of two variables, $z=f(u,v)$, as shown in Figure 1.2. Holding one parameter constant, u, defines an isoparametric

curve on the surface. *Step size* along this curve determines the interval between points on the isoparametric curve. Step-size can be determined according to a specified maximum chordal deviation of the tool path from the original curve. *Step-over* determines the intervals at which the other parameter, *v,* is fixed, generating a series of isoparametric curves.

Given the tool diameter, the *step-over* determines the resulting cusp height produced by machining along adjacent isoparametric curves. While machining along two adjacent isoparametric curves defined by a constant step-over interval, varying cusp heights will be produced as the angle of inclination of the surface varies. Using a step-over based on the maximum cusp height being equal to the specified tolerance of the surface, cusp height can vary between zero and the specified tolerance between adjacent tool paths. Any cusp height below the specified tolerance is a point of redundant machining, where step-over could have been increased to produce a shorter overall tool path length.

Additionally, the relationship between the parametric co-ordinates and corresponding Cartesian co-ordinates is not always uniform. Therefore the accuracy and efficiency of the isoparametric approach will vary with surface geometry [Elber, Cohen, 1993]. This deficiency is demonstrated in the isoparametric machining of a fan blade [Huang, Oliver, 1994]

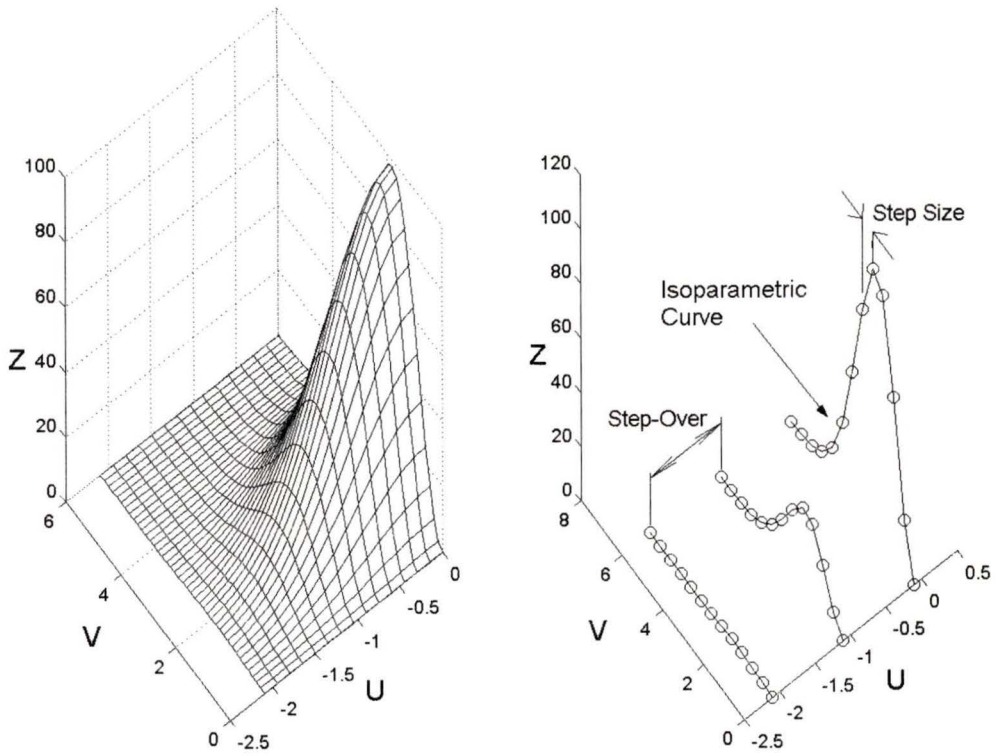

Figure 1.2 Isoparametric Curves: Step-Over and Step-Size

1.2.2. Plane-Surface Intersection Machining

Parallel plane-surface intersection machining has become the most common tool path programming approach for surface geometries [Jensen and Anderson, 1993]. By specifying the desired milling direction, a series of parallel cutting planes can be generated, and the tool path is found along the intersection of the cutting planes and the surface as shown in Figure 1.3. The tool path lies on these intersecting curves.

The major advantage of this method is that the milling direction can be specified by the user and is not limited to the parametric co-ordinate axes [Chen *et al.*, 1993]. Also, the machining of multiple adjoining surfaces is simplified when curves from different surfaces are joined into a single tool path [Bobrow, 1985].

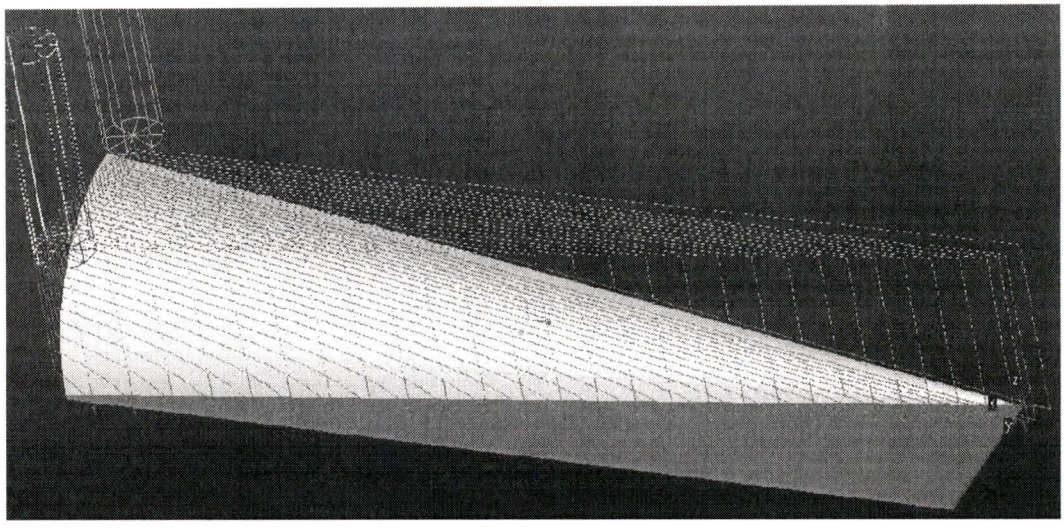

Figure 1.3 Parallel Plane Machining

In some cases the calculation of intersecting curves can be computationally intensive. The computation load can be reduced by using both parallel and non-parallel planes intersecting with the design surface to create planar tool paths for ball-mills [Huang and Oliver, 1992]. Calculating tool paths for end-mills is computationally more involved than the calculation for ball-mills.

As with isoparametric methods, tool paths generated using the plane-surface intersection method are in general not the most efficient, as step-over between adjacent tool paths is determined by the maximum scallop height produced while machining along a given plane. This results in redundant machining.

1.2.3. Isocusp Machining

Isocusp tool paths are tool paths that produce a constant cusp height across the surface. In isocusp machining the step-over between adjacent tool paths is determined by the resulting cusp height between tool paths. This principle is discussed and demonstrated by generating isocusp tool paths for an extruded part generated in Pro-E [Suresh and Yang, 1994]. Due to lack of geometry matching between the design surface and the cutter, manufactured surfaces always have a degree of roughness, determined by cusp height between tool paths. Step-over is maximized when the cusp height between adjacent tool

paths equals the specified tolerance of the surface. Isocusp tool paths are generated where the cusp height equals a constant value, usually equal to the specified tolerance of the surface. Figure 1.4 shows the horizontal projection of isocusp cutter locations along the contour lines of a quarter sphere.

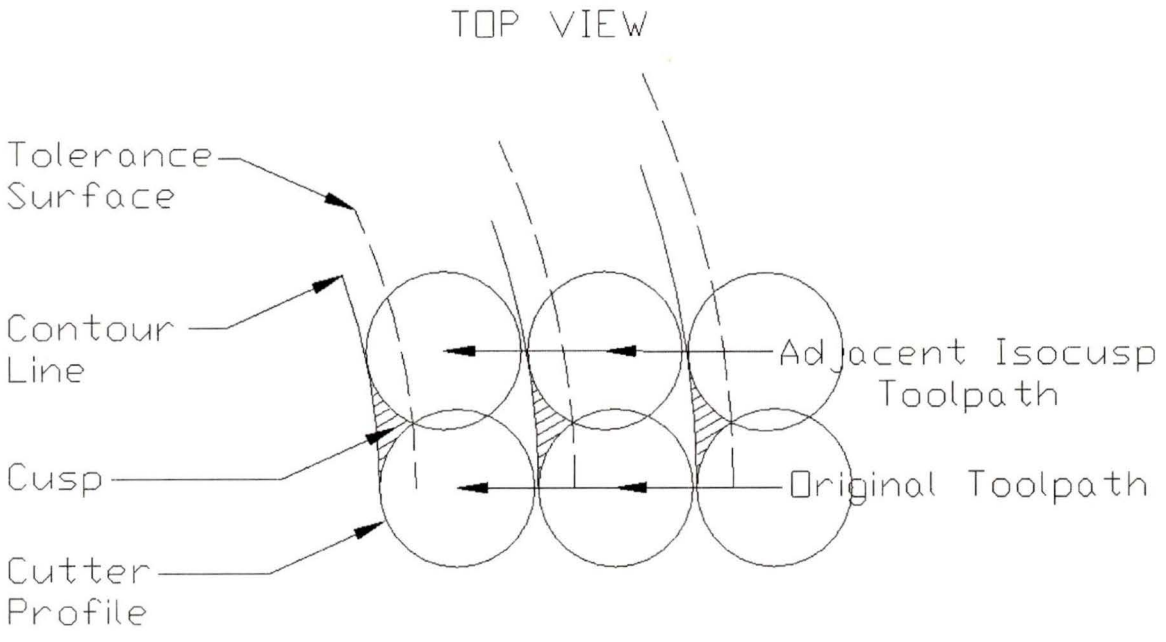

Figure 1.4 Isocusp Machining

This method is effective in maximizing step-over, thus eliminating redundant machining, but does not in general generate the most efficient tool paths [Sarma and Dutta, 1997] as the isocusp tool paths deviate from the steepest path, as shown in Figure 2.25.

1.2.4. Steepest Directed Tree Machining

The best geometry match between an end-mill cutter and a sculptured surface is obtained when the cutter is moved along lines of steepest surface slope [Vickers and Quan, 1989]. The steepest directed tree approach [Maeng and Vickers 1996] generates a tool path that guides an end-mill in the steepest direction upward along a triangulated surface model representation of the sculptured surface. Tool paths start from the bottom of the surface and follow the steepest slope trajectory through points on the surface mesh. These tool paths merge as they move upwards towards the summit of the surface. By optimizing the geometry matching between the cutter and the design surface, the effective cutting edge is

maximized, which in turn maximizes the step-over between adjacent tool paths, minimizing the overall tool path length.

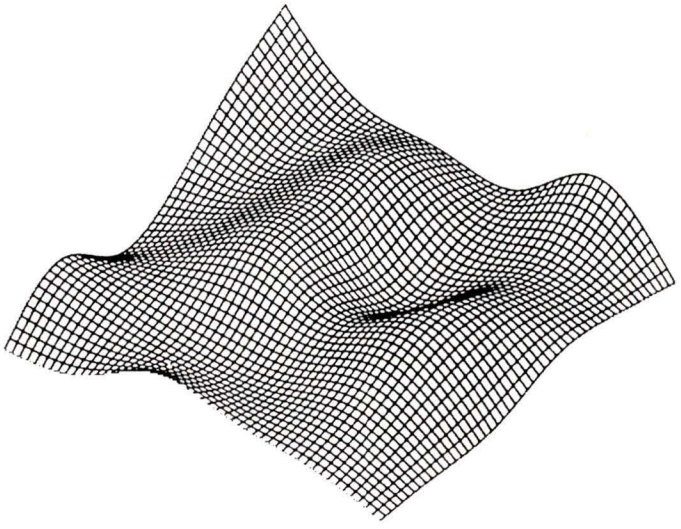

Figure 1.5 Mesh Sculptured Surface

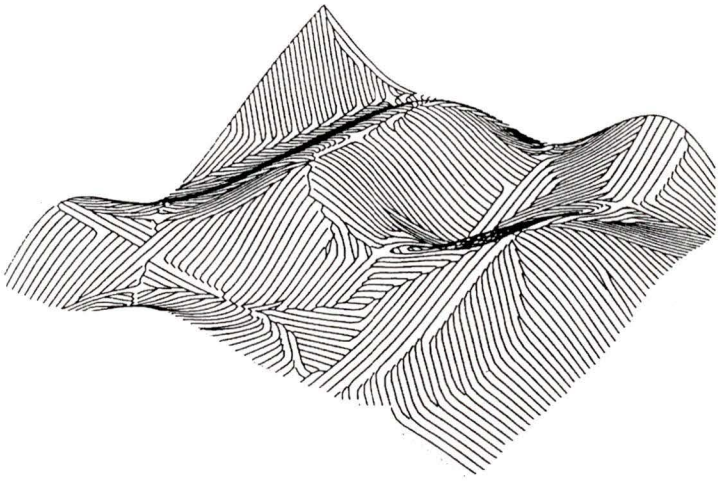

Figure 1.6 Tool paths Generated Using the Steepest Directed Tree Method

Using this strategy to machine a convex sculptured surface produces a series of steepest paths that overlap as they move towards the summit, causing redundant machining between adjacent tool paths.

1.2.5. Steepest Directed Isocusp Machining

Steepest Directed Isocusp (SDIC) machining is the combination of steepest directed tool paths and isocusp tool paths to produce a total tool path that maximizes the machining efficiency of an end-mill cutter [Chen, 2002]. As mentioned above, isocusp machining can maximize step-over between adjacent tool paths by setting the cusp height equal to the tolerance of the surface, but step-over drops off as the tool path deviates from the steepest directed path. Steepest directed machining maximizes the projected effective cutting edge of the cutter, which maximizes step-over between adjacent tool paths, but redundant machining occurs as the steepest paths merge towards the summit of the sculptured surface. By strategically combining steepest directed and isocusp machining, the optimum step-over is obtained while limiting redundant machining.

Steepest directed paths are uniformly spaced across the sculptured surface, bounding regions of isocusp machining. Uniform spacing between the steepest paths decreases redundant machining as the steepest paths converge at the summit of the sculptured surface. The regions bounded by the steepest paths are covered by isocusp tool paths which are successively offset from the original steepest path, as shown in Figure 1.7. The bounding steepest paths limit the number of isocusp tool paths offset from the steepest path, decreasing the loss in projected effective cutting edge length associated with deviation from the steepest path.

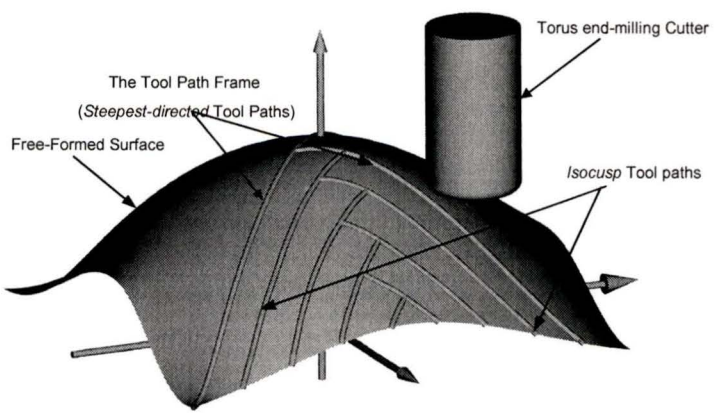

Figure 1.7 Steepest Directed Isocusp Tool path

Sculptured surfaces can be machined using a variety of cutters ranging from spherical ball-mills to flat end-mills. Although the use of spherical ball-mills simplifies the calculation of cutter locations across the sculptured surface, the step-over between adjacent ball-mill tool paths is less than or equal to the step-over between adjacent end-mill tool paths along a given surface. Increasing step-over decreases the overall tool-path length, and decreases overall machining time. Machining sculptured surfaces using an end-mill is demonstrably more efficient than using a ball-mill [Vickers and Quan, 1989]. The SDIC method generates tool paths for end-mill machining of sculptured surfaces based on the combination of the isocusp criteria and the steepest directed tree criteria explained above.

In the SDIC work, Chen generates SDIC tool paths to machine a horizontal half cylinder. For a given surface tolerance, the number of evenly spaced steepest directed tool paths is varied, and a minimum tool path length is found. A general procedure for generating SDIC tool paths on sculptured parts in finish machining is described [Chen, Vickers, and Dong, 2001]

1.3. Research Focus

The purpose of this thesis is to examine and quantify the benefits of using the SDIC tool path generation method for a series of basic primitive shapes as well as general concave and convex surfaces. These basic primitive shapes are chosen to show the effect of angle of inclination and steepest path placement on SDIC tool path length. An algorithm is presented which generates the SDIC tool path for general convex and concave sculptured surfaces. The results of the SDIC method are presented and compared with conventional tool path generation methods for these surfaces. Since feed rate is fixed during the machining process, tool path length is directly proportional to machining time. Therefore machining efficiency of various tool path generation methods can be compared by comparing tool path lengths.

1.4. Thesis Organization

In Chapter 2 the effective cutting edge is introduced and the effective cutting edge length is derived in terms of cutter radius, surface tolerance, surface curvature, and angle of inclination. The effective cutting edge length of end-mills is compared to the effective cutting edge of ball-mills. In order to illustrate the variation of effective cutting edge length over sculptured surfaces, the effective cutting edge length is derived in terms of x,y,z co-ordinates for various three dimensional geometric primitive surfaces and plotted on these surfaces.

In Chapter 3 the algorithm for generating steepest directed isocusp tool paths is presented. These tool paths are made up of isocusp cutter locations and steepest path cutter locations. The procedure for determining isocusp cutter locations is presented. Steepest path cutter locations are found by approximating the gradient of the sculptured surface. It is shown that the surface gradient runs perpendicular to the contour lines of a surface, and this property is used to approximate the steepest path over the surface. The steepest path can be approximated by following paths normal to the contour lines of the sculptured surface. The procedure for determining cutter locations along the steepest path is presented. The generation of SDIC tool paths on concave and convex surfaces is presented.

In Chapter 4 SDIC tool paths for various three-dimensional geometric primitives and a free-form sculptured surface are presented and compared to tool paths generated using isoparametric methods and surface-plane intersection methods. The benefits and drawbacks of using the SDIC method are discussed and presented.

Conclusions are drawn and presented in Chapter 5.

CHAPTER 2 EFFECTIVE CUTTING EDGE LENGTH ON SCULPTURED SURFACES

In order to examine and discuss the benefits of the SDIC tool path for machining sculptured surfaces, the concept of an effective cutting edge is presented for both end mills and ball mills.

The *effective cutting edge* (ECE) is the intersection of the cutting tool surface and the tolerance surface. The ECE is a function of tool radius, surface tolerance, the angle of inclination of the sculptured surface, and the radius of curvature of the sculptured surface. Closed form equations are found relating these variables for both end-mills and ball-mills on a series of primitive shapes. From these equations, the ECE length can be found at every point along a sculptured surface, given the angle of inclination. ECE length is found and plotted across the following three dimensional primitive geometric surfaces to give an understanding of how ECE length varies with surface tolerance, tool radius, and angle of inclination of the machined surface:

- planes,
- horizontal cylinders,
- spheres,
- vertical cones, and
- horizontal cones,

Choosing three-dimensional primitive surfaces facilitates the derivation of closed-form expressions for the effective cutting edge length in terms of (x,y,z) position on the surface. These closed forms expressions allow the ECE_{length} to be plotted over the surfaces.

2.1. Effective Cutting Edge of End-Mills

2.1.1. Definition

The effective cutting edge, ECE, of an end-mill on a curved surface is found by projecting the cutting surface in the tool feed direction. At any given cutter location, the cutting surface of the end-mill makes an angle with the surface normal, known as the *angle of inclination*, as shown in Figure 2.1.

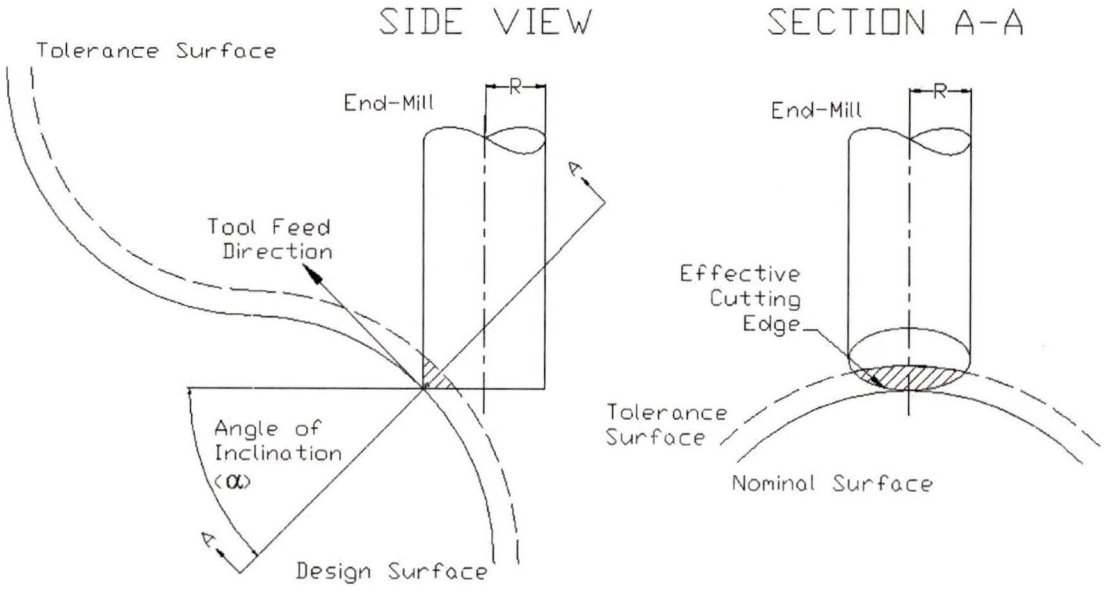

Figure 2.1 Effective Cutting Edge of End-Mills

The angle of inclination (α) is the angle the surface normal ($\vec{N}$) makes with the horizontal plane ($\vec{H}$) as shown in Figure 2.2.

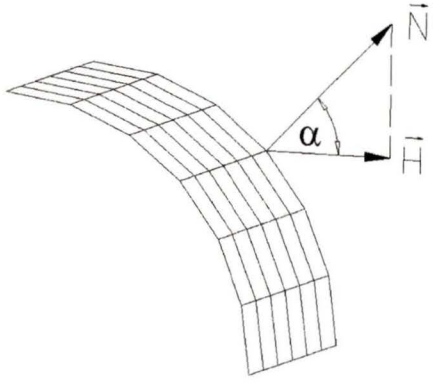

Figure 2.2 Angle of Inclination

The angle of inclination is determined using the property of dot-products between vectors:

$$\cos(\alpha) = \frac{\vec{N} \bullet \vec{H}}{|\vec{N}||\vec{H}|}$$
$$\alpha = \cos^{-1}\left(\frac{\vec{N} \bullet \vec{H}}{|\vec{N}||\vec{H}|}\right) \quad (1)$$

Effective cutting edge length (ECE_{length}) is defined as the distance between the endpoints of the ECE, not the true length of the cutting edge, as shown in Figure 2.3.

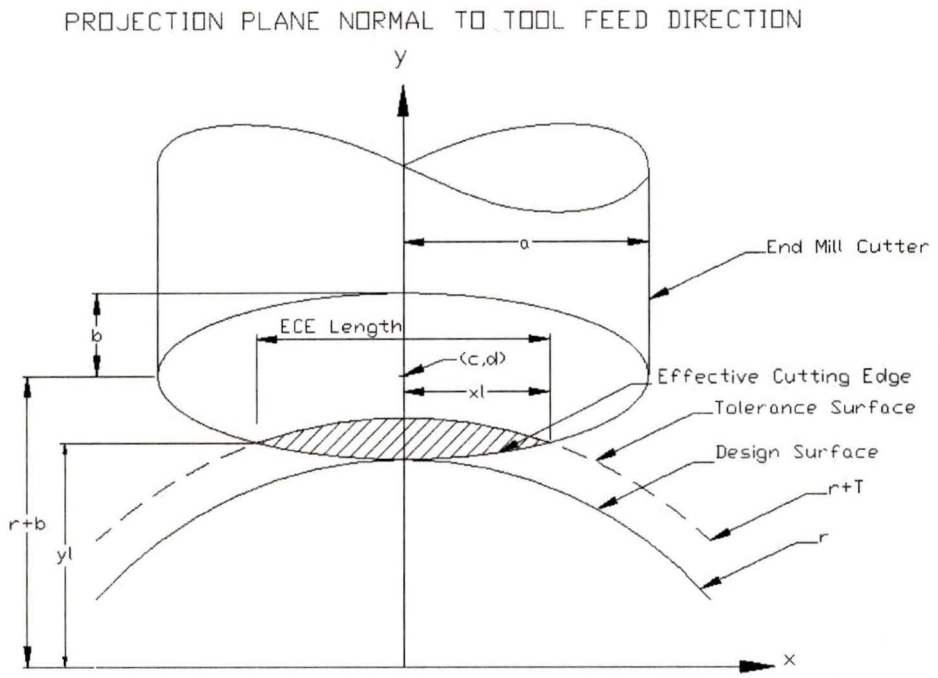

Figure 2.3 Effective Cutting Edge Length

The projection of the cutting surface of an end-mill in the tool feed direction is an ellipse (Figure 2.3). The equation of an ellipse centered at *(c,d)* is

$$\frac{(x-c)^2}{a^2} + \frac{(y-d)^2}{b^2} = 1 \quad (2)$$

where the x and y axes intersect at the centre of curvature of the design surface as shown in Figure 2.3. The major axis of the ellipse (a) equals the radius of the end-mill (R), and r is the radius of curvature of the design surface. The ellipse is centered at $(0,r+b)$. Substituting these values into Equation 2 gives

$$\frac{x^2}{R^2}+\frac{(y-(r+b))^2}{b^2}=1 \tag{3}$$

The projection of the end-mill in the plane of tool feed direction with respect to the side view of the end-mill is shown in Figure 2.4. The angle of inclination (α) is the angle the surface normal makes with the horizontal plane.

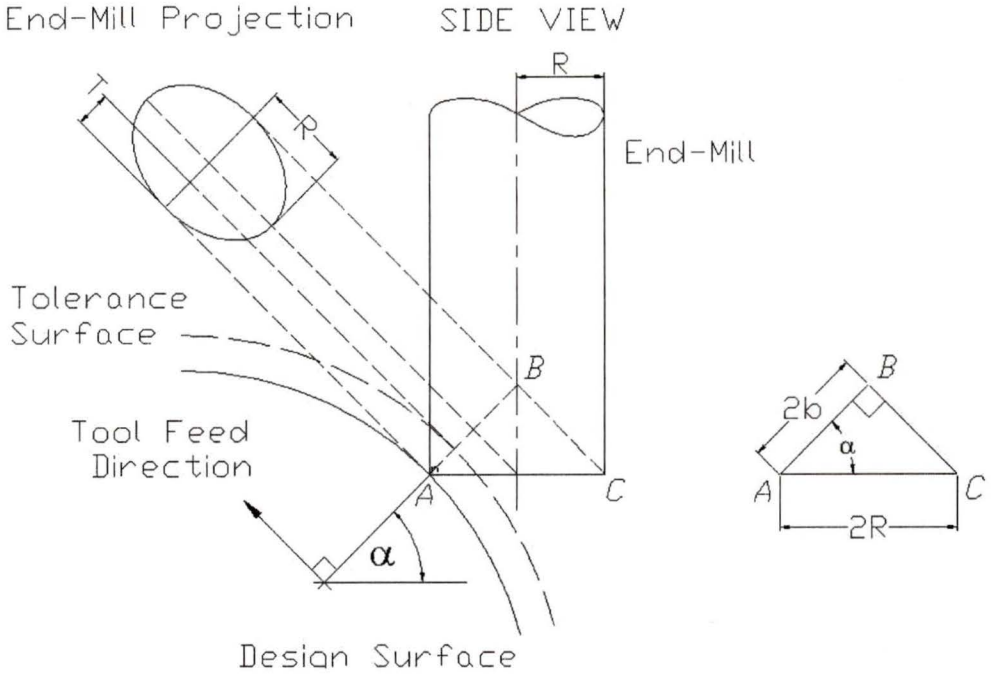

Figure 2.4 End-Mill Projection and the Angle of Inclination

There is a trigonometric relationship between the minor axis of the end-mill projection, *b*, and the angle of inclination of the cutter, *α*.

$$\cos(\alpha)=\frac{2b}{2R}=\frac{b}{R}$$
$$b=R\cos(\alpha) \tag{4}$$

The co-ordinates of the intersection point between the tolerance surface and the projection of the end-mill are (x_l,y_l). The ECE_{length} is found in terms of x_l, as shown in Figure 2.3.

$$ECE_{length}=2x_l \tag{5}$$

Equation 3 is rearranged as an expression for x_l when $y=y_l$

$$x_l = R\sqrt{1-\left(\frac{\left(y_l-(r+b)\right)^2}{b^2}\right)} \tag{6}$$

and this expression can be substituted into Equation 5 to give ECE_{length} in terms of x_l and y_l.

$$ECE_{length} = 2R\sqrt{1-\left(\frac{\left(y_l-(r+b)\right)^2}{b^2}\right)} \tag{7}$$

The equation of the end-mill projection in terms of R and α is found by substituting Equation 3 into Equation 4:

$$\frac{x^2}{R^2}+\frac{(y-(r+R\cos(\alpha)))^2}{R^2\cos^2(\alpha)}=1 \tag{8}$$

The equation of the tolerance surface is

$$x^2+y^2=(r+T)^2 \tag{9}$$

Solving Equations 8 and 9 for y gives the expression for y_l

$$y_l=\frac{-\frac{2(r+R\cos(\alpha))}{\cos^2(\alpha)}+\sqrt{\left(\frac{2(r+R\cos(\alpha))}{\cos^2(\alpha)}\right)^2-4\left(-\tan^2(\alpha)\right)\left(R^2-(r+T)^2-\frac{(r+R\cos(\alpha))^2}{\cos^2(\alpha)}\right)}}{2\left(-\tan^2(\alpha)\right)} \tag{10}$$

Substituting this expression for y_l into Equation 7 gives the ECE_{length} in terms of cutter radius, R, surface tolerance, T, angle of inclination, α, and radius of curvature of the design surface, r:

$$ECE_{length} = 2R\sqrt{1-\left(\frac{\left(y_l-\left(r+R\cos(\alpha)\right)\right)^2}{R^2\cos^2(\alpha)}\right)} \tag{11}$$

When the radius of curvature greatly exceeds the radius of the cutting tool, the ECE_{length} approaches the ECE_{length} for machining a ruled surface. For an end-mill machining a ruled surface

$$y_l = r+T \tag{12}$$

this expression can be substituted into Equation 11 to give a simplified equation for the ECE_{length} of an end-mill on a ruled surface:

$$ECE_{length} = 2R\sqrt{1-\left(\frac{\left(r+T-(r+R\cos(\alpha))\right)^2}{R^2\cos^2(\alpha)}\right)} = 2R\sqrt{1-\left(\frac{\left(T-R\cos(\alpha)\right)^2}{R^2\cos^2(\alpha)}\right)} \qquad (13)$$

This equation for the ECE length of an end-mill on a ruled surface is equivalent to the equation for the cross-feed of an end-mill on a flat surface given in Equation 21, page 175 [Vickers, Ly, 1990]. Figure 2.5 shows the ruled surface ECE_{length} is a reasonable approximation to the actual ECE_{length} when the radius of curvature is much greater than the radius of the tool.

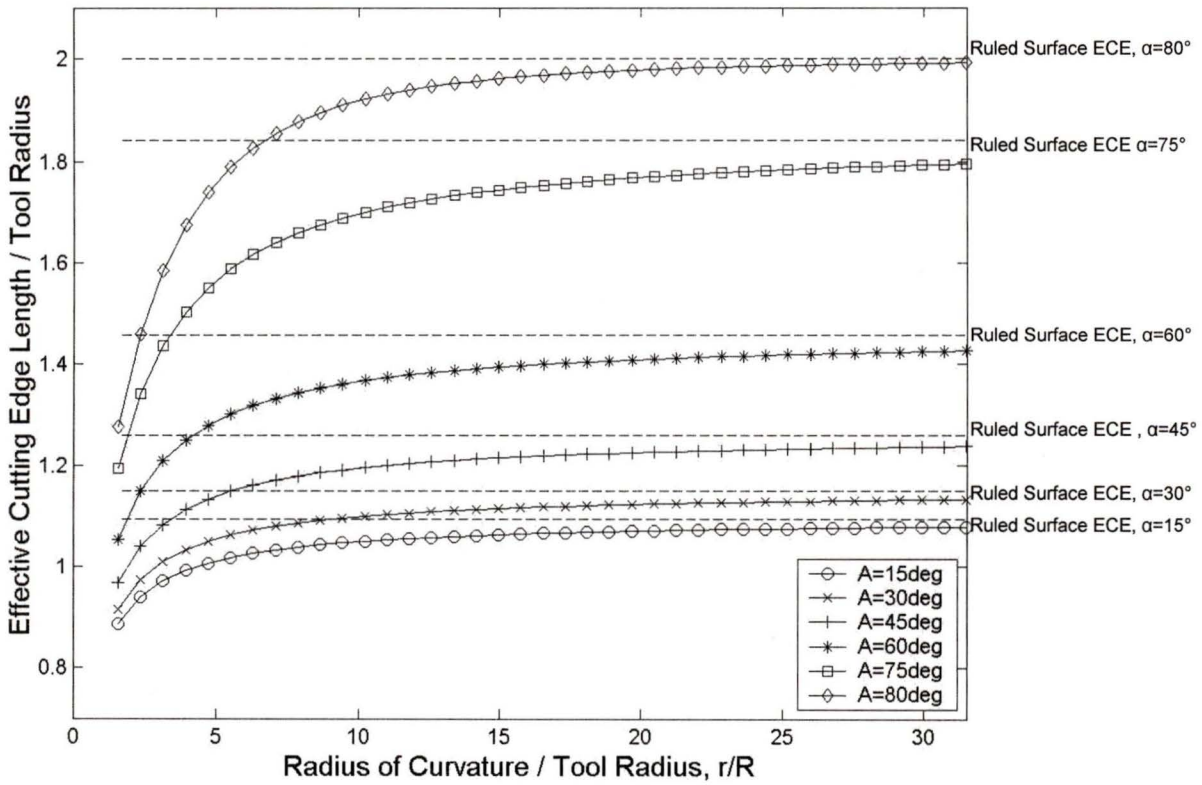

Figure 2.5 ECE_{length} for Ruled and Curved Surfaces vs. Angle of Inclination

The accuracy of this approximation for different tolerances increases as the radius of curvature of the design surface is increased while the angle of inclination remains constant, as shown in Figure 2.6. The approximation approaches the true value as the ratio of radius of curvature by tool radius (r/R) increases.

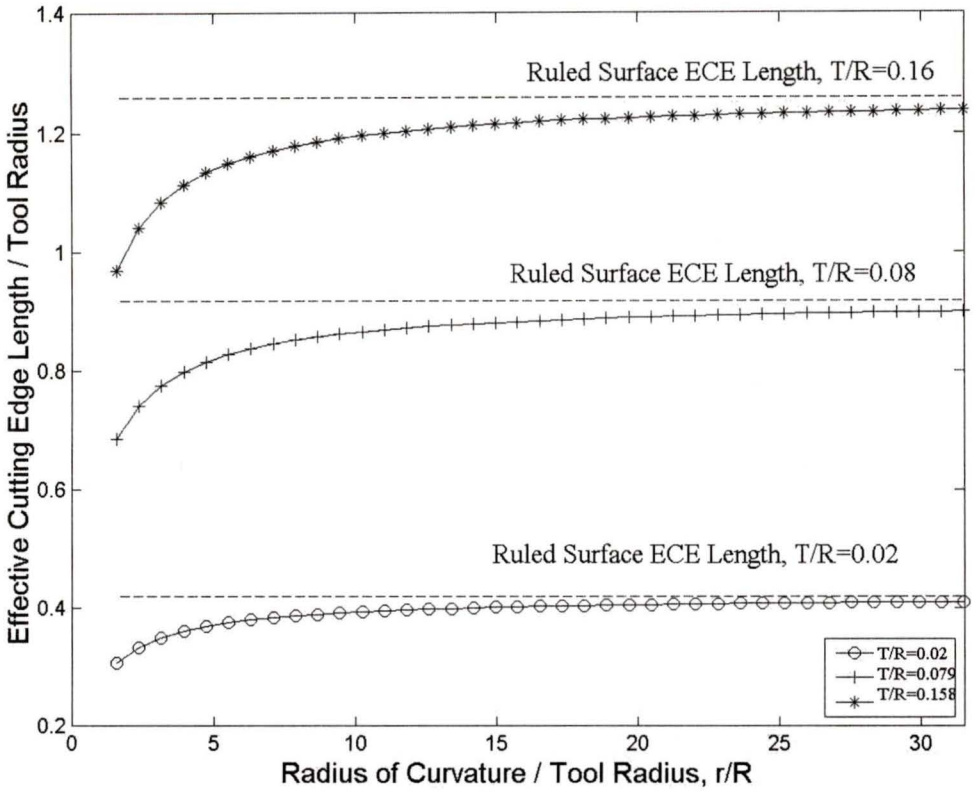

Figure 2.6 ECE_{length} for Ruled and Curved Surfaces vs. Tolerance

2.1.2. Critical Angle

The effective cutting edge reaches a maximum when the tolerance surface intersects the projection of the major axis of the projected ellipse as shown in Figure 2.7. This occurs when the effective cutting edge equals the end-mill diameter. The critical angle of inclination ($\alpha_{critical}$) is the angle where the maximum effective cutting edge occurs. $\alpha_{critical}$ can be found by differentiating Equation 13 and setting it equal to zero.

$$\frac{d(ECE_{length})}{d\alpha} = \frac{d}{d\alpha}\left(2R\sqrt{1-\left(\frac{(T-R\cos(\alpha))^2}{R^2\cos^2(\alpha)}\right)}\right) \tag{14}$$

$$= \frac{2T(T-R\cos(\alpha))\tan(\alpha)}{R\cos^2\alpha\sqrt{1-\left(\frac{(T-R\cos(\alpha))^2}{R^2\cos^2(\alpha)}\right)}} = 0$$

The minimum ECE_{length} for an end-mill is found when α=0 and the maximum is found

when $\alpha=\alpha_{critical}$, where

$$\alpha_{critical} = arc\cos\left(\frac{T}{R}\right) \tag{15}$$

When α exceeds the critical angle of inclination, $\alpha_{critical}$, the ECE_{length} reaches its maximum at the tool diameter, while the cusp height decreases below the tolerance surface and vanishes as the angle of inclination approaches 90° as shown in Figure 2.7.

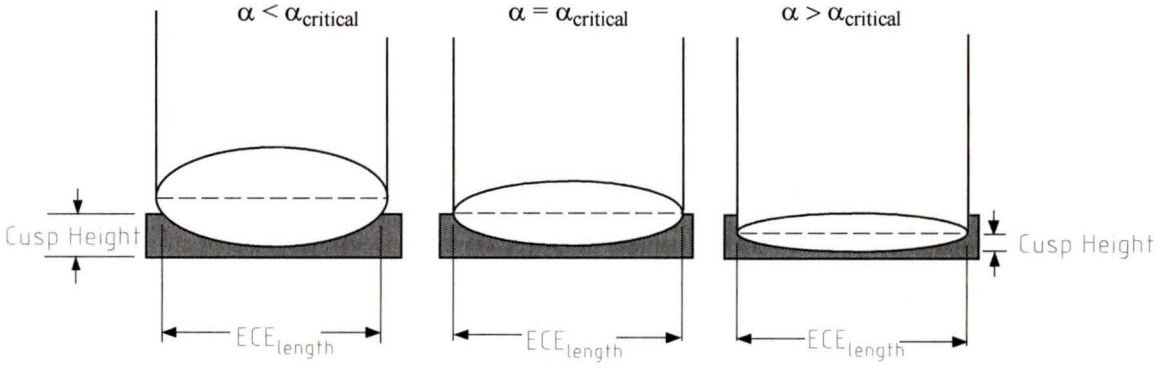

Figure 2.7 Cusp Height Past the Critical Angle of Inclination

2.2. Effective Cutting Edge of Ball-Mills

The projection of the cutting surface of a ball-mill of radius R in the tool feed direction remains a circle of radius R as the angle of inclination is varied between 0-90°, as shown in Figure 2.8.

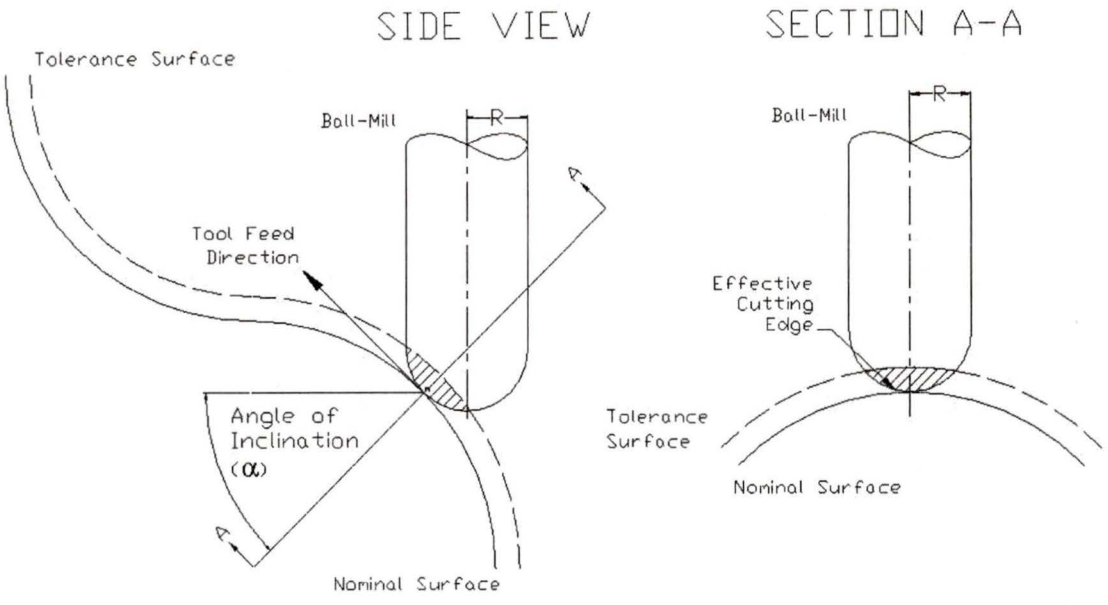

Figure 2.8 ECE and ECE_{length} of a Ball-Mill Along a Sculptured Surface

The equation for a circle of radius R, centered at (c,d) is

$$(x-c)^2+(y-d)^2=R^2 \tag{16}$$

where the x and y axes intersect at the centre of curvature of the design surface as shown in Figure 2.9).

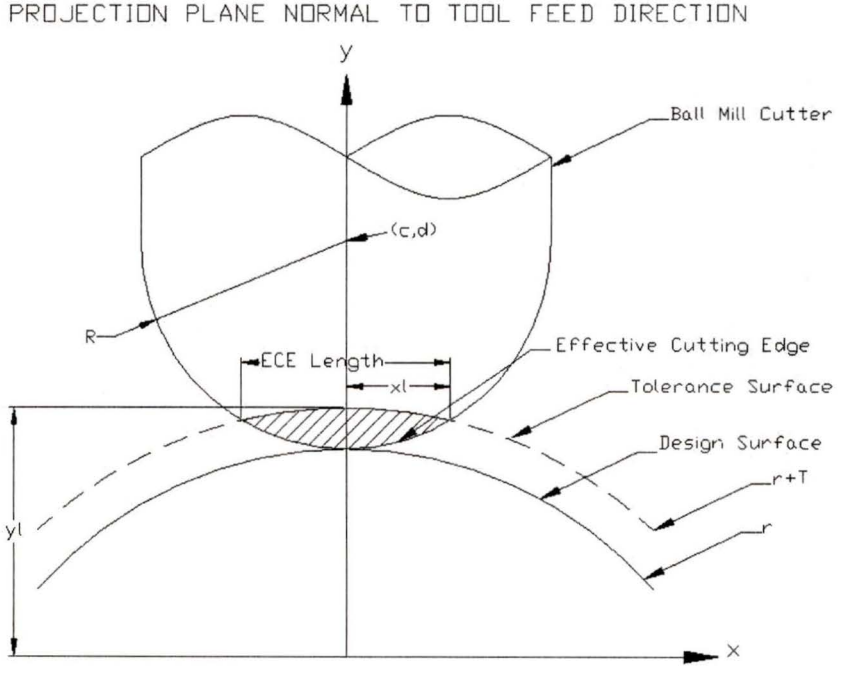

Figure 2.9 ECE_{length} of a Ball-Mill

The equation of the circular projection of the ball-mill in Figure 2.9 is:

$$x^2 + (y-(r+R))^2 = R^2 \tag{17}$$

$$x = \pm\sqrt{R^2 - (y-(r+R))^2} \tag{18}$$

and the equation of the tolerance surface is:

$$x^2 + y^2 = (r+T)^2 \tag{19}$$

Solving Equations 17 and 19 for y_l, the y co-ordinate of the intersection of the surfaces, gives:

$$y_l = \frac{(r+T)^2 + (r+R)^2 - R^2}{2(r+R)} \tag{20}$$

The length of the effective cutting edge is found in terms of x_l as shown in Figure 2.9:

$$ECE_{length} = 2x_l \tag{21}$$

Combining Equations 18 and 21 gives an expression for ECE_{length} in terms of cutter radius, R, radius of curvature, r, and y:

$$ECE_{length} = 2\sqrt{R^2 - (y_l - (r+R))^2} \tag{22}$$

Substituting the expression for y_l into Equation 20 gives an expression for ECE_{length} in terms of cutter radius, R, specified tolerance, T, and radius of curvature, r:

$$ECE_{length} = 2\sqrt{R^2 - \left(\frac{(r+T)^2 + (r+R)^2 - R^2}{2(r+R)} - (r+R)\right)^2} \tag{23}$$

This expression is equal to the ECE_{length} of an end-mill when the angle of inclination equals zero. When the radius of curvature greatly exceeds the radius of the cutting tool, the ECE_{length} approaches the ECE_{length} for machining a ruled surface. For a ball-mill machining a ruled surface:

$$y_l = r + T \tag{24}$$

Substituting this expression into Equation 20 gives the equation for the ECE_{length} of an end-mill machining a ruled surface:

$$ECE_{length} = 2\sqrt{R^2 - (T-R))^2} = 2\sqrt{2TR - T^2} \tag{25}$$

This equation is equivalent to the equation for the cross-feed of a ball-mill machining a flat surface given in Equation 19, page 175 [Vickers, Ly, 1990].

2.3. Effective Cutting Edge Length of End-Mills Compared to Ball Mills on a Ruled Surface

The effective cutting edge of an end-mill cutter on a ruled surface is calculated using Equation 13 and compared to the effective cutting edge length of a ball-mill cutter on a ruled surface using Equation 23, both cutters machining at various angles of inclination and various ratios of tolerance by tool radius (*T/R*), as shown in Figure 2.10.

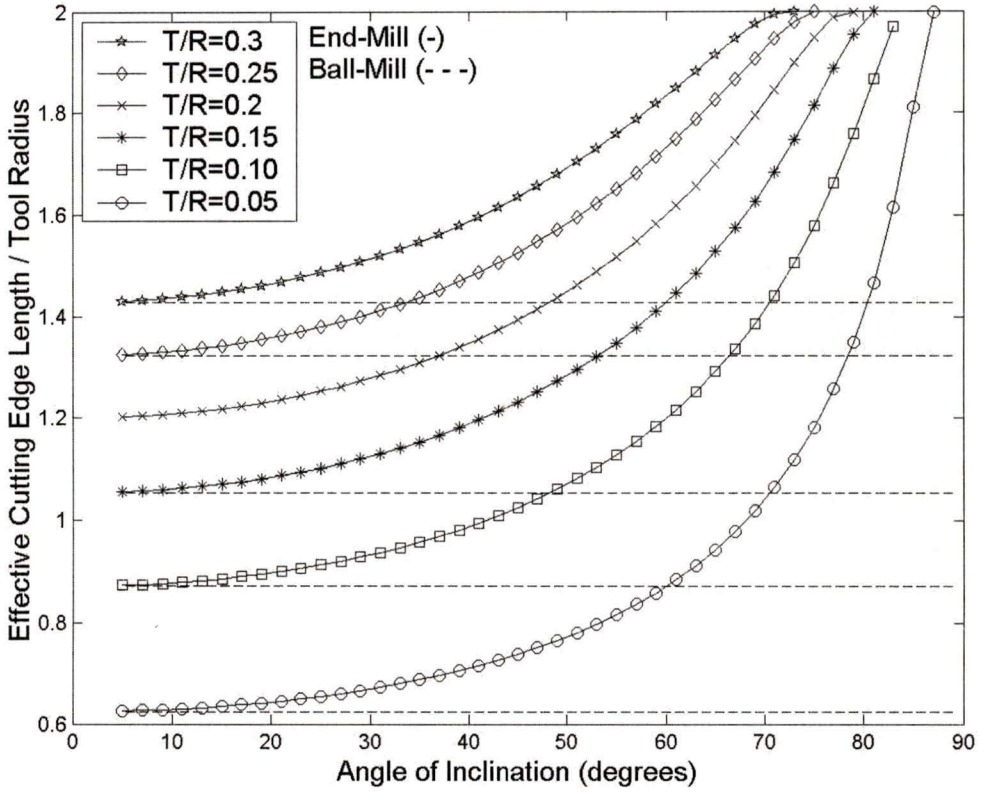

Figure 2.10 Effective Cutting Edge Length vs. Angle of Inclination

A ratio of ECE_{length} for end-mills (Equation 13) vs. ECE_{length} for ball-mills (Equation 25) may be given as:

$$\frac{ECE_{EM}}{ECE_{BM}} = \frac{2R\sqrt{1-\left(\frac{\left(T-R\cos(\alpha)\right)^2}{R^2\cos^2(\alpha)}\right)}}{2\sqrt{2TR-T^2}} = \frac{R\sqrt{1-\left(\frac{\left(T-R\cos(\alpha)\right)^2}{R^2\cos^2(\alpha)}\right)}}{\sqrt{2TR-T^2}} \tag{26}$$

This can be rearranged in terms of *T/R* to give:

$$\frac{ECE_{EM}}{ECE_{BM}} = \frac{ECE_{EM}/R}{ECE_{BM}/R} = \frac{\sqrt{1-\left(\frac{(T-R\cos(\alpha))^2}{R^2\cos^2(\alpha)}\right)}}{\sqrt{2\left(\frac{T}{R}\right)-\left(\frac{T}{R}\right)^2}} = \sqrt{\frac{2\left(\frac{T}{R}\right)}{\frac{\cos(\alpha)}{2\left(\frac{T}{R}\right)-\left(\frac{T}{R}\right)^2}} - \frac{\left(\frac{T}{R}\right)^2}{\cos^2(\alpha)}} \quad (27)$$

As the angle of inclination increases, the ECE_{length} of end-mills greatly exceeds the ECE_{length} of ball mills as shown in Figure 2.11. In the region beyond the critical angle of inclination, the ECE_{length} of the end-mill equals the tool diameter as shown in Figure 2.7. In this region the cusp height decreases from the isocusp tolerance value as the angle of inclination approaches 90°.

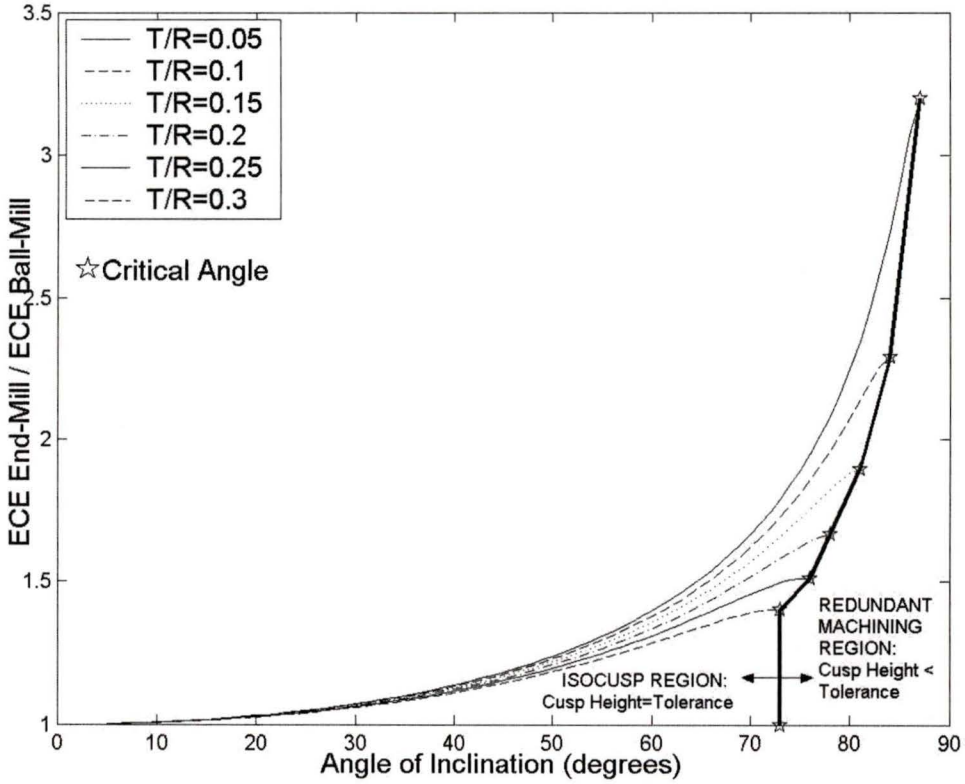

Figure 2.11 End-mill ECE_{length} by Ball-Mill ECE_{length} vs. Angle of Inclination

2.4. ECE_{length} in terms of *x,y,z* Position on a Surface

To illustrate the distribution of ECE_{length} on curved surfaces, ECE_{length} is calculated and displayed for the following three dimensional primitive surfaces:

- planes,
- horizontal cylinders,
- spheres,
- vertical cones, and
- horizontal cones.

For these surfaces the angle of inclination can be expressed in terms of *(x,y,z)* co-ordinates, an expression for ECE_{length} in terms of *x,y,z* co-ordinates may be found and plotted. ECE_{length} is plotted as shading density, where lighter shading represents higher ECE_{length}, and darker shading represents lower ECE_{length}.

2.4.1. Planes

The equation for a plane through $P_o(x_o,y_o,z_o)$ normal to $\vec{N} = A\hat{i} + B\hat{j} + C\hat{k}$ is given as

$$f(x,y,z) = A(x-x_0) + B(y-y_0) + C(z-z_0) = 0 \tag{28}$$

The surface normal, $\vec{N}$, and the horizontal projection of the surface normal, $\vec{H}$, are:

$$\begin{aligned} \vec{N} &= \nabla f = A\hat{i} + B\hat{j} + C\hat{k} \\ \vec{H} &= A\hat{i} + B\hat{j} \end{aligned} \tag{29}$$

The angle of inclination is found using Equation 1:

$$\alpha = arc\cos\left(\sqrt{\frac{A^2+B^2}{A^2+B^2+C^2}}\right) \tag{30}$$

The effective cutting edge length for an end-mill, ECE_{length} is found using Equation 13:

$$ECE_{length} = 2\sqrt{\frac{2TR}{\sqrt{\frac{A^2+B^2}{A^2+B^2+C^2}}} - \frac{T^2}{\frac{A^2+B^2}{A^2+B^2+C^2}}} \tag{31}$$

ECE_{length} has been plotted over a plane defined through $P_o(0,0,0)$ normal to $\vec{N} = -1\hat{i} + 0\hat{j} + 1\hat{k}$. Because the angle of inclination is constant all over the plane, the ECE_{length} is also constant as shown in Figure 2.12.

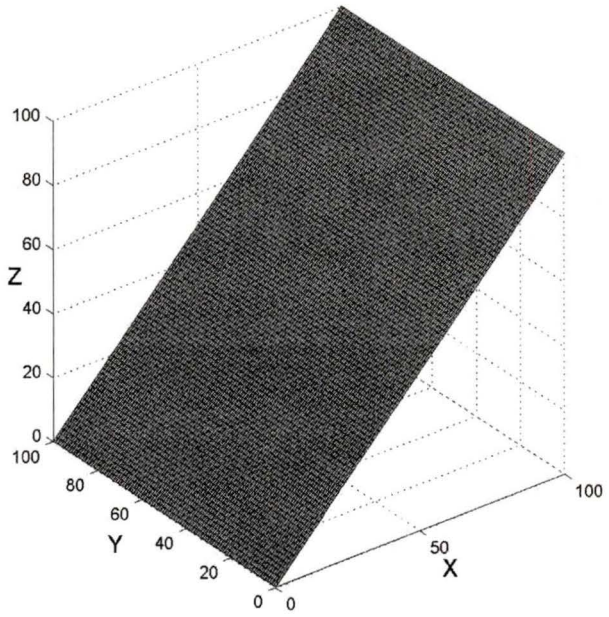

Figure 2.12 Constant ECE_{length} over a Planar Surface

2.4.2. Horizontal Cylinders

The equation for a cylinder with its axis along the x-axis, centered at (y_0,z_0) is

$$f(x,y,z) = (y-y_0)^2 + (z-z_0)^2 - r^2 = 0 \tag{32}$$

where the equation for the surface normal vector, $\vec{N}$, and the horizontal projection of the normal vector, $\vec{H}$ are

$$\vec{N} = \nabla f = (2y-2y_0)\hat{j} + (2z-2z_0)\hat{k} = (y-y_0)\hat{j} + (z-z_0)\hat{k} \tag{33}$$

$$\vec{H} = (2y-2y_0)\hat{j} = (y-y_0)\hat{j} \tag{34}$$

The angle of inclination is found as the angle between $\vec{N}$ and $\vec{H}$, using Equation 1:

$$\alpha = arc\cos\left(\sqrt{\frac{(y-y_0)^2}{(y-y_0)^2 + (z-z_0)^2}}\right) \tag{35}$$

The ECE_{length} of an end-mill over the cylinder surface is found using Equation 13

$$ECE_{length} = 2\sqrt{\frac{2TR}{\sqrt{\frac{(y-y_0)^2}{(y-y_0)^2+(z-z_0)^2}}} - \frac{T^2}{\frac{(y-y_0)^2}{(y-y_0)^2+(z-z_0)^2}}} \tag{36}$$

The distribution of the ECE_{length} over the cylindrical surfaces for increasing *R/T* ratios is shown in Figure 2.13 to Figure 2.15. As the ratio of *R/T* increases, the critical angle decreases, and the ECE_{length} reaches its maximum over more of the surface.

2.4.3. Spheres

The equation for a sphere of radius r and centre (x_o,y_o,z_o) is given as

$$f(x,y,z) = (x-x_o)^2 + (y-y_o)^2 + (z-z_o)^2 - r^2 = 0 \tag{37}$$

where the equation for the surface normal vector, $\vec{N}$, and the horizontal projection of the normal vector, $\vec{H}$ are

$$\vec{N} = \nabla f = (2x-2x_o)\hat{i} + (2y-2y_o)\hat{j} + (2z-2z_o)\hat{k} \tag{38}$$

$$\vec{H} = (2x-2x_o)\hat{i} + (2y-2y_o)\hat{j} + (2z-2z_o)\hat{k} \tag{39}$$

The angle of inclination of inclination is found as the angle between $\vec{N}$ and $\vec{H}$ using Equation 26:

$$\alpha = arc\cos\left(\sqrt{\frac{(x-x_o)^2+(y-y_o)^2}{(x-x_o)^2+(y-y_o)^2+(z-z_o)^2}}\right) \tag{40}$$

The ECE_{length} of an end-mill over the sphere surface is found using Equation 13:

$$ECE_{length} = 2\sqrt{\frac{2TR}{\sqrt{\frac{(x-x_o)^2+(y-y_o)^2}{(x-x_o)^2+(y-y_o)^2+(z-z_o)^2}}} - \frac{T^2}{\frac{(x-x_o)^2+(y-y_o)^2}{(x-x_o)^2+(y-y_o)^2+(z-z_o)^2}}} \tag{41}$$

The distribution of ECE_{length} is plotted over the surface of a sphere centered at *(0,0,0)* with a radius of 35mm. ECE_{length} is maximized when the angle of inclination is maximized, near the top of the sphere As the ratio of tolerance offset by tool radius (T/R) is increased, the critical angle of inclination decreases, and the ECE_{length} reaches its maximum over more of the surface, as shown in Figure 2.16 to Figure 2.17.

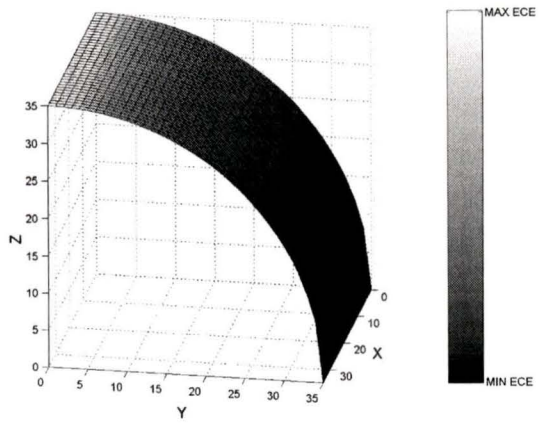

Figure 2.13 ECE_{length} on a Cylindrical Surface, T/R=0.05

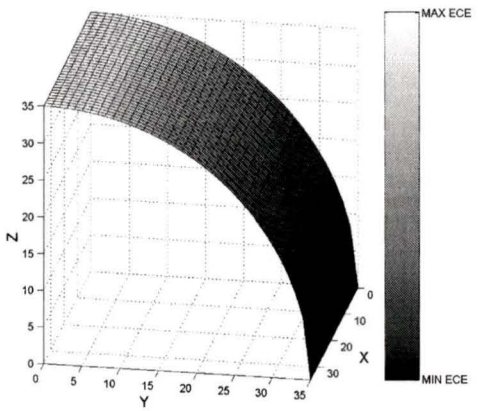

Figure 2.14 ECE_{length} on a Cylindrical Surface, T/R=0.15

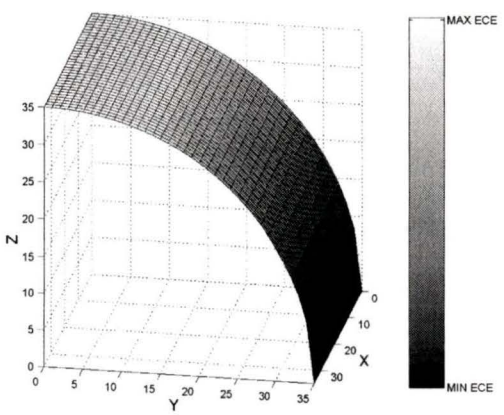

Figure 2.15 ECE_{length} on a Cylinder Surface, T/R=0.3

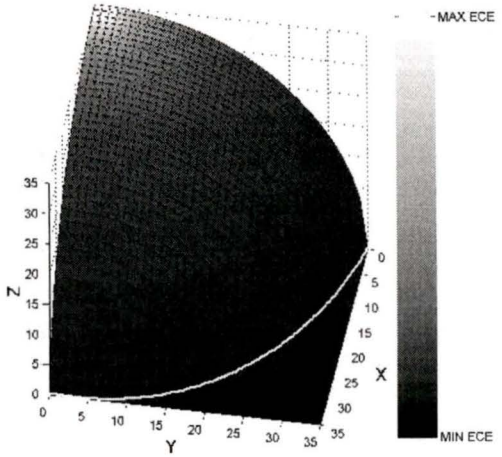

Figure 2.16 ECE_{length} on a Spherical Surface, T/R=0.05

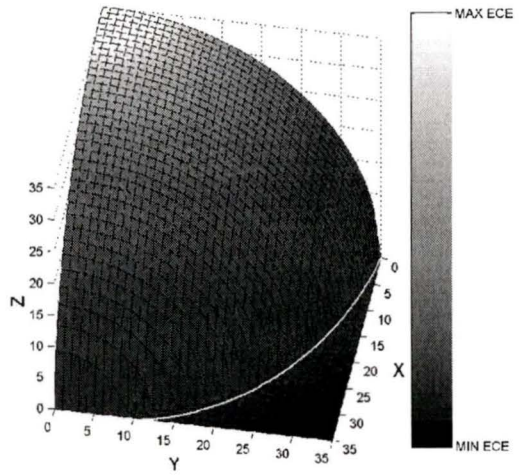

Figure 2.17 ECE_{length} on a Spherical Surface, T/R=0.15

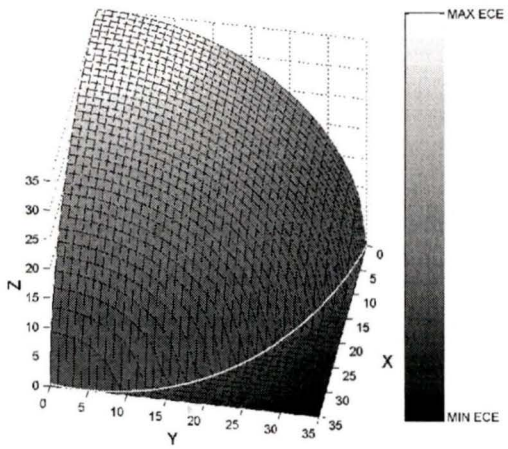

Figure 2.18 ECE_{length} on a Spherical Surface, T/R=0.30

2.4.4. Vertical Cones

The equation for a vertical cone with its axis parallel to the z-axis, centered at (x_o,y_o), forming an angle β with the z-axis, with a maximum radius of r_{max} is:

$$f(x,y,z) = (x-x_o)^2 + (y-y_o)^2 - (r_{\max} - z\tan(\beta))^2 = 0 \tag{42}$$

where the equation for the surface normal vector, $\vec{N}$, and the horizontal projection of the normal vector, $\vec{H}$ are

$$\begin{aligned} \vec{N} &= \nabla f = (2x-2x_o)\vec{i} + (2y-2y_o)\vec{j} + (2z\tan^2(\beta) - 2r_{\max}\tan(\beta))\hat{k} \\ \vec{H} &= (2x-2x_o)\vec{i} + (2y-2y_o)\vec{j} \end{aligned} \tag{43}$$

The angle of inclination is found as the angle between $\vec{N}$ and $\vec{H}$ using Equation 26:

$$\alpha = arc\cos\left(\sqrt{\frac{(x-x_o)^2 + (y-y_o)^2}{(x-x_o)^2 + (y-y_o)^2 + (z\tan^2(\beta) - r_{\max}\tan(\beta))^2}}\right) \tag{44}$$

The ECE_{length} of an end-mill over the cone surface is found using Equation 13:

$$ECE_{length} = 2\sqrt{\frac{2TR}{\sqrt{\frac{(x-x_o)^2 + (y-y_o)^2}{(x-x_o)^2 + (y-y_o)^2 + (z\tan^2(\beta) - r_{\max}\tan(\beta))^2}}} - \frac{T^2}{\frac{(x-x_o)^2 + (y-y_o)^2}{(x-x_o)^2 + (y-y_o)^2 + (z\tan^2(\beta) - r_{\max}\tan(\beta))^2}}} \tag{45}$$

The distribution of the ECE_{length} over the surface of a cone centered through (0,0,*z*), forming and angle β=45° wit the z-axis, and with a maximum radius of 35 is shown in Figure 2.19. For all vertical cones, the angle of inclination is always constant everywhere on the surface of the cone, therefore the ECE_{length} is also constant everywhere on the surface.

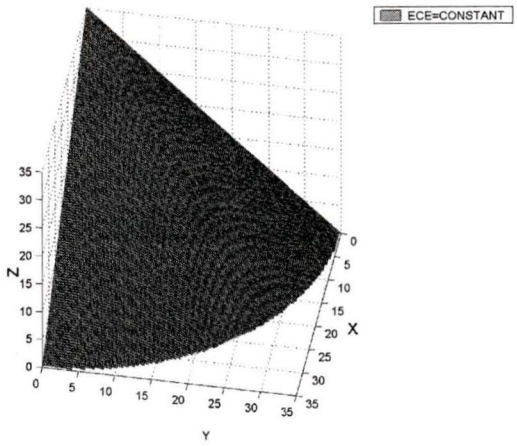

Figure 2.19 ECE_{length} on a Vertical Cone

2.4.5. Horizontal Cones

The equation for a horizontal cone with its axis parallel to the x-axis centered at (x_o,y_o) forming an angle β with the x-axis is:

$$f(x,y,z) = x^2 \tan^2(\beta) - (y-y_o)^2 - (z-z_o)^2 = 0 \tag{46}$$

where the equation for the surface normal vector, $\vec{N}$, and the horizontal projection of the normal vector, $\vec{H}$ are

$$\begin{aligned} \vec{N} &= \nabla f = (x\tan^2\beta)\hat{i} + (-y+y_o)\hat{j} + (-z+z_o)\hat{k} \\ \vec{H} &= (x\tan^2\beta)\hat{i} + (-y+y_o)\hat{j} \end{aligned} \tag{47}$$

The angle of inclination of inclination is found as the angle between $\vec{N}$ and $\vec{H}$, using Equation 26:

$$\alpha = arc\cos\left(\sqrt{\frac{\left(x\tan^2(\beta)\right)^2 + (-y+y_o)^2}{\left(x\tan^2(\beta)\right)^2 + (-y+y_o)^2 + (-z+z_o)^2}}\right) \tag{48}$$

The ECE_{length} over the cylinder surface is found using Equation 13:

$$ECE_{length} = 2\sqrt{\frac{2TR}{\frac{\sqrt{\left(x\tan^2(\beta)\right)^2 + (-y+y_o)^2}}{\sqrt{\left(x\tan^2(\beta)\right)^2 + (-y+y_o)^2 + (-z+z_o)^2}}} - \frac{T^2}{\frac{\left(x\tan^2(\beta)\right)^2 + (-y+y_o)^2}{\left(x\tan^2(\beta)\right)^2 + (-y+y_o)^2 + (-z+z_o)^2}}} \tag{49}$$

The distribution of the ECE_{length} over the surface of a horizontal cone with its axis centered on $(x,0,0)$, forming an angle of 10° with the x-axis is shown in Figure 2.20 to

Figure 2.22. The ECE_{length} is maximized along the ridge of the cone running along the line of intersection between the cone and the plane y=*0*.

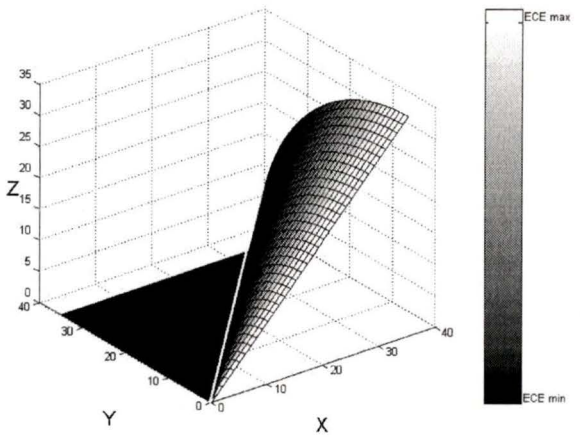

Figure 2.20 ECE_{length} on a Horizontal Cone, T/R=0.05

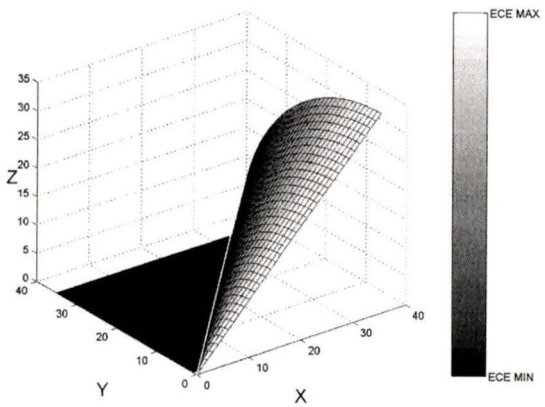

Figure 2.21 ECE_{length} on a Horizontal Cone, T/R=0.15

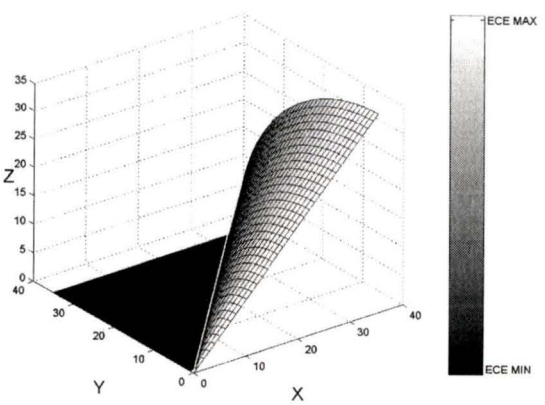

Figure 2.22 ECE_{length} on a Horizontal Cone, T/R=0.3

2.5. Effective Cutting Edge in Isocusp Machining

Cusp height is determined by the projection of adjacent cutter locations normal to the direction of tool feed as shown in Figure 2.23. Isocusp tool paths are generated when the step-over between adjacent cutter locations is determined by setting the cusp height equal to the specified tolerance of the surface. When step-over is maximized, overall tool path length can be minimized because the surface will be machined using the fewest number of adjacent tool paths.

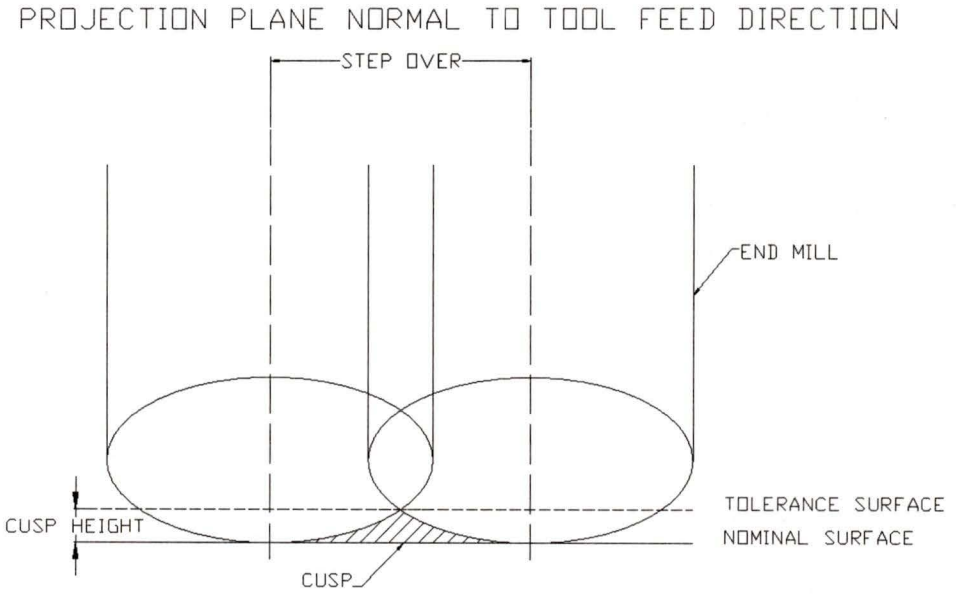

Figure 2.23 Cusp Height

Isocusp machining does not always provide the shortest overall tool path length because step-over is also determined by the projection of the ECE of the tool. As the tool travels in the tool feed direction, it carves out a furrow which is the projection of the ECE_{length} in the direction of tool feed. When the tool feed direction is in the steepest directed path, the projected ECE_{length} is maximized. The projection of the ECE_{length} in the direction of tool feed decreases as the tool feed direction deviates from the steepest path as shown in Figure 2.24.

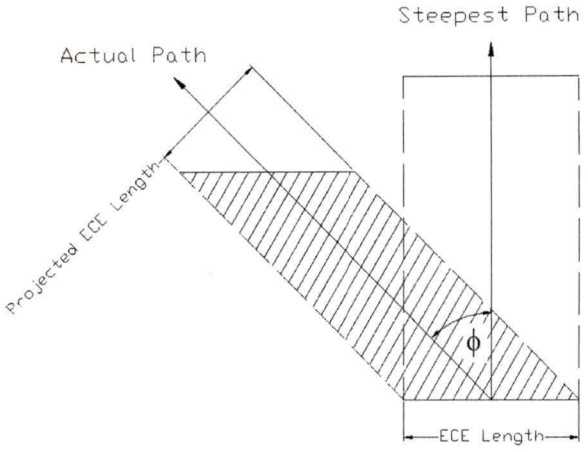

Figure 2.24 Projected $ECE_{length(projected)}$ and Angle of Deviation(φ)

The relationship between the projected effective cutting edge length ($ECE_{length(projected)}$) and the angle of deviation (ϕ) is

$$ECE_{length(\,projected\,)} = ECE_{length}\cos(\phi)\,. \tag{50}$$

Isocusp machining maximizes step-over based on cusp height, but it does not ensure the projection of the effective cutting edge length in the direction of tool feed is also maximized. For example, on a convex sculptured surface isocusp tool paths beginning from a steepest directed path will progressively deviate from the steepest direction, decreasing the projected ECE_{length} as shown in Figure 2.25. This results in an increase in overall tool path length. The strategy of steepest directed machining is introduced to maximize the projected effective cutting edge of the cutter.

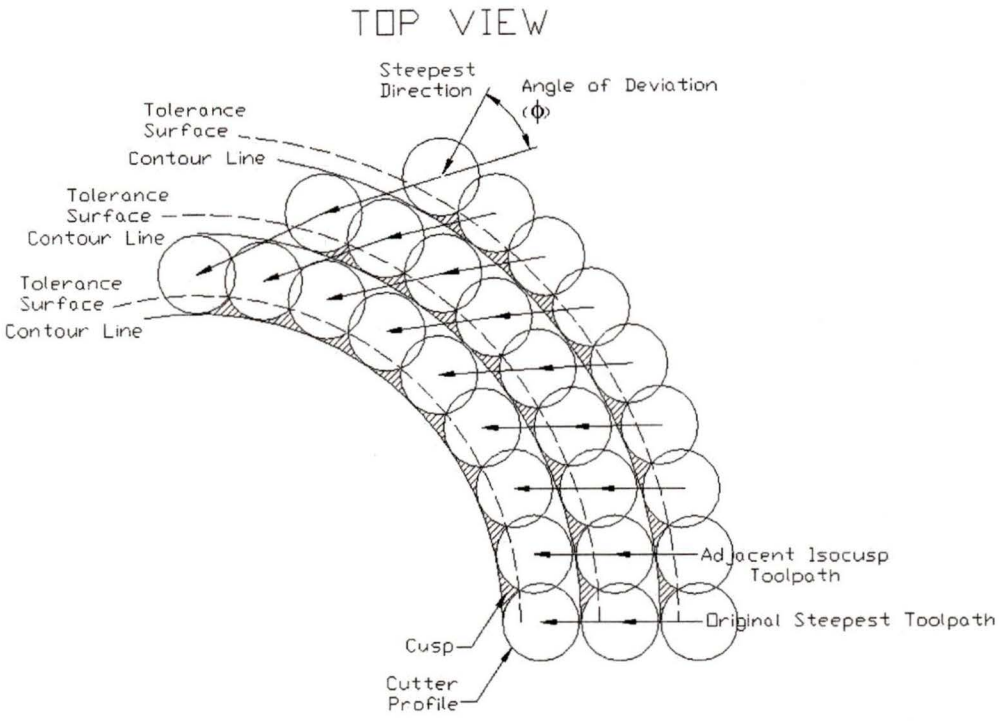

Figure 2.25 Progressive Deviation of the Isocusp Tool path from the Steepest Direction

2.6. Effective Cutting Edge in Steepest Directed Machining

The concept of steepest directed machining is based on the Steepest Directed Tree tool path generation scheme [Maeng, 1996]. Tool paths are generated along several steepest slope trajectories on the surface, starting from the bottom of the surface and moving upwards. On convex sculptured surfaces, these tool paths gradually merge as they move upwards. The goal using the steepest directed tool path is to maximize the projected *effective cutting edge* length of the end-mill, which maximizes step-over between adjacent tool paths and minimizes overall tool path length.

The steepest directed tool paths on a convex curved surface gradually merge as they move upwards. As they merge, effective cutting edges begin to overlap, resulting in overmachining as shown in Figure 2.26. A combination of steepest directed paths and isocusp tool paths is required to produce a minimum tool path length.

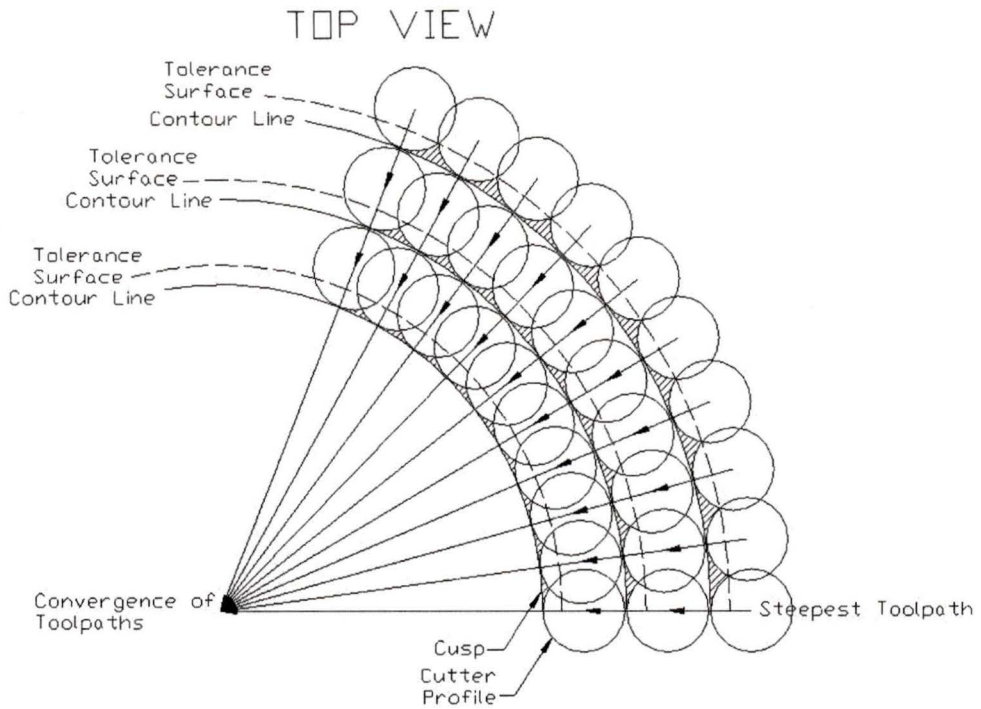

Figure 2.26 Redundant Machining Caused By Converging Steepest Paths

The SDIC method of tool path generation aims to minimize overall tool path length by combining isocusp machining (Section 1.2.3) and steepest directed machining (Section 1.2.4). Isocusp machining determines step-over based on an isocusp finish equal to the specified tolerance of the surface, while steepest directed machining gives the largest projection of the *effective cutting edge* in the cutting direction, minimizing the number of passes needed to machine the surface area.

CHAPTER 3 STEEPEST DIRECTED ISOCUSP TOOL PATH GENERATION

In order to machine complex sculptured surfaces, a series of command codes is required to guide and control the spindle and table of the CNC mill. These codes are generated based on the design surface geometry and specified machining parameters. The numerical instructions are generated by first reducing the dimensionality of the surface to that of contour lines. Next, the contour lines reduced to a set of points, called *nodes,* as shown in Figure 3.1.

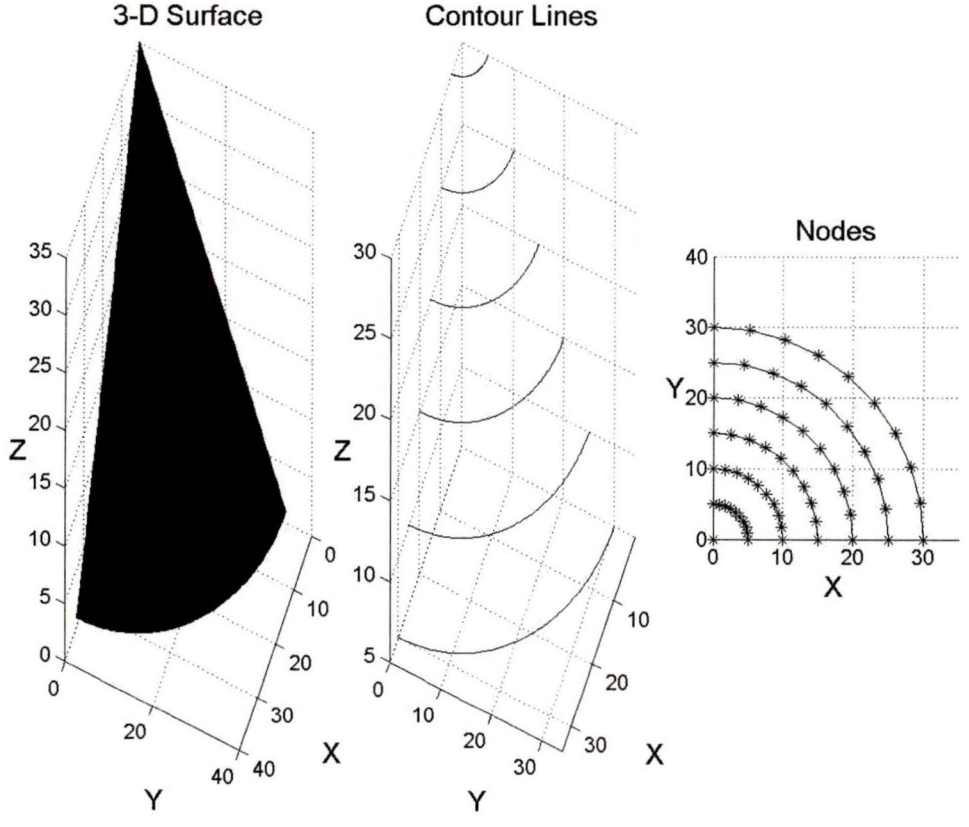

Figure 3.1 Reduction of Surface Geometry for Tool Path Calculation

The SDIC tool path is formed by a skeleton of evenly spaced steepest directed tool paths which form the boundaries for isocusp regions on the surface. The isocusp regions are covered by isocusp tool paths. Cutter locations along these steepest directed tool paths

and isocusp tool paths are selected based on the steepest path and isocusp criteria, respectively. Along each contour line, starting with cutter locations along the steepest path, adjacent cutter locations are found based on the isocusp criteria. Cutter locations from the lowest to the highest contour line are ordered to produce the SDIC tool paths, as shown in Figure 3.2.

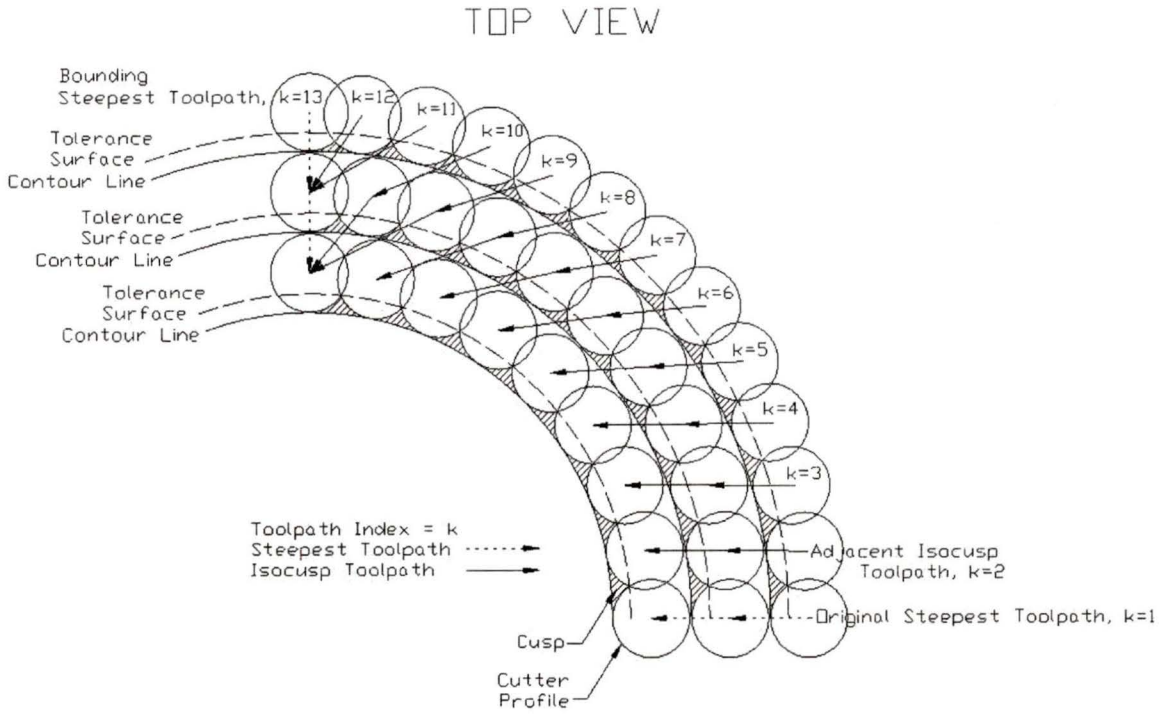

Figure 3.2 SDIC Cutter Locations, Convex Surface

Isocusp cutter locations are determined using an iterative algorithm. Similarly, cutter locations along the steepest directed path are determined using an iterative algorithm which approximates the steepest path between the nodes of the contour lines.

3.1. Isocusp Cutter Location Calculations

Isocusp cutter locations are found selecting the cutter locations that gives the closest cusp height that falls within the tolerance of the sculptured surface. Cusp height is defined as the distance between the intersection of adjacent cutter profiles and the design surface. Starting from a known base cutter location, cusp heights are found by calculating the intersection of cutter locations corresponding to neighbouring nodes along the contour

line. The cutter location corresponding to a cusp height that is closest to, but does not exceed, the projection of the tolerance surface is selected as an isocusp cutter location. This new cutter location is used as the next base cutter location for evaluating new cusp heights along the curve. The scheme continues until the end of the isocusp region is reached. Isocusp regions are bounded by steepest directed paths.

The projection of the tolerance surface onto a horizontal cross-section of the surface is needed to find the isocusp cutter locations along the contour. The tolerance surface, offset normal to the design surface, is projected along a horizontal plane at the same z height as the contour line, as shown in Figure 3.3.

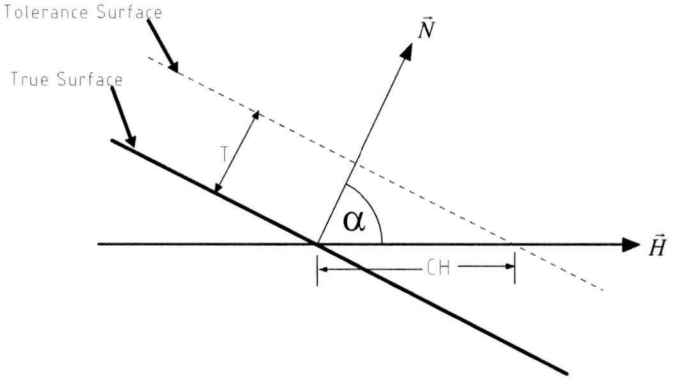

Figure 3.3 Projection of the Tolerance Surface Along Contour Plane

The cusp height along the horizontal surface defined by the contour line is determined using the angle of inclination of the design surface:

$$CH = \frac{T}{\cos(\alpha)} \tag{51}$$

The *(x,y)* co-ordinates of the cutter center *(a,b)* and *(c,d)* are found by offsetting the cutter profile by its radius normal to the contour line, as shown in Figure 3.4. The normal vectors $(\vec{H}_1, \vec{H}_2)$ are unit vectors normal to the tangent vectors, which are the vectors joining the neighbouring nodes on the contour line.

$$
\begin{aligned}
a &= x_1 + \vec{H}_{1x} \bullet R \\
b &= y_1 + \vec{H}_{1y} \bullet R \\
c &= x_2 + \vec{H}_{2x} \bullet R \\
d &= y_2 + \vec{H}_{2y} \bullet R
\end{aligned}
\tag{52}
$$

When machining a convex surface, the cutter radius is offset *outside* the contour line. When machining a concave surface, the cutter is offset *inside* the contour line. The equations for the cutter profiles are:

$$(x-a)^2 + (y-b)^2 = R^2 \tag{53}$$

$$(x-c)^2 + (y-d)^2 = R^2 \tag{54}$$

The coordinates of the intersections of the two circles (x,y) are found by solving Equations 53 and 54.

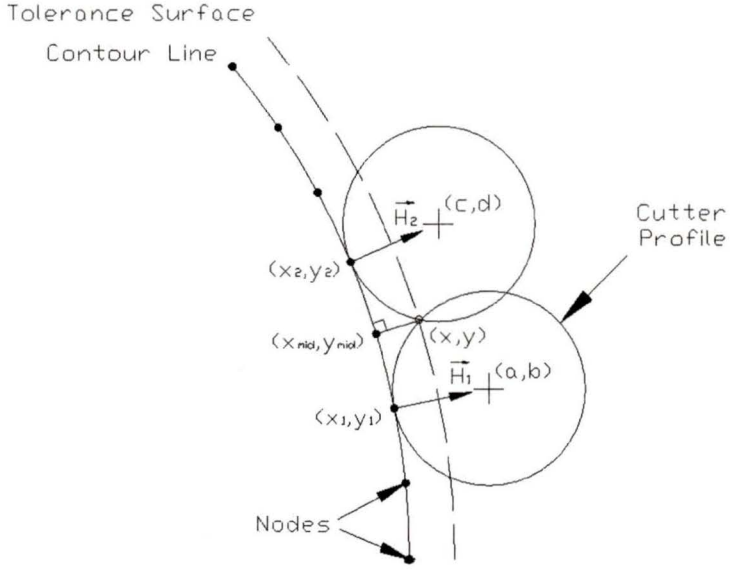

Figure 3.4 Cusp Height Determination, Convex Surface

There are two intersections of the cutter profiles–the closest solution to the surface contour is used. The cusp height is found using the midpoint of the two nodes in consideration. The midpoint (x_{mid},y_{mid}) is determined by finding the closest point on the contour line to the intersection of the circles. The cusp height for the two cutter locations is found by:

$$cuspheight = \sqrt{(x_{mid} - x)^2 + (y_{mid} - y)^2} \tag{55}$$

Cusp height is compared to the projection of the tolerance surface. If the cusp height is less than the projection of the of the tolerance surface, the procedure moves on to the next node. Using the same values of (x_1,y_1) and new values of (x_2,y_2). New cutter locations give new circle intersections (x,y) giving a new cusp height. If cusp height is less than the specified tolerance, the process is repeated until the cusp height is greater than or equal to the projection of the tolerance surface. When this occurs, the cutter location from the previous iteration is used in the tool path, and this location is used as the new base cutter location (a,b) in determining the next isocusp cutter location. The entire process repeats until isocusp cutter locations have been determined across the surface contour. The following pseudocode describes how the concepts explained above are implemented.

Synopsis: *CUTTERLOCATION=isocusp(NODES,T)*

Input: *NODES –array of points along the contour lines of the surface*

Subfields *NODES.x –x co0-ordinate for node*

NODES.y –y co-ordinate for node

Return: *CUTTERLOCATION –array of new kernel locations and normals*

Subfields *CUTTERLOCATION.x –x co-ordinate for kernel*

CUTTERLOCATION.y –y co-ordinate for kernel

Procedure

begin

j=1;

i=1; *{initialize array indexes}*

dx=NODES(i).x - NODES(i+1).x;

dy=NODES(i).y - NODES(i+1).y;

H_x*=dy;* H_y*=-dx;* *{Hx, Hy –x and y components of normal}*

$a = NODES(i).x + H_x \bullet R$

$b = NODES(i).y + H_y \bullet R$ *{calculate original cutter location (c,d)}*

i=i+1;

for *each node along the contour line*

dx=NODE(i).x-NODE(i+1).x;

dy=NODE(i).y-NODE(i+1).y;

Hx=dy; Hy=-dx; *{use neighbouring node to determine normal, N}*

$c = NODES(i).x + H_x \bullet R$

$d = NODES(i).y + H_y \bullet R$

$(x-a)^2+(y-b)^2=R^2$

$(x-c)^2+(y-d)^2=R^2$ *{calculate intersection of cutters, (x,y)}*

{find the midpoint , (x_{mid},y_{mid})closet point to intersection}

$cuspheight=\sqrt{(x_{mid}-x)^2+(y_{mid}-y)^2}$ *{find cuspheight}*

if *cuspheight>tolerance*

(c,d)=(NODES(j-1).x,NODES(j-1).y); {go back to last nde since CH>T}

CUTTERLOCATION(j)=(c,d); {store previous cutter location in tool path}

j=j+1; {increment index to cutter location}

(a,b)=(c,d); {set base co-ordinates for next iteration}

end *{end if}*

i=i+1; {increment NODE index}

end *{end for loop}*

end *{end program}*

The accuracy of this iterative algorithm for finding cutter locations that approximate an isocusp finish is directly dependent on the resolution of the contour line. If the curve is made up of many nodes, cusp heights are found that are much closer to the projected tolerance. When the spacing of these nodes becomes greater, the approximation of an isocusp surface loses accuracy, as shown in Figure 3.5.

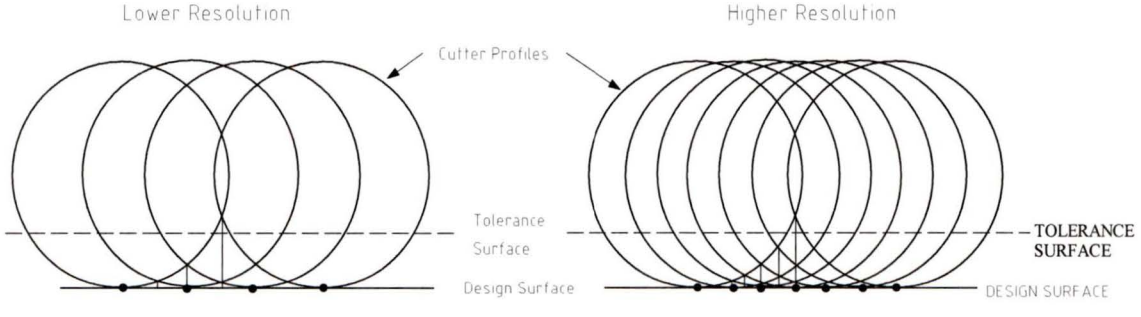

Figure 3.5 Isocusp Accuracy vs. Contour Line Resolution

In some cases the resolution of the contour line is insufficient, and produces a cusp height between neighbouring cutter locations that is less than the tolerance offset. In this case, the iterative algorithm cannot move forward along the nodes of the contour line. To solve this problem, interpolation can be used to create more neighbouring nodes for the existing nodes of the contour line. Since the original design surface has been specified to its

original resolution, increasing the number of nodes along these contour lines through linear interpolation will not change the final shape of the curve. Therefore, linear interpolation can be used to provide a better approximation to an isocusp surface when more nodes are needed along the surface contour lines as shown in Figure 3.6. In this figure, two additional linearly interpolated nodes are calculated within each pair of original nodes.

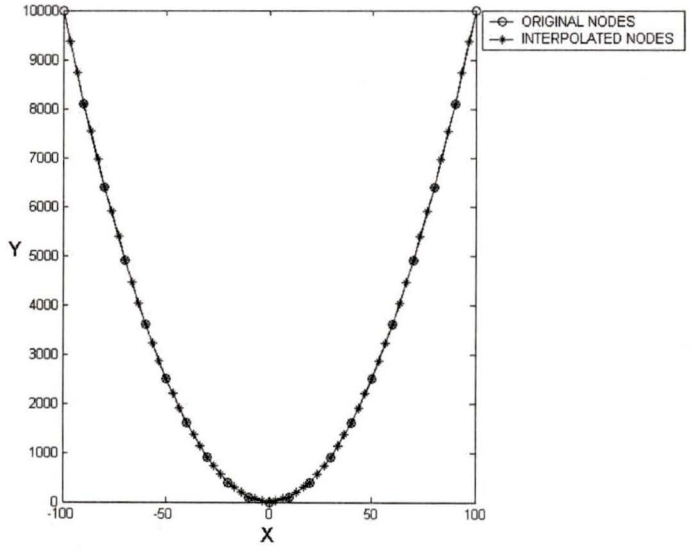

Figure 3.6 Linear Interpolation Along Surface Contour Lines

3.2. Steepest Path Calculation

The steepest path is found by approximating the gradient on the surface. The horizontal component of the gradient is equal to the normal vector at any point along a contour line as described in Chapter 3. If a differentiable function $z=f(x,y)$ has a constant value c along a smooth curve s

$$s(t) = g(t)\hat{i} + h(t)\hat{j} \tag{56}$$

making s a contour line of f, then

$$f(g(t), h(t)) = c \tag{57}$$

Differentiating both sides of Equation 57 with respect to t leads to the equations

$$\frac{d}{dt}\left(f(g(t),h(t))\right)=\frac{d}{dt}(c)=0$$
$$\frac{\partial f}{\partial x}\frac{dg}{dt}+\frac{\partial f}{\partial y}\frac{dh}{dt}=0 \tag{58}$$

This latest equation is in the form of the result of a dot-product of two vectors. The dot-product of two perpendicular vectors is zero. Therefore the following vectors are perpendicular:

$$\left(\frac{\partial f}{\partial x}\hat{i}+\frac{\partial f}{\partial y}\hat{j}\right)\bullet\left(\frac{dg}{dt}\hat{i}+\frac{\partial h}{\partial t}\hat{j}\right)=0 \tag{59}$$

where

$$\nabla f=\left(\frac{\partial f}{\partial x}\hat{i}+\frac{\partial f}{\partial y}\hat{j}\right)$$
$$\frac{ds}{dt}=\left(\frac{dg}{dt}\hat{i}+\frac{dh}{dt}\hat{j}\right) \tag{60}$$

Therefore the gradient of a differentiable function of two variables is always normal to the function's level curves [Finney, Thomas, 1994].

The horizontal projection of this vector matches the definition of the gradient of *z(x,y)* as shown in Figure 3.7

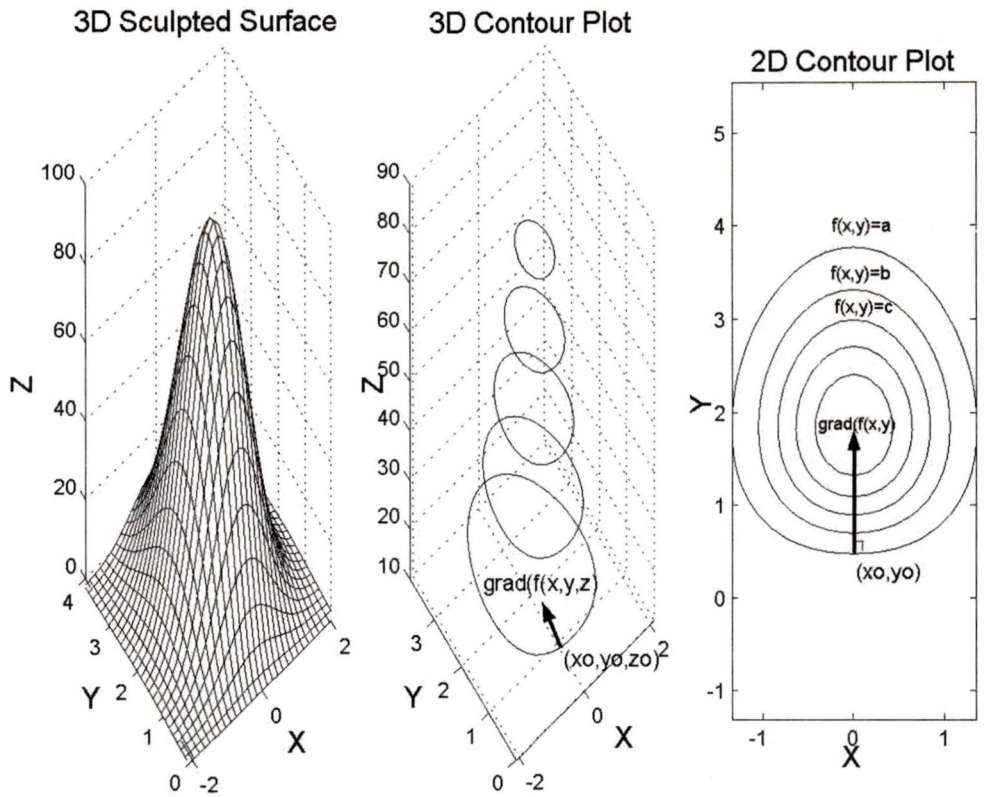

Figure 3.7 Gradient Normal to Contour Lines

The gradient at any point on a surface is always normal to the contour line passing through this point. This is demonstrated by plotting surface gradients along the contour lines of planes, horizontal cylinders, spheres, vertical cones, and horizontal cones, as shown in Figure 3.8 to 3.12.

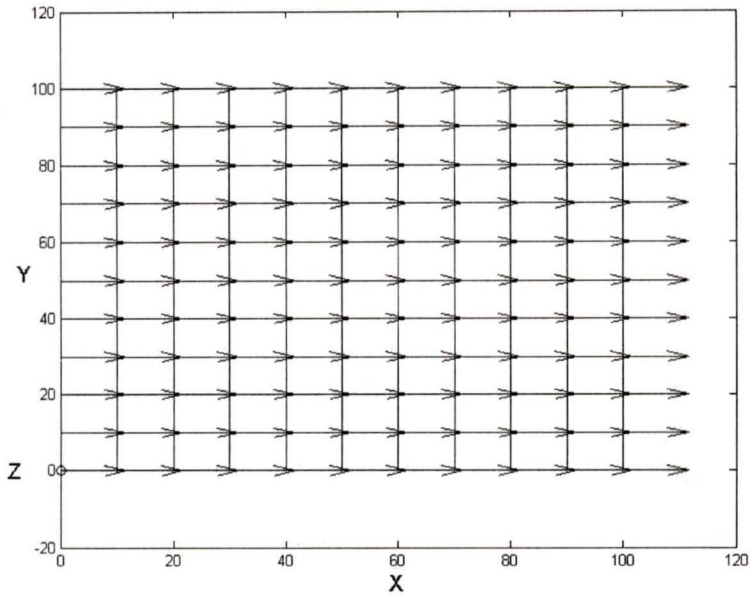

Figure 3.8 Gradient on a Planar Surface

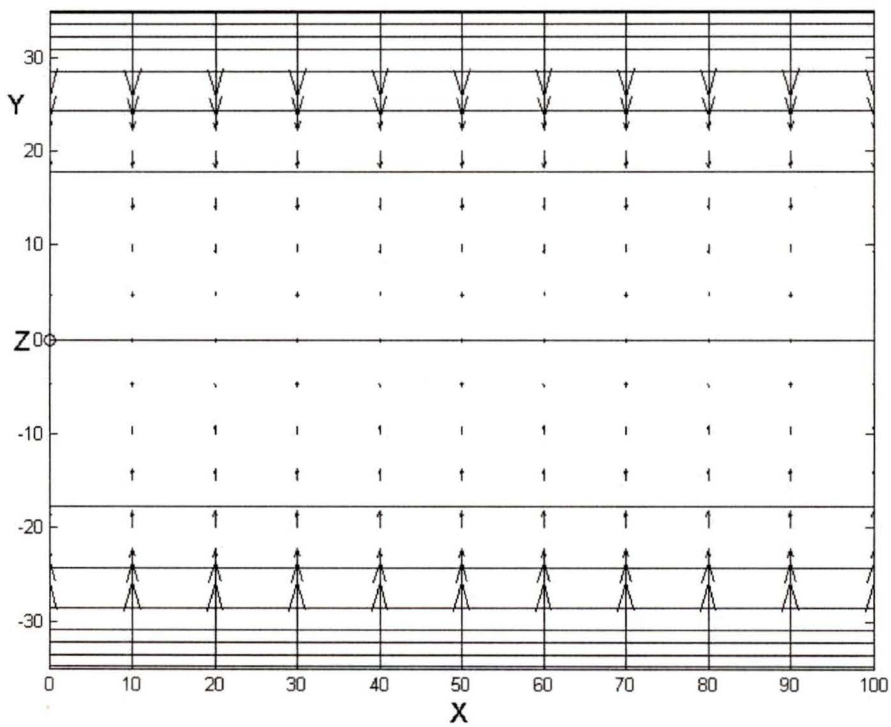

Figure 3.9 Gradient on a Cylindrical Surface

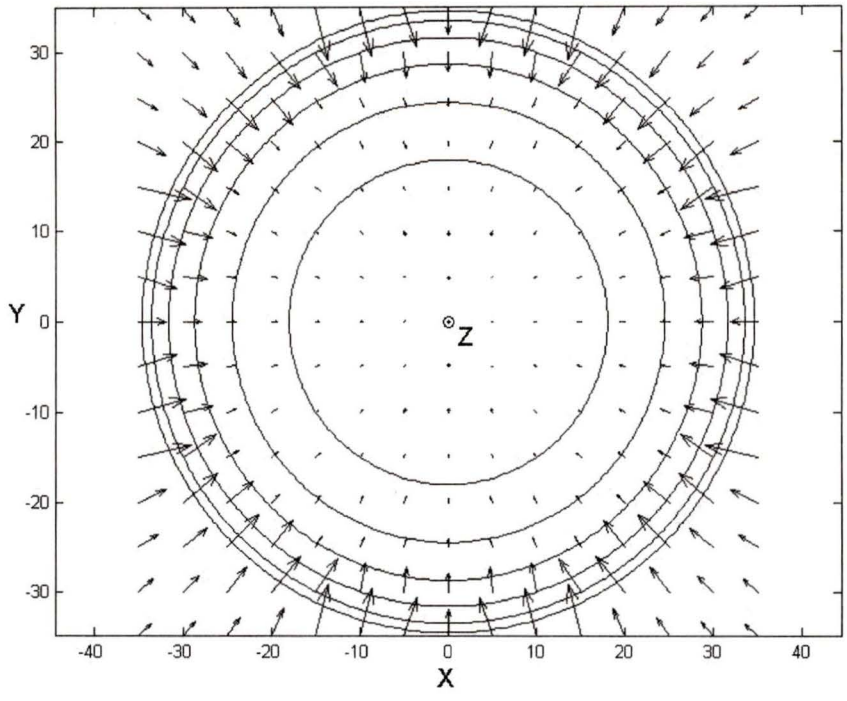

Figure 3.10 Gradient on a Sphere

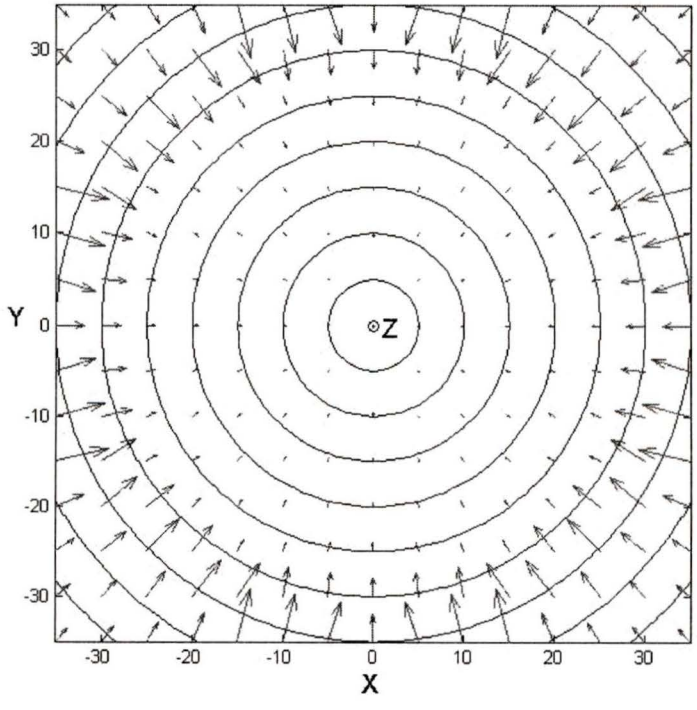

Figure 3.11 Gradient on a Vertical Cone

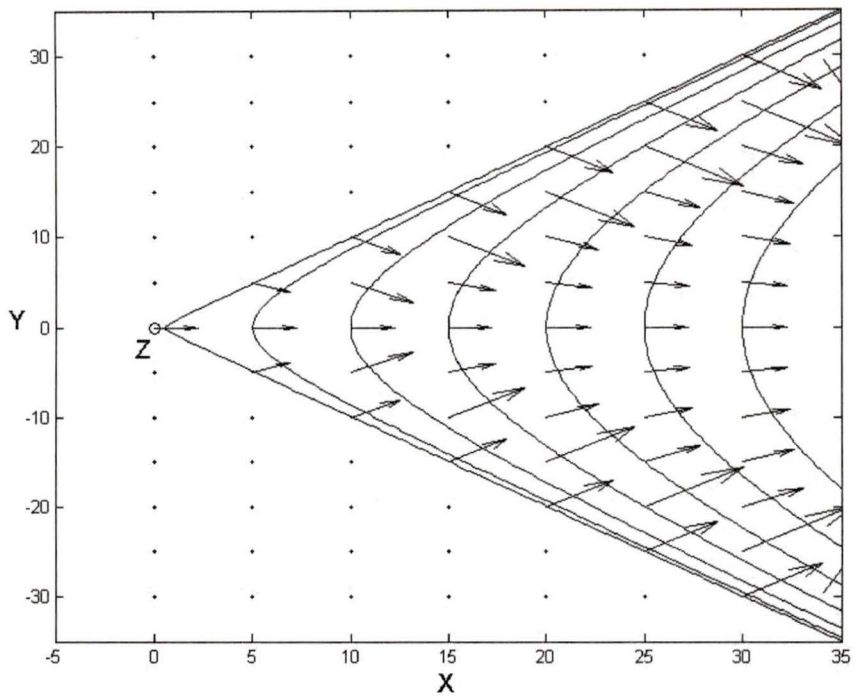

Figure 3.12 Gradient on a Horizontal Cone

Given the starting point of the steepest path on the bottommost contour line, the steepest path is approximated by identifying and linking those nodes on successive contour lines which lie closest to the projection of the gradient. Nodes identified and used to make up the steepest path are called *kernels.* The distance (*dist*) between a node (A) and the normal vector to a given contour line ($\vec{N}$) is determined by

$$dist = \frac{\left|\overrightarrow{AB} \times \vec{N}\right|}{\left|\vec{N}\right|} \tag{61}$$

as shown in Figure 3.13.

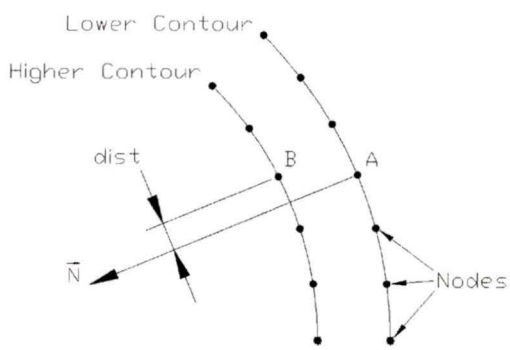

Figure 3.13 Steepest Path Approximation

This process of identifying kernels on successive contour lines is repeated until a series of kernels have been identified that can be linked from the bottom contour line to the top contour line. The cutter locations needed to machine along this steepest path are found by projecting the tool radius normal to the contour line at each kernel.

The following pseudocode describes how the concepts explained above are implemented.

Synopsis: KernelNEW=steepest(NODES,KernelOLD)

Input: *NODES –array of points along the contour lines of the surface*
Subfields *NODES.x -x co-ordinate for node*
NODES.y –y co-ordinate for node
KernelOLD –kernel locations, normals from previous contour line
Subfields *KernelOLD.x –x co-ordinate for kernel*
KernelOLD.y –y co-ordinate for kernel
KernelOLD.Nx –x component of normal
KernalOLD.Ny –y component of normal
Return: KernelNEW –array of new kernel locations and normals
Subfields *KernelNEW.x –x co-ordinate for kernel*
KernelNEW.y –y co-ordinate for kernel
KernelNEW.Nx –x component of normal
KernalNEW.Ny –y component of normal

Procedure:
begin
i=1; {initialize index}
j=1; {initialize index}
firstTIME=1; {initialize firstTIME flag}
for *each node along the contour line*

$$dist = \frac{\left|\left((KernelOLD(i).x - NODE(i).x)\hat{i} + (KernelOLD(i\_.y - NODE(i).y)\hat{j}) \times \vec{N}\right)\right|}{\left|\vec{N}\right|}$$

if *firstTIME=1;*
distOLD=dist; {setting distOLD=dist for first iteration}
firstTIME=0; {turning firstTIME flag off}

```
        end {end if}
        if dist<=distOLD
                distOLD=dist;
                KernelNEW(j)=NODE(i);
                j=j+1; {increment KernelNEW}
                KernelNEW(i).Nx=(NODE(i).y - NODE(i+1).y)
                KernelNEW(i).Ny=(NODE(i).x - NODE(i+1).x)
        end {end if}
        i=i+1;
end {end for}
end {end program}
```

As with the iterative isocusp algorithm, the accuracy of the numerical approximation to the steepest path is directly affected by the number of nodes available on a contour line. When required, linear interpolation can be used to define more nodes along contour lines, producing a more accurate approximation to the steepest path.

3.3. Steepest Directed Isocusp Tool path

The steepest directed isocusp tool path is determined by combining the cutter locations found using the steepest directed path and the isocusp algorithms described above.

Machining parameters are specified including end-mill radius, surface tolerance offset, and the number of steepest paths. Using this information the kernels of the steepest path are found, starting at the bottom contour line and moving up to the top contour line of the surface. The steepest paths are the boundaries, dividing the design surface into areas where isocusp tool paths are found. The steepest paths are uniformly spaced around the lowest contour line in the machined examples.

The index of the nodes selected as kernels for the steepest path are used to limit the area of isocusp calculation. This strategy results in a surface machined in several regions by isocusp tool paths bounded by steepest tool paths. If the node resolution is high enough

to produce a satisfactory tool path, the cutter locations are organized into tool paths and post-processed into G-CODE, as shown in Figure 3.14

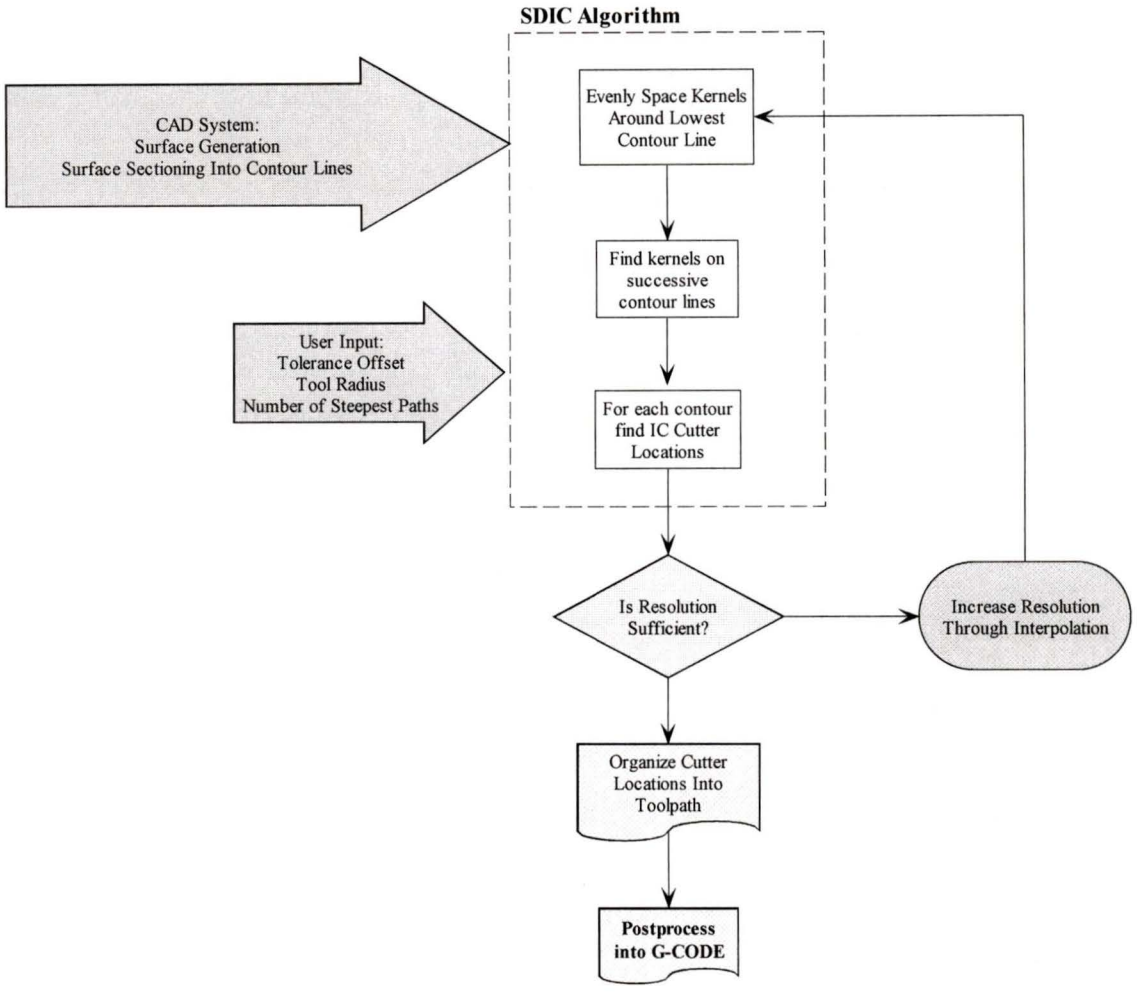

Figure 3.14 SDIC Flowchart

Indices are used to identify cutter locations in successive tool paths. In convex machining the number of adjacent cutter locations along a level curve decreases as the height of the contour line increases. Conversely, in concave machining, the number of cutter locations increases as the height of the contour line increases. Cutter locations with the same index are joined to form the tool path. The tool path is terminated when there is no cutter location for the specific index of the tool path on the next contour line, or when the final contour line is reached as shown in Figure 3.2.

3.4. Laced and Unlaced SDIC Tool paths

Unlaced tool paths are made up of cutter locations starting along a steepest path with successive cutter locations offset based on the isocusp criteria up to the next bounding steepest path, as shown in Figure 3.15. Generation of the unlaced SDIC tool path is described in the preceding sections.

Laced tool paths are tool paths calculated from two starting points, two boundaries defined by steepest paths. Isocusp cutter locations are found on the inside of each border and successive cutter locations are offset from these tool paths. Successive cutter locations are found until isocusp cutter locations completely cover the bounded area, as shown in Figure 3.15.

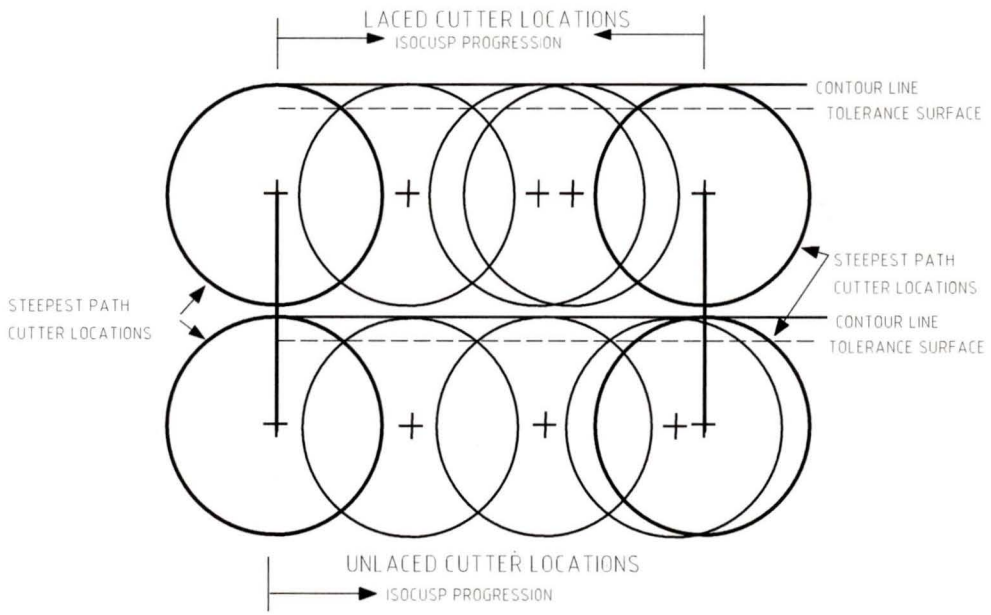

Figure 3.15 Laced and Unlaced Cutter Locations

The solutions for laced and unlaced tool path lengths were basically similar except for integer effects. More specifically, due to the discrete nature of the cutter location selection and the finite resolution of the contour lines, the positioning of the bounding steepest paths and isocusp cutter locations was not always identical for similar surface sections, as shown in Figure 3.16. The simpler unlaced tool paths were adopted for this work.

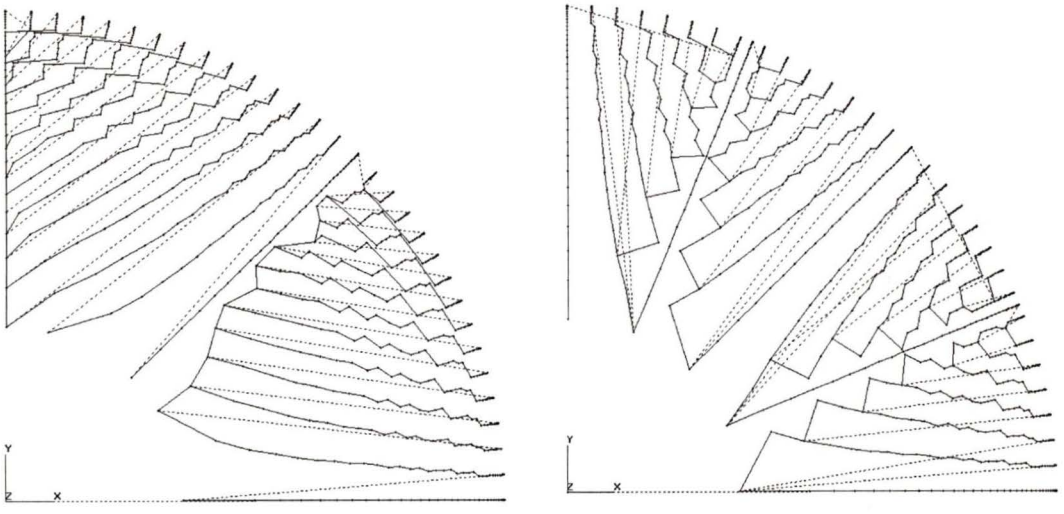

Figure 3.16 Unlaced and Laced SDIC Tool paths

3.5. SDIC Tool path Generation for Concave and Convex Surfaces

The SDIC generation algorithm described in this chapter can be used to calculate tool paths for concave or convex surfaces. In calculating SDIC tool paths for convex surfaces, the cutter locations are offset outside the contour lines, since the tool will be machining on the outside of the convex surface. For concave surfaces the cutter locations are offset inside the concave contour line, as shown in Figure 3.17.

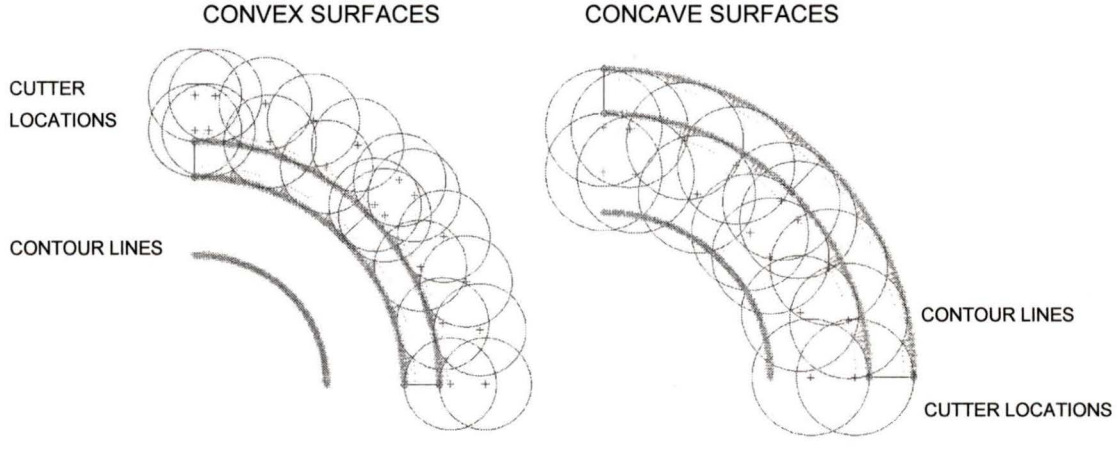

Figure 3.17 Convex and Convex SDIC Tool paths

Using this approach, regions of concavity and convexity must be identified and separated prior to SDIC tool paths generation. For example SDIC tool paths were generated for the

following concave/convex sculptured surface (shown in Figure 3.18). The surface was separated into areas of concavity and convexity, and SDIC tool paths were found for each section.

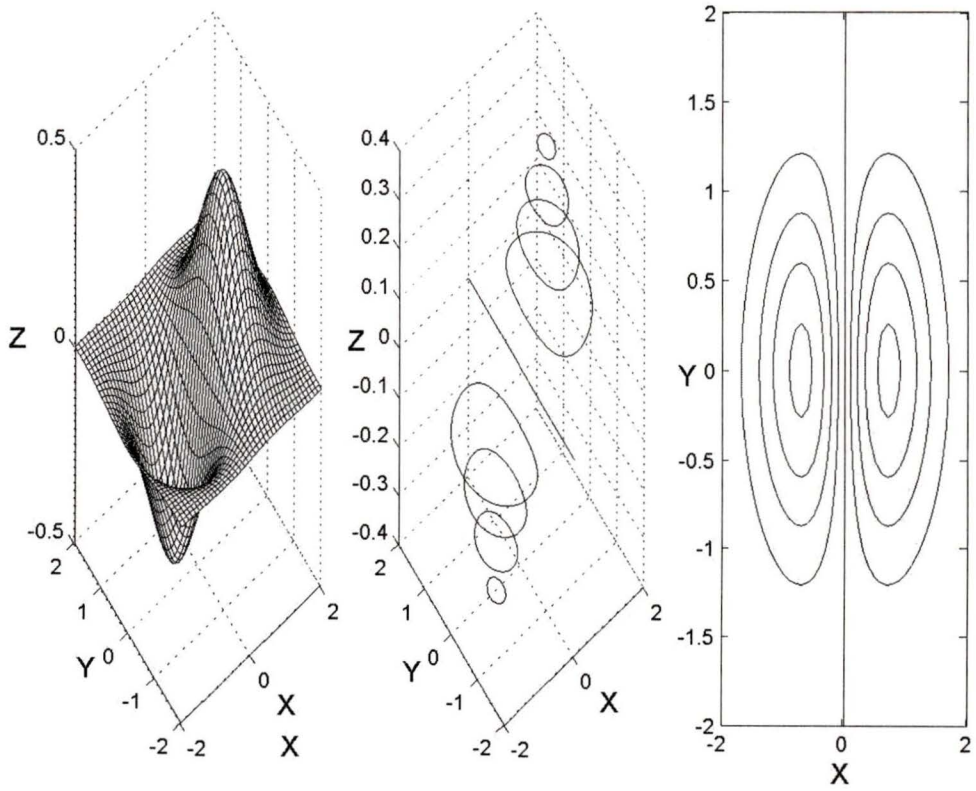

Figure 3.18 Concave / Convex Sculptured Surface

CHAPTER 4 CNC MACHINING OF SURFACES USING THE SDIC TOOL PATH

SDIC, isocusp, and isoparametric tool paths were generated for the following surfaces:

- Planes
- Horizontal cylinders
- Spheres
- Vertical cones
- Horizontal cones of various cone angles
- Convex freeform surface
- Concave freeform surface

SDIC tool paths were generated using the algorithm presented in Chapter 3. The minimum SDIC tool path length is found by calculating the SDIC tool path for different numbers of steepest paths, until the minimum is found.

Isoparametric tool paths were generated by following isoparametric lines over the design surface. In the case of planes, horizontal cylinders, and vertical cones, isoparametric lines are coincident with steepest directed paths. For these surfaces the isoparametric tool path is comprised of a series of steepest directed paths. The step-over between adjacent isoparametric tool paths was determined using the isocusp criteria along the bottommost contour line. Since the convex and concave freeform surfaces were expressed in terms of $z=f(x,y)$, isoparametric lines lie parallel to the x and y planes. For these surfaces, isoparametric tool paths were coincident with isocusp tool paths parallel to the x and y planes.

The isocusp tool paths are generated for all surfaces using the plane surface intersection method described in Section 1.2.2. The offset between adjacent intersecting planes is determined by the maximum cusp height between adjacent slices being less than the surface tolerance. These tool paths are generated in *Pro-MANUFACTURING* from

models generated in *Pro-ENGINEER* . Critical variables affecting the resulting tool paths are the cutting direction, cutting tool dimensions, the retraction plane for the tool, the allowable chordal deviation of the design surface, and allowable cusp height (referred to as scallop height in *Pro-MANUFACTURING*). Cutting direction was parallel to the x or y planes. In cases where changes in cutting direction will change the overall tool path length, different cutting directions were calculated and their tool paths are presented. Chordal deviation was set to 0.1mm, and the allowable cusp height was set equal to the desired tolerance of the surface, 0.1mm.

During surface machining, the end-mill travel at a fixed feed rate. A faster feed rate is used during tool retraction, return, and plunging. Distances traveled during retraction, return, and plunging are included in the total toolpath length for each method.

The SDIC, isocusp, and isoparametric tool paths were all generated for a half inch end-mill (R=6.35mm) and surface tolerance equal to 0.1mm. Equivalent retraction planes were used for the tool paths being compared. The surfaces were machined from Ren-Shape corrugated fiberboard using a 3-axis CNC mill.

4.1. Inclined Plane

SDIC tool paths were generated for an inclined plane, length=100mm, height=50mm, angle of inclination=45°, with a surface tolerance of 0.1mm, as shown in Figure 4.9.

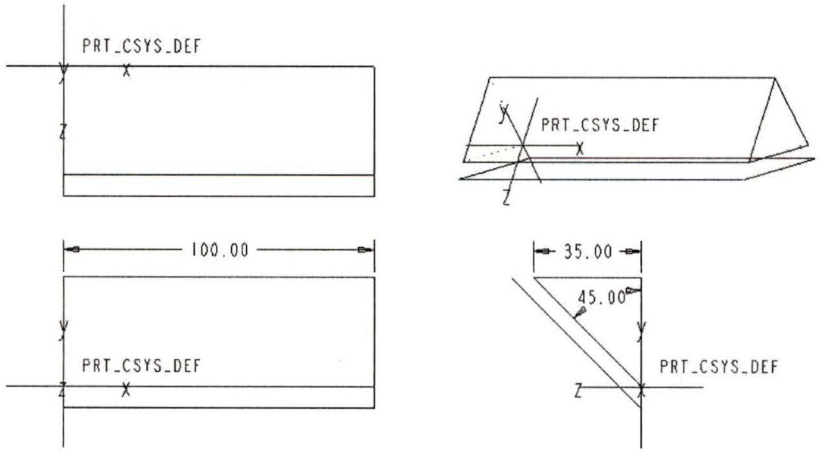

Figure 4.1 Inclined Plane

The shortest SDIC tool path was generated with three steepest directed paths, as shown in Figure 4.2.

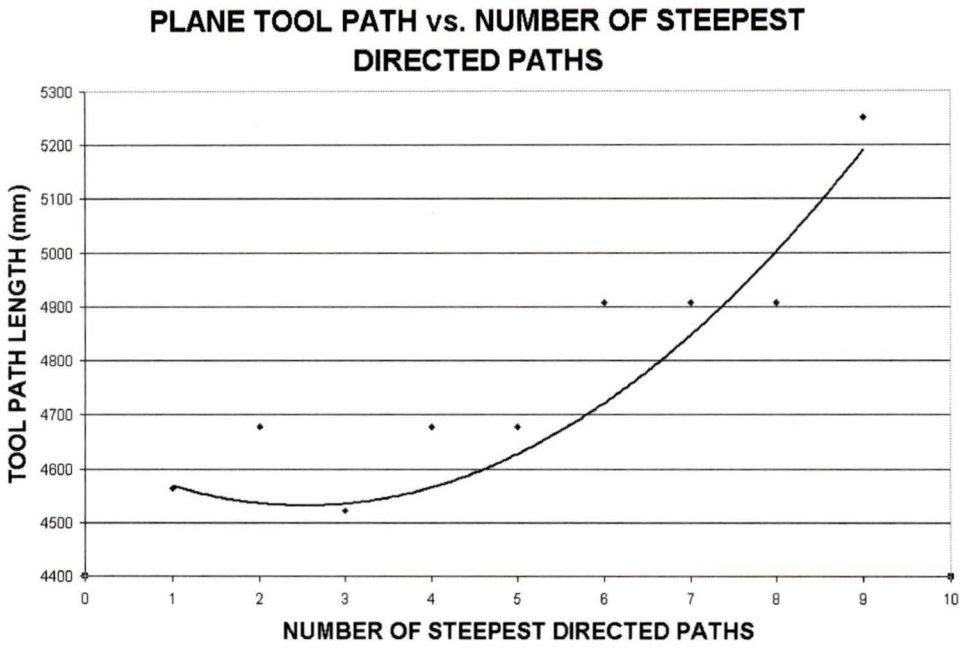

Figure 4.2 Inclined Plane: SDIC Tool Path Length vs. Number of Steepest Directed Paths.

The SDIC, isoparametric, and isocusp tool paths are shown in Figure 4.3. Since the angle of inclination is always constant at any point on a planar surface, as shown in Figure 2.12, isocusp tool paths will remain at a fixed offset distance from adjacent tool paths on a planar surface. Therefore the SDIC tool path for a planar surface is a series of parallel tool paths, all parallel to the steepest paths. The optimum SDIC tool path is found with one steepest path. This is equivalent to the isoparametric tool path where adjacent tool paths are spaced to produce a constant cusp height equal to the tolerance of the surface. Machining isocusp tool paths parallel to the x axis is highly inefficient in this case since the x-axis runs perpendicular to the steepest directed path of the surface. This inefficiency is reflected by the large number of tightly packed adjacent tool paths required to machine the surface.

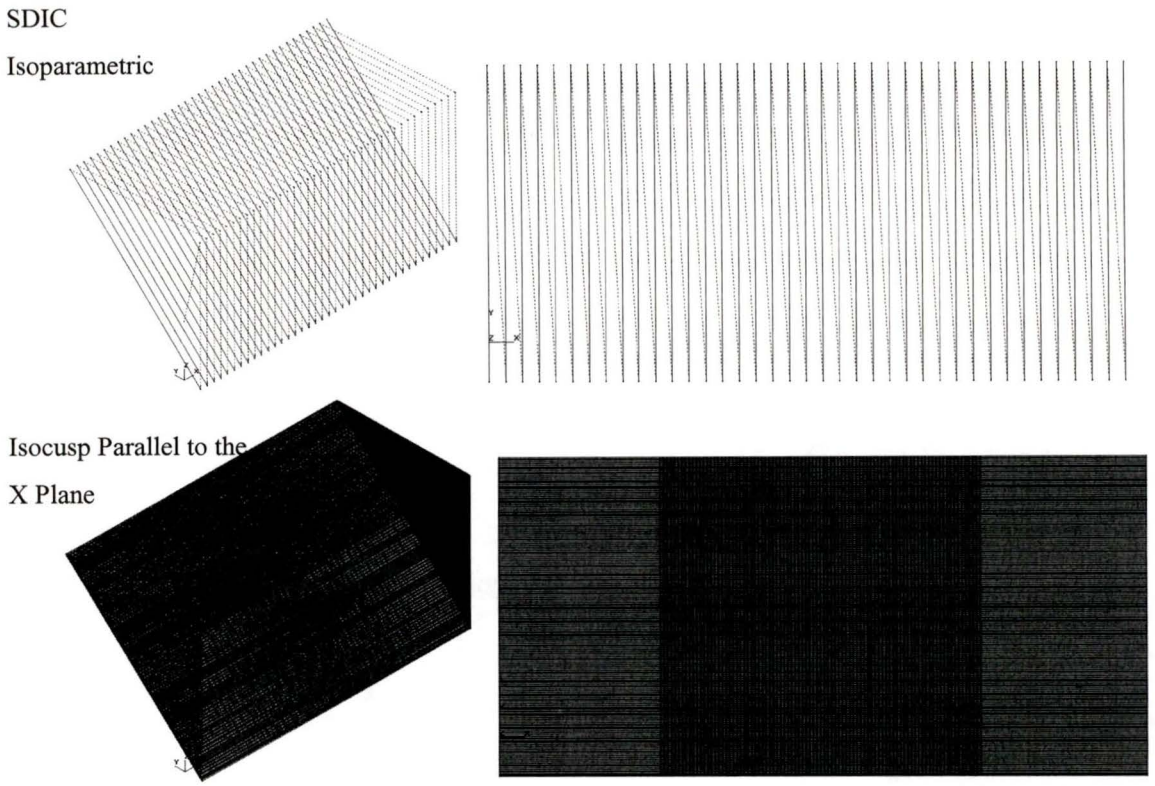

Figure 4.3 Plane Tool Paths: Optimal SDIC, Isoparametric, and Isocusp

The tool path lengths for SDIC, isocusp, and isoparametric tool paths are shown in Figure 4.4. The optimum SDIC tool path is 31.6% shorter than the isocusp tool path parallel to the *y* plane, and 95.1% shorter than the isocusp parallel to the *x* plane.

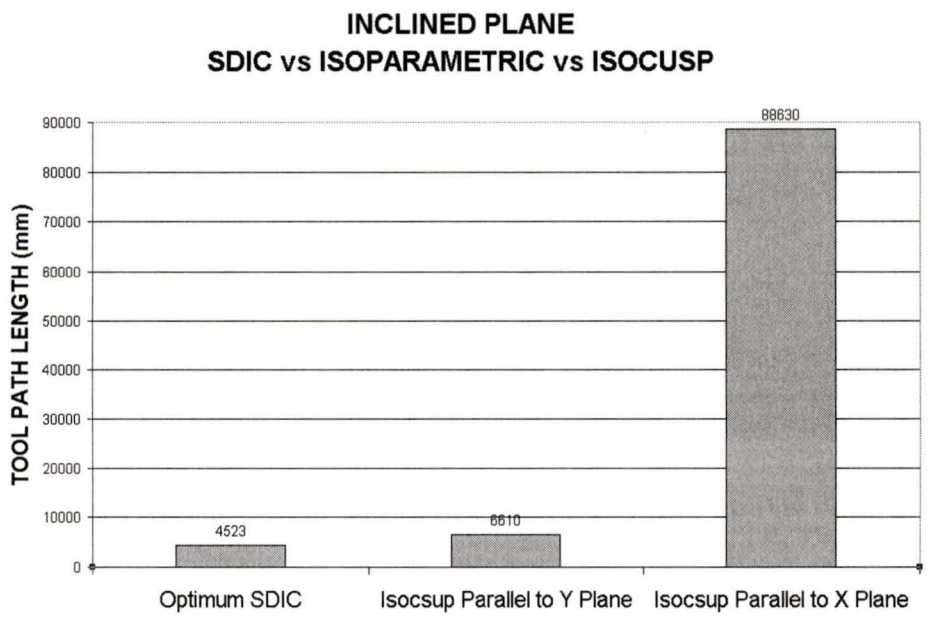

Figure 4.4 Plane Tool Path Length Comparisons

4.2. Horizontal Cylinder

SDIC tool paths were generated for a convex horizontal cylinder, radius=35mm,. length=100mm, with a surface tolerance of 0.1mm, as shown in Figure 4.5.

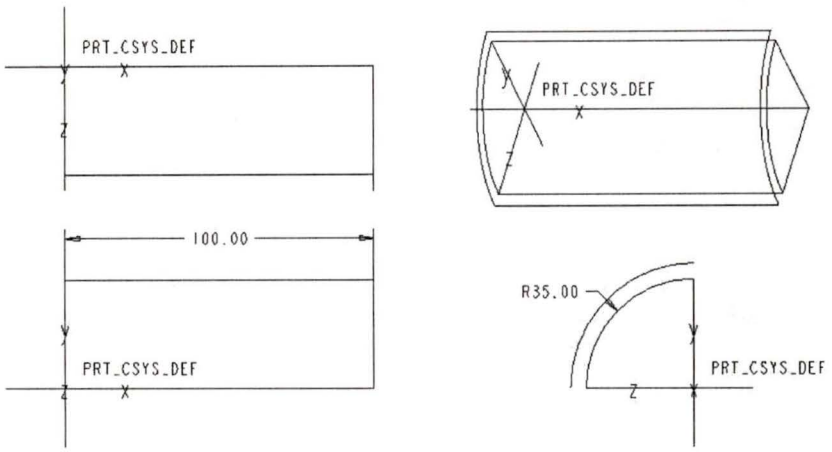

Figure 4.5 Horizontal Cylinder

The shortest SDIC tool path was generated with six steepest directed paths, as shown in Figure 4.6.

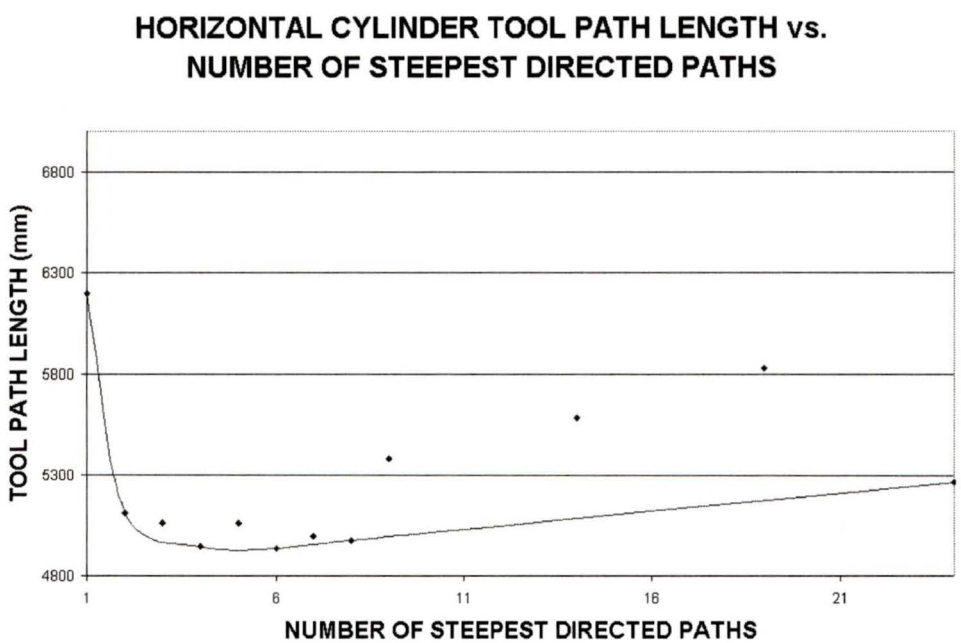

Figure 4.6 Horizontal Cylinder: SDIC Tool Path Length vs. Number of Steepest Directed Paths

The SDIC, isoparametric, and isocusp tool paths are shown in Figure 4.7. Machining isocusp tool paths parallel to the x axis is highly inefficient in this case since the x-axis runs perpendicular to the steepest directed path of the surface. This inefficiency is reflected by the large number of tightly packed adjacent tool paths required to machine the surface. The spacing between adjacent tool paths increases as the angle of inclination of the surface increases, near the top of the cylinder.

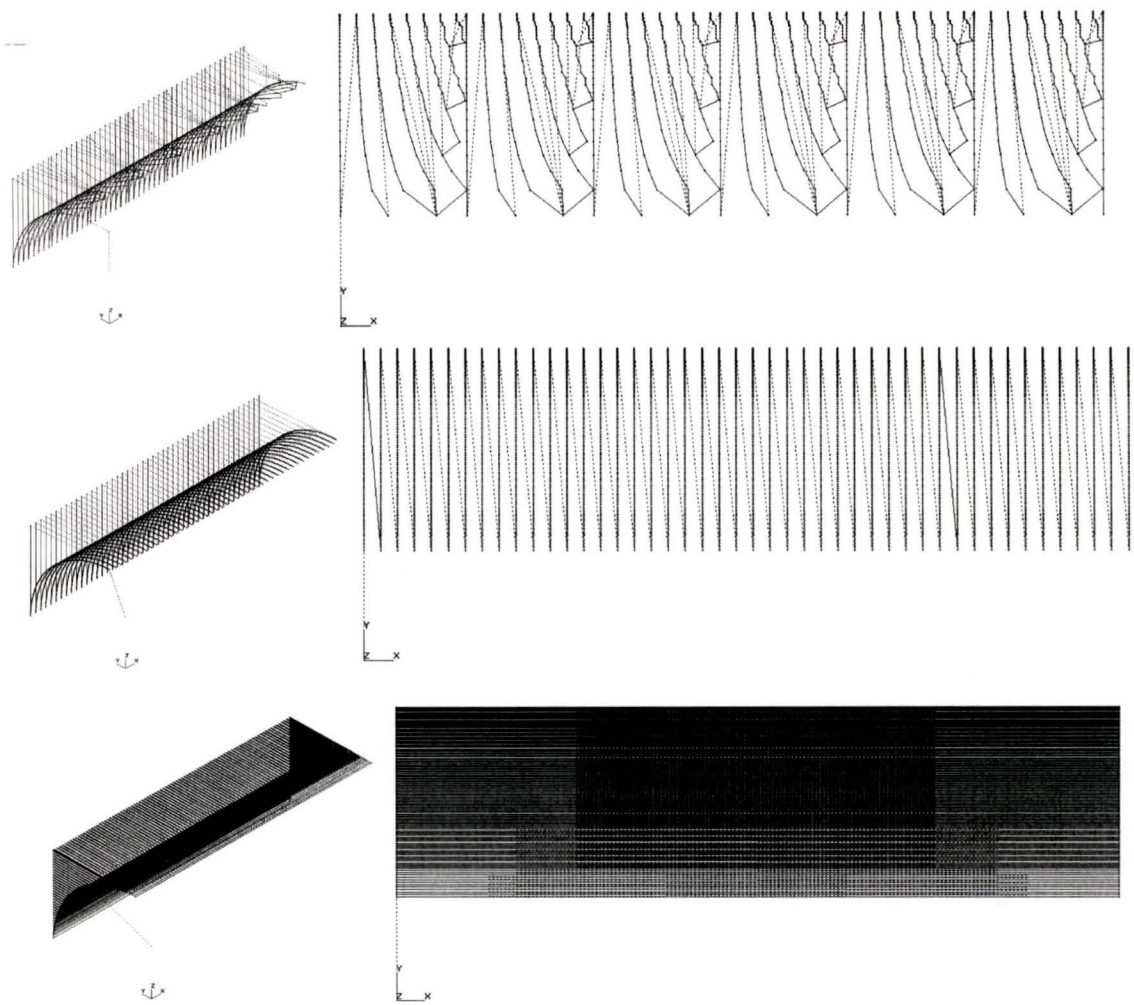

Figure 4.7 Horizontal Cylinder Tool Paths: Optimum SDIC, Isoparametric, and Isocusp

The tool path lengths for SDIC, isocusp, and isoparametric tool paths are shown in Figure 4.8. The optimum SDIC tool path length is 13.7% shorter than the isoparametric tool path length, and 88.3% shorter than the isocusp tool path length parallel to the X-axis.

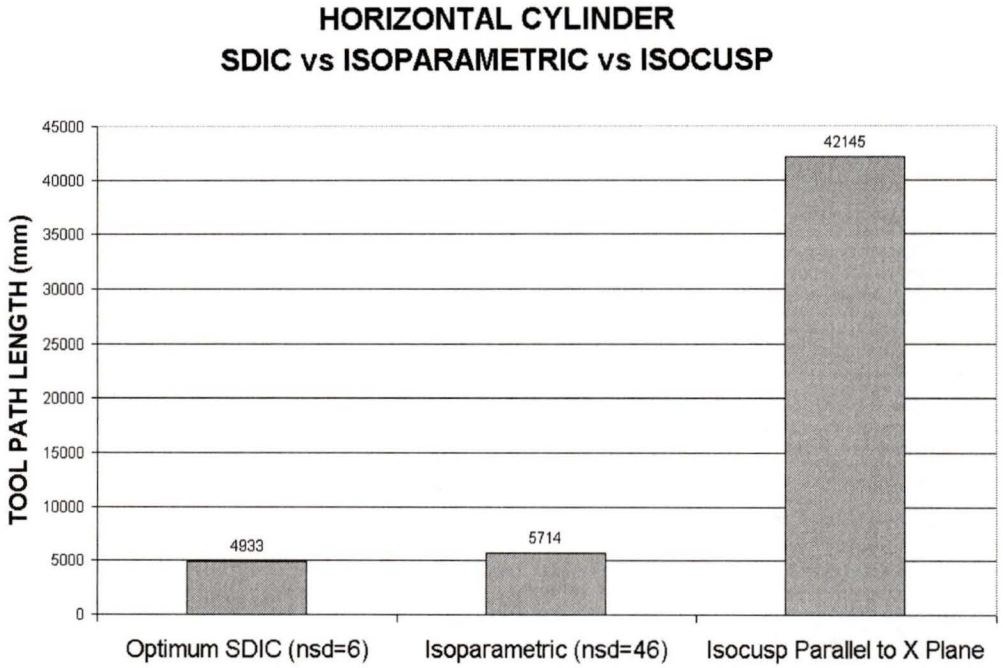

Figure 4.8 Horizontal Cylinder Tool Path Length Comparison

4.3. Sphere

SDIC tool paths were generated for a convex quarter sphere, radius=35mm, with a surface tolerance of 0.1mm, as shown in Figure 4.9.

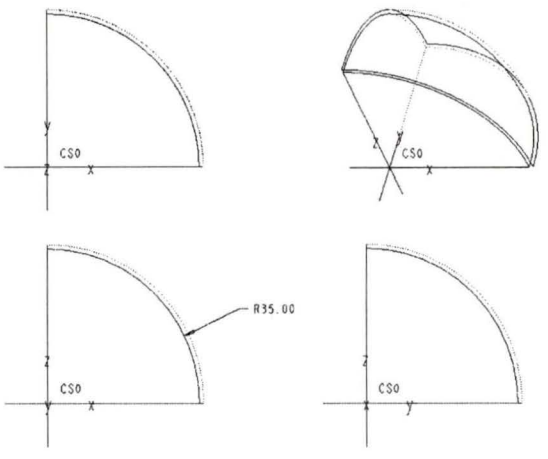

Figure 4.9 Quarter Sphere

The shortest SDIC tool path was generated with three steepest directed paths, as shown in Figure 4.10.

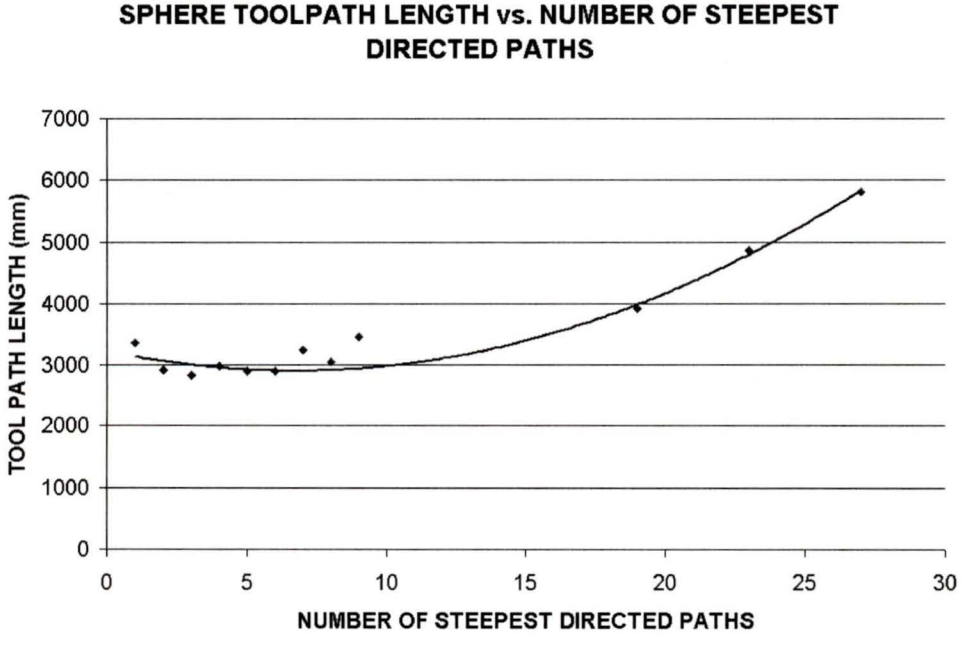

Figure 4.10 Sphere: SDIC Tool Path Length vs. Number of Steepest Directed Paths

The SDIC, isocusp, and isoparametric tool paths are shown in Figure 4.11.

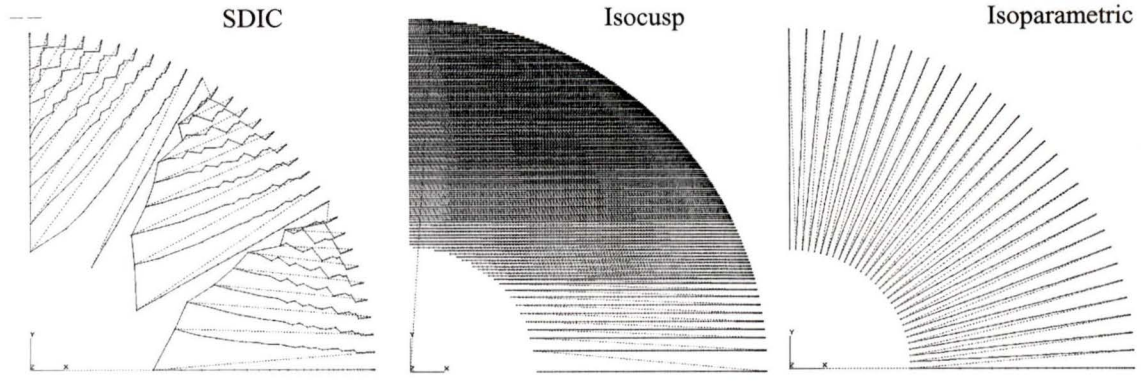

Figure 4.11 Sphere: Optimal SDIC, Isoparametric, and Isocusp Tool Paths

Quarter sphere surfaces machined using these toolpaths are shown in Figure 4.12.

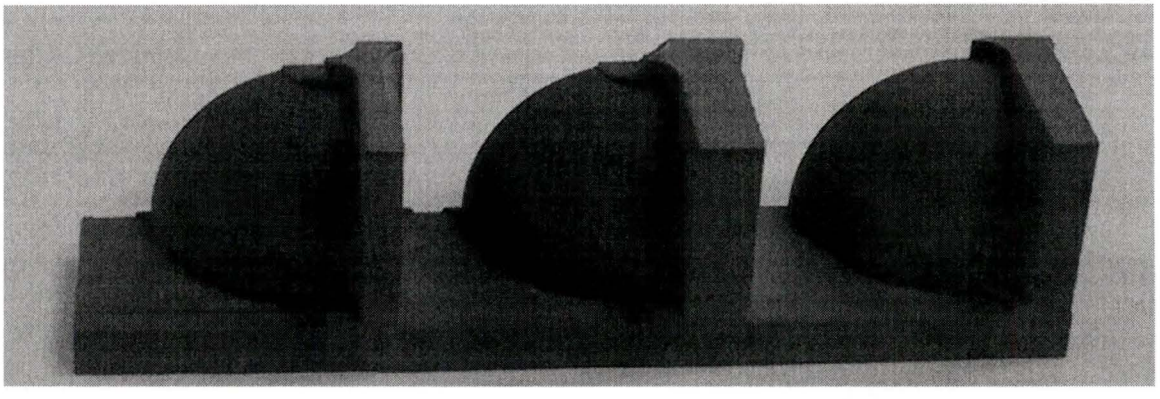

Figure 4.12 Machined Quarter Spheres (L to R): SDIC, Isocusp, Isoparametric

A terraced isocusp tool path was also generated for comparison in Figure 4.13. This tool path is parallel to the z-plane, machining the surface in horizontal sections, with step-over determined by the maximum cusp height between cuts. The tool path lengths for SDIC, isocusp, and isoparametric tool paths are shown in Figure 4.13. The optimum SDIC tool path is 15.2% shorter than tool path generated by the isoparametric, 80.0% shorter than the isocusp tool path, and 86.3% shorter than the terraced tool path.

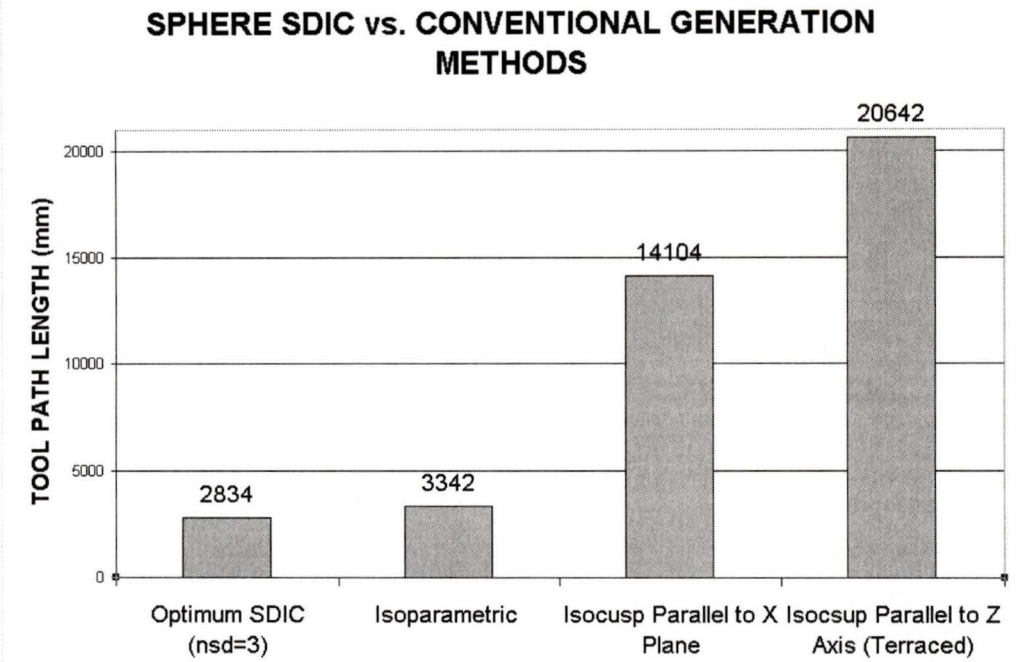

Figure 4.13 Sphere Tool Path Length Comparison

4.4. Vertical Cone

SDIC tool paths were generated for a convex quarter vertical cone, radius=35mm, with a surface tolerance of 0.1mm, as shown in Figure 4.14.

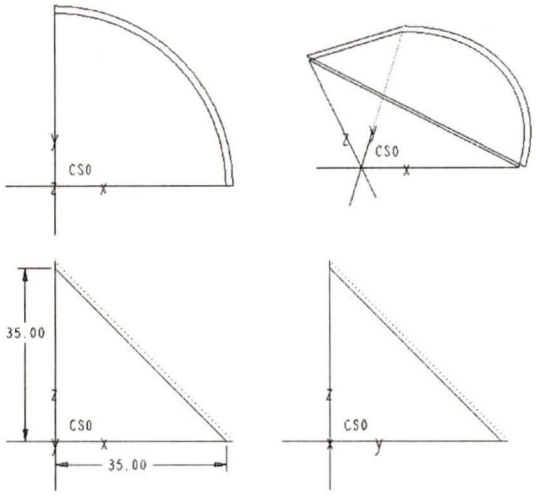

Figure 4.14 Vertical Cone

The shortest SDIC tool path was generated with three steepest directed paths, as shown in Figure 4.15.

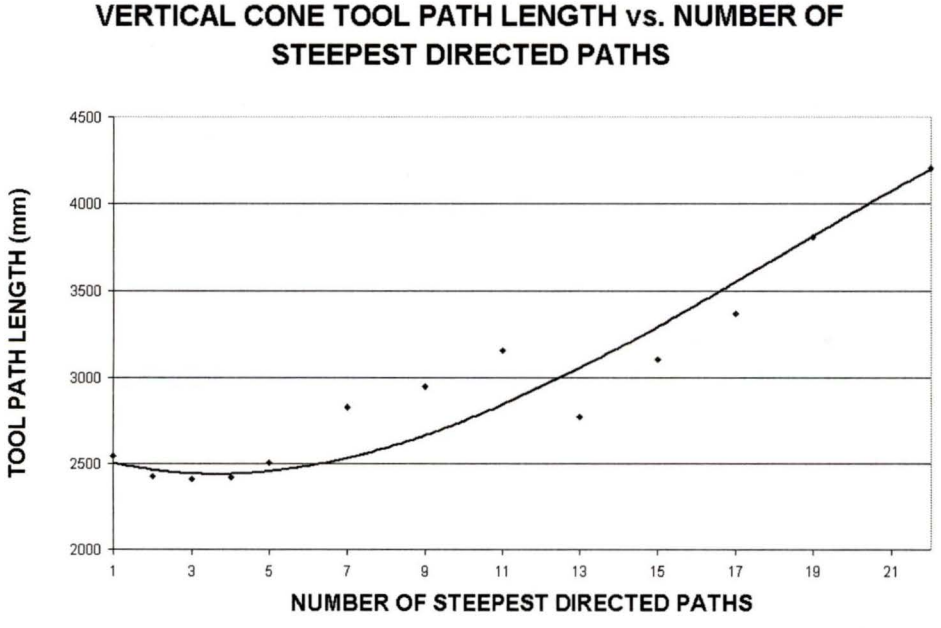

Figure 4.15 Vertical Cone: SDIC Tool Path Length vs. Number of Steepest Directed Paths

The SDIC, isoparametric, and isocusp tool paths are shown in Figure 4.16

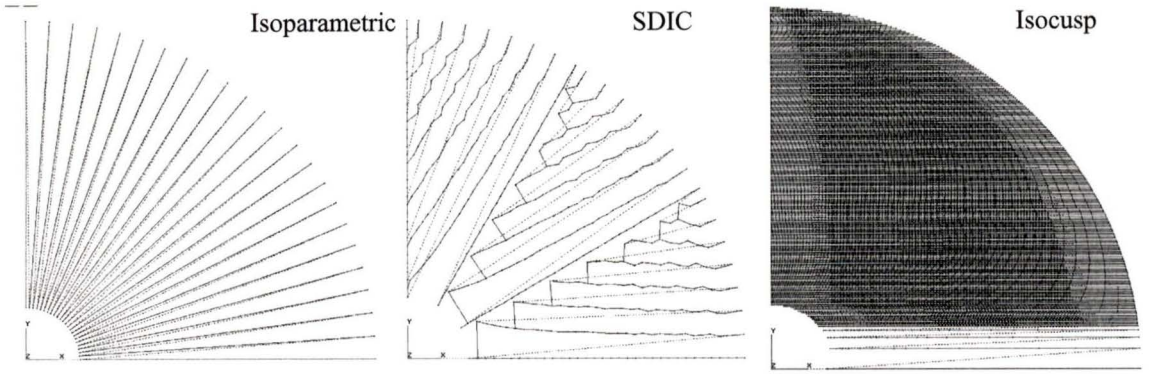

Figure 4.16 Vertical Cone Tool Paths: Optimal SDIC, Isoparametric, and Isocusp Tool Paths

Quarter vertical cone surfaces machined using these toolpaths are shown in Figure 4.17.

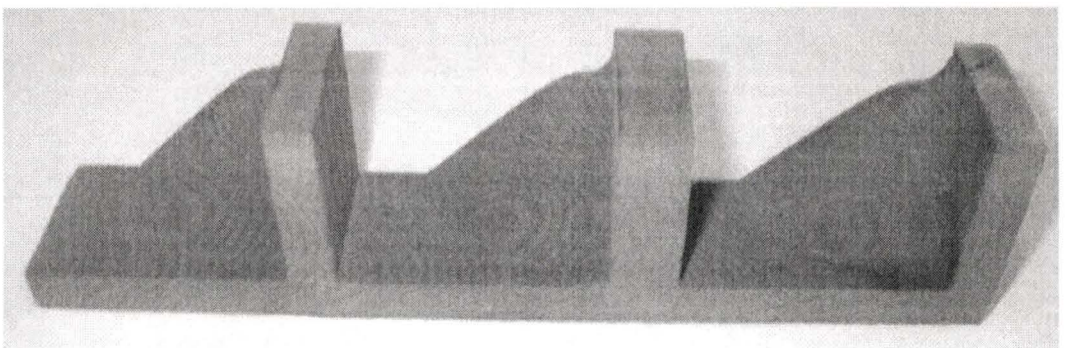

Figure 4.17 Machined Vertical Cones (L to R): Isoparametric, SDIC, Isocusp

A terraced isocusp tool path was also generated for comparison in Figure 4.18. This tool path is parallel to the z-plane, machining the surface in horizontal sections, with step-over determined by the maximum cusp height between cuts. The tool path lengths for SDIC, isocusp, and isoparametric tool paths are shown in Figure 4.18. The optimum SDIC tool path is 11.4% shorter than isoparametric tool path, 91.7% shorter than the isocusp tool path, and 91.2% shorter than the terraced tool path.

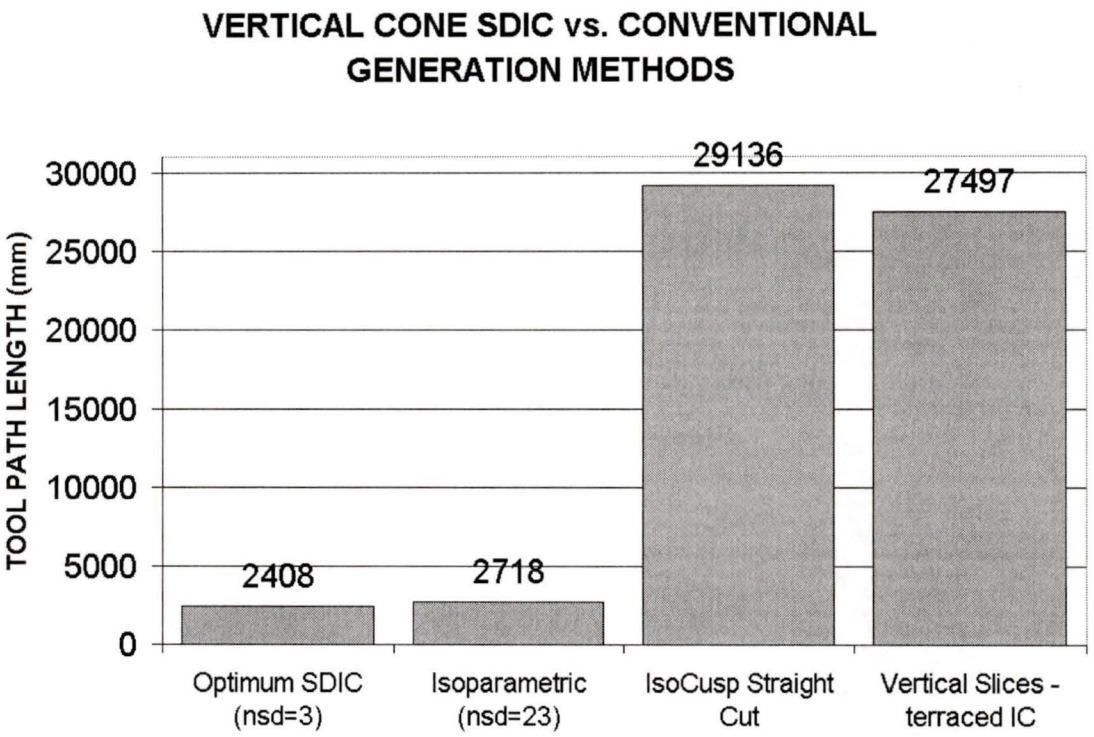

Figure 4.18 Vertical Cone Tool Path Length Comparison

4.5. Horizontal Cone

SDIC tool paths were generated for a convex quarter horizontal cone, radius=35mm, forming a 10° cone with its axis, with a surface tolerance of 0.1mm, as shown in Figure 4.19.

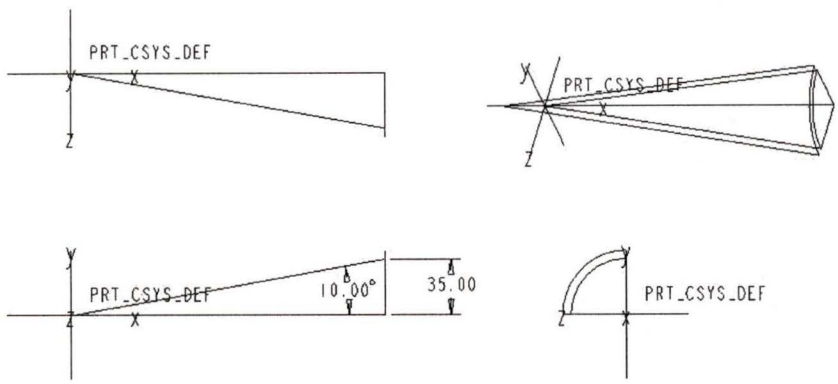

Figure 4.19 Horizontal Cone, Cone Angle=10°

The shortest SDIC tool path was generated with nine steepest directed paths, as shown in Figure 4.20.

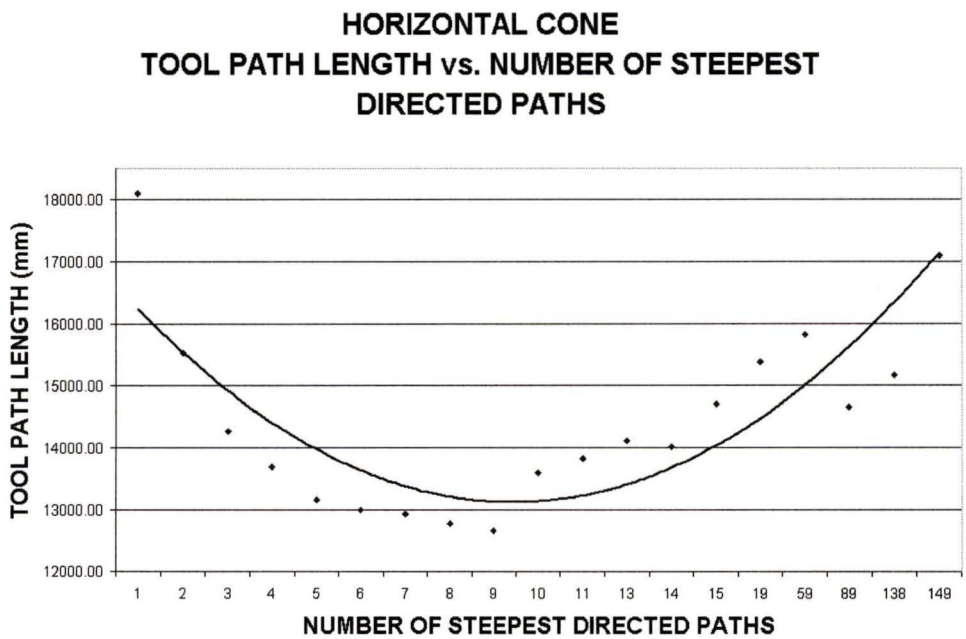

Figure 4.20 Horizontal Cone: SDIC Tool Path Length vs. Number of Steepest Directed Paths

The SDIC, isoparametric, and isocusp tool paths are shown in Figure 4.16

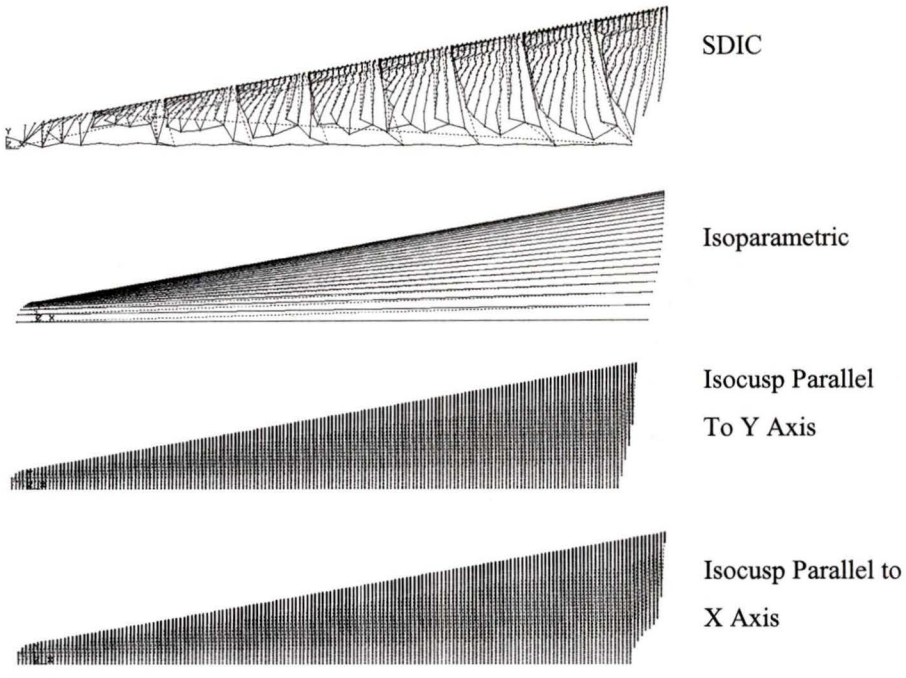

Figure 4.21 Horizontal Cone Tool paths: Optimal SDIC, Isoparametric, Isocusp Parallel to the Y Axis, Isocusp Parallel to the X-Axis

Horizontal cone surfaces machined using these toolpaths are shown in Figure 4.22.

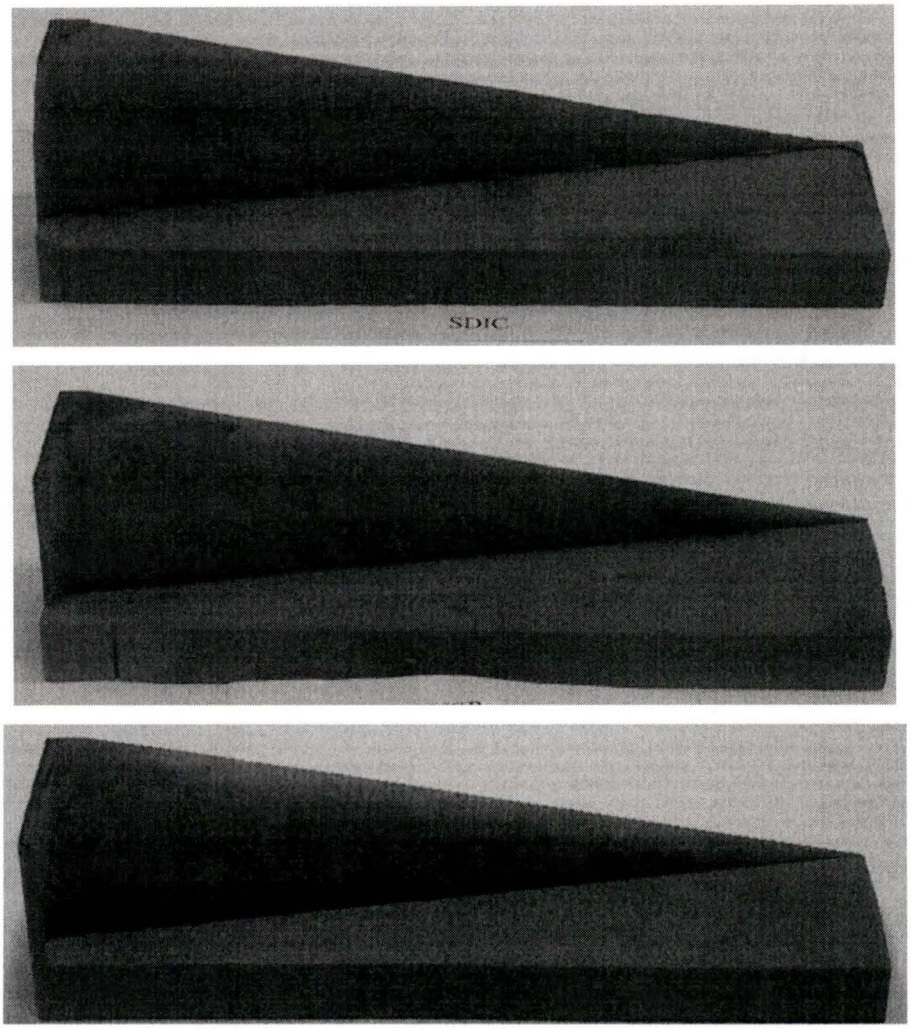

Figure 4.22 Machined Horizontal Cones (Top to Bottom): SDIC, Isocsup Parallel to Y Plane, Isocsup Parallel to X Plane

The tool path lengths for SDIC, isocusp, and isoparametric tool paths are shown in Figure 4.23. The optimum SDIC tool path is 30.2% shorter than the isoparametric tool path, 36.3% shorter than the isocusp tool path parallel to the y axis, methods, and 53.6% shorter than the isocusp tool path parallel to the x axis.

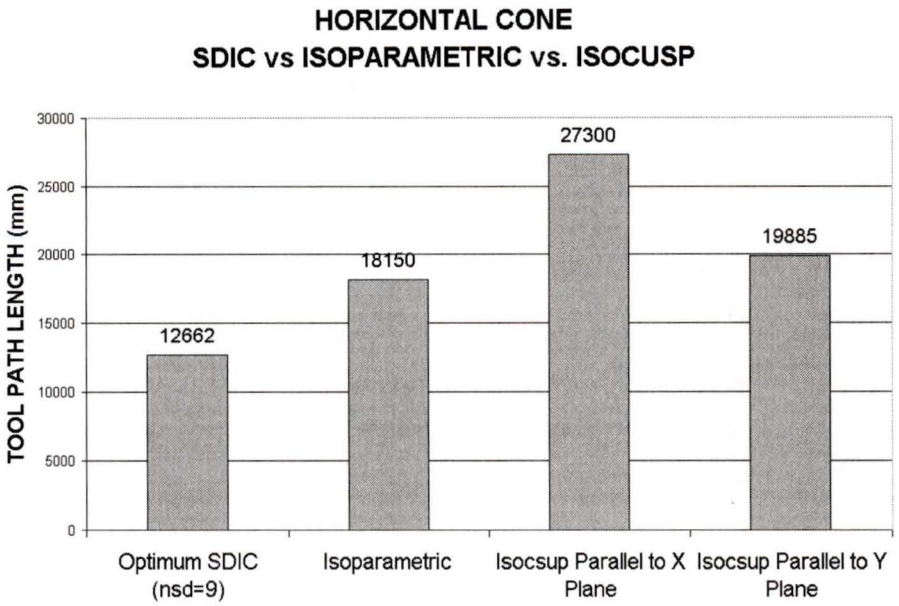

Figure 4.23 Horizontal Cone Tool Path Length Comparison

4.6. Horizontal Cone – Various Angles

In order to demonstrate the significance of the angle of inclination of the surface on cutting efficiency, as discussed in Chapter 2, SDIC tool paths were generated for horizontal cones with increasing cone angles. The SDIC tool paths for horizontal cones with cone angles of 10°, 15°, 30°, and 45° are shown in Figure 4.24

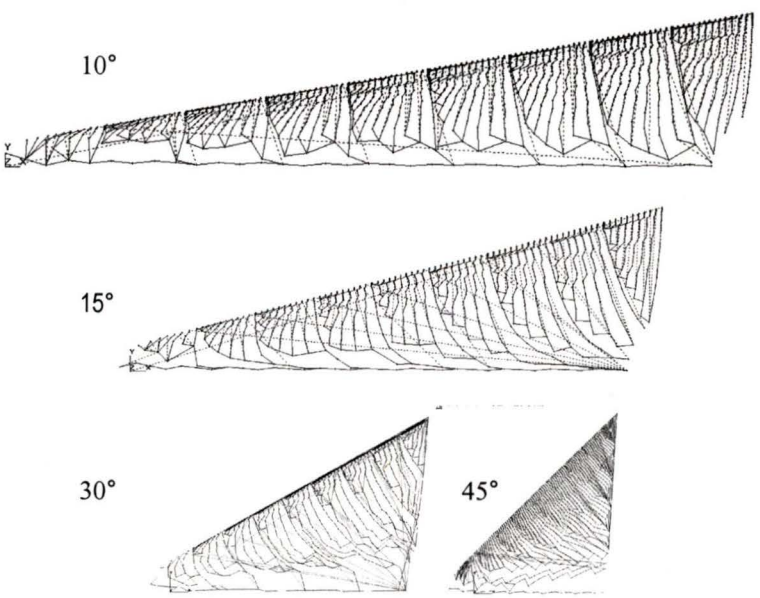

Figure 4.24 Horizontal Cones with Varying Cone Angle:10°,15°,30°, and 45°

To examine the effect of cone angle on overall SDIC tool path length, overall tool path lengths were divided by the surface area of the horizontal cone, as shown in Figure 4.25. As the cone angle decreases, a greater portion of the surface area is at a higher angle of inclination than for higher cone angles. A higher angle of inclination over the surface gives a higher effective cutting edge length over the surface, and a decrease in the tool path length/surface area ratio.

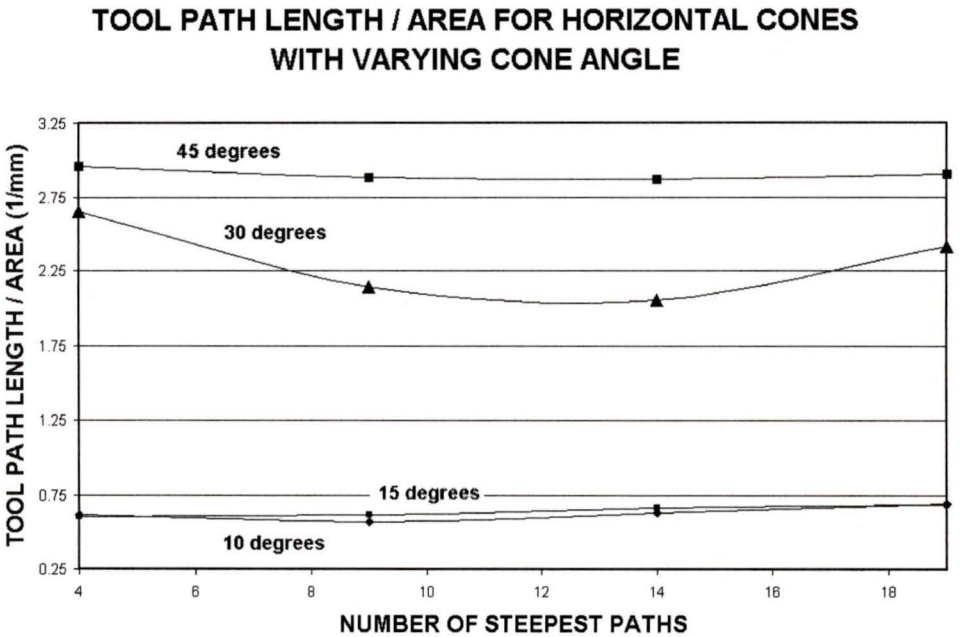

Figure 4.25 TPL/Area for Horizontal Cones with Various Cone Angles

4.7. Freeform Sculptured Surface–Convex

SDIC tool paths were generated for a convex freeform surface, with a surface tolerance of 0.1mm, as shown in Figure 4.26. This sculptured surface is chosen for machining because of its variations in surface curvature The surface was defined using the following equation

$$z = 100\left(\frac{x}{60}\right)^{e^{\left(-\left(\frac{x}{60}\right)^2-\left(\frac{y}{30}\right)^2\right)}}$$
$$0 \le x \le 150 \qquad (62)$$
$$0 \le y \le 60$$

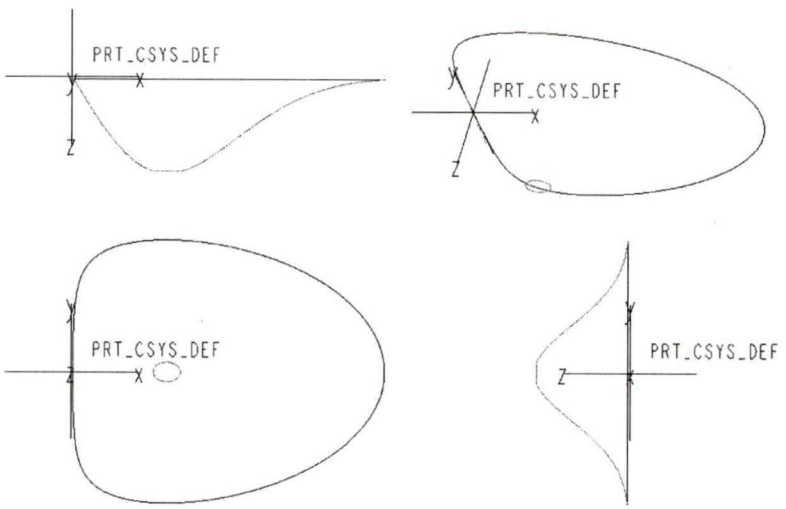

Figure 4.26 Freeform Surface

The shortest SDIC tool path was generated with five steepest directed paths, as shown in Figure 4.27.

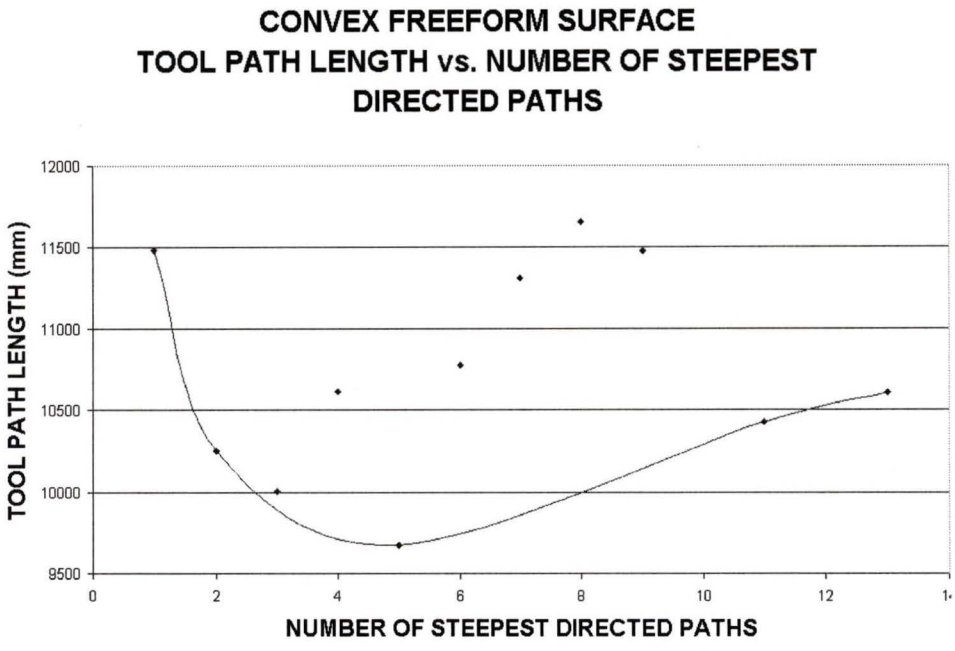

Figure 4.27 Convex Freeform Surface: SDIC Tool Path Length vs. Number of Steepest Directed Paths

Since this convex surface was defined in the form $z=f(x,y)$, isoparametric slices in terms of x or y steps are equivalent to slices created with the surface-plane intersection method, when the plane is coincident with the x and y planes. The isoparametric tool path found using x slices and y slices is equivalent to the isocusp tool path found using surface plane intersection parallel to the x and y planes. These solutions will be presented as the isocusp solutions, with cutting direction parallel to the x and y planes respectively. The SDIC and isocusp tool paths are shown in Figure 4.28. Notice how the step-over between adjacent tool paths in the isocusp solution parallel to the y plane greatly increases as the cut direction approached the steepest path direction.

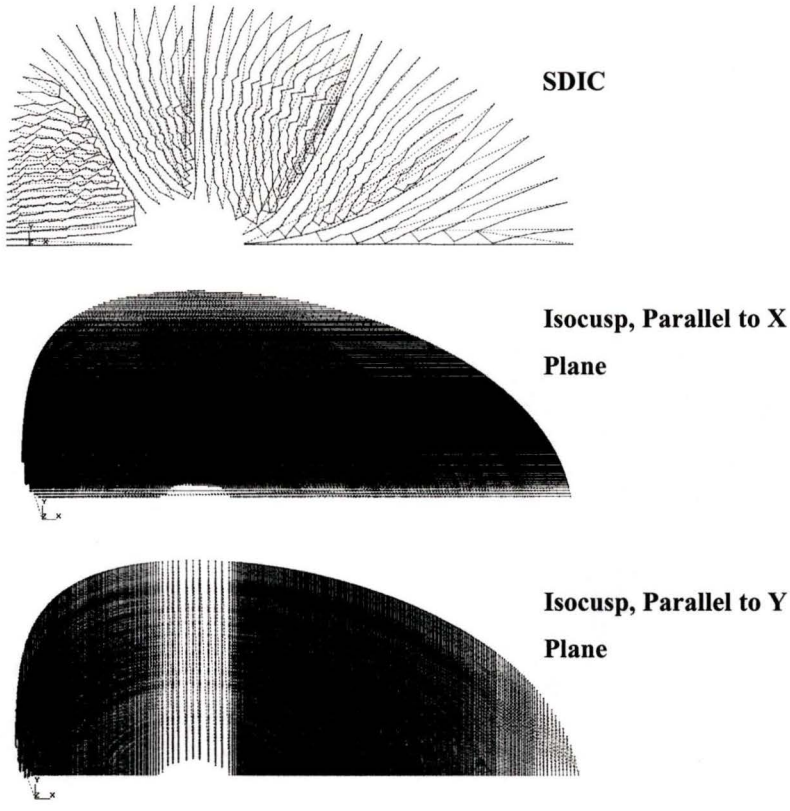

Figure 4.28 Freeform Convex Tool Paths: SDIC, Isocusp Parallel to the X Plane,, Isocusp Parallel to Y Plane

Freeform convex surfaces machined using these toolpaths are shown in Figure 4.29.

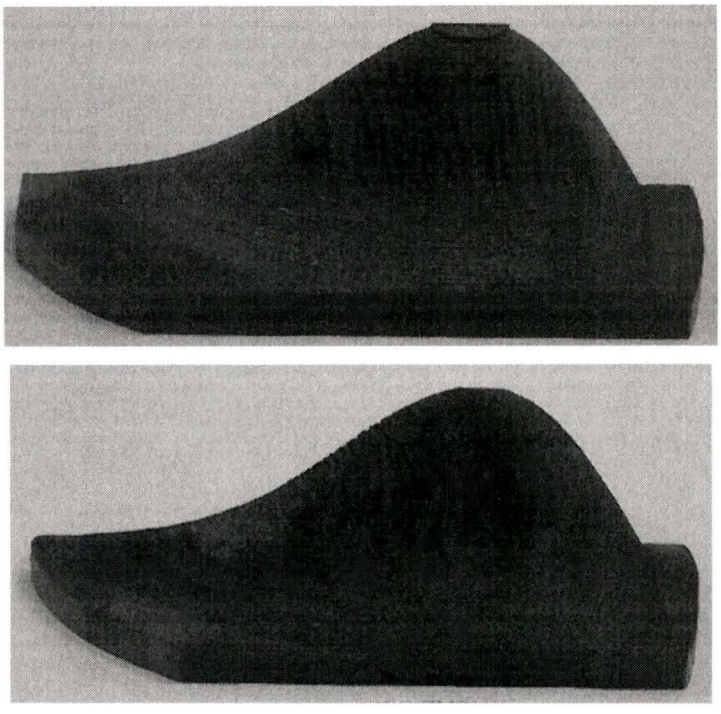

Figure 4.29 Machined Freeform Convex Surfaces (Top to Bottom): SDIC, Isocusp

The tool path lengths for SDIC and isocusp tool paths are shown in Figure 4.30. The optimum SDIC tool path is 88.0% shorter than isoparametric tool path and 91.7% shorter than the isocusp tool path parallel to the *x* axis.

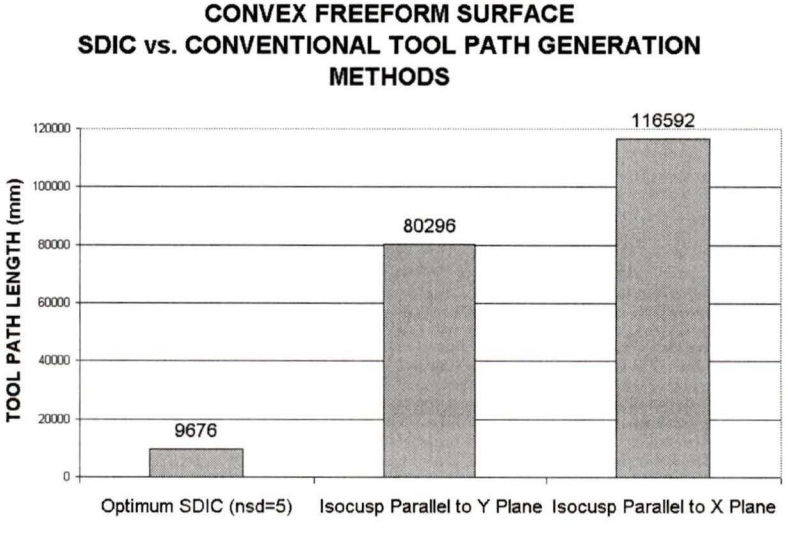

Figure 4.30 Convex Freeform Surface: Tool Path Length Comparison

4.8. Freeform Sculptured Surface–Concave

SDIC tool paths were generated for a concave freeform surface. The surface has a tolerance of 0.1mm. The surface was generated suing the following equation

$$z = 50 - 100\left(\frac{x}{60}\right)^{e^{\left(-\left(\frac{x}{60}\right)^2-\left(\frac{y}{30}\right)^2\right)}}$$
$$0 \le x \le 150 \qquad (63)$$
$$0 \le y \le 60$$

The shortest SDIC tool path was generated with three steepest directed paths, as shown in Figure 4.31.

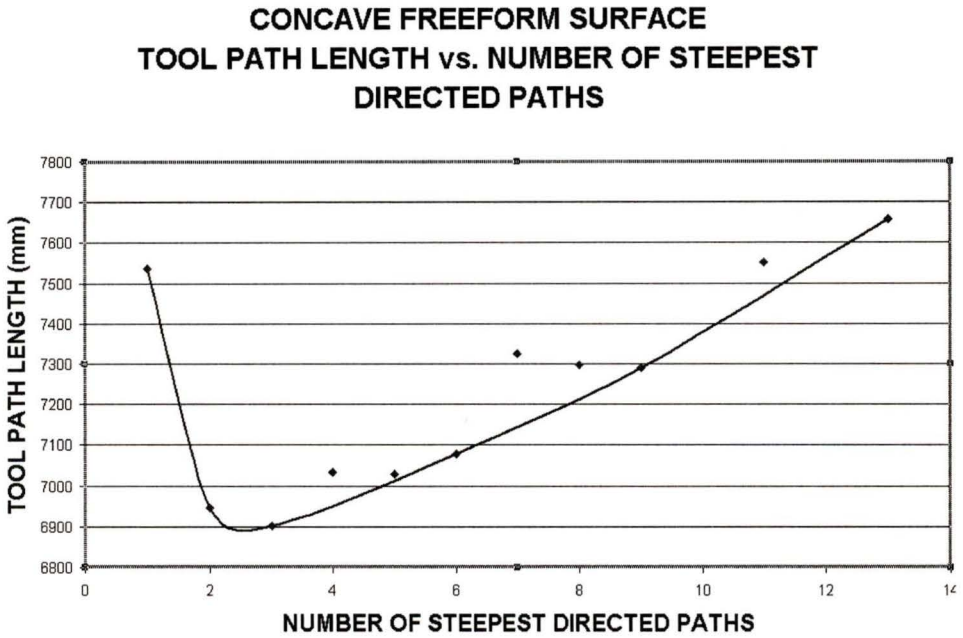

Figure 4.31 Concave Freeform Surface: SDIC Tool Path Length vs. Number of Steepest Directed Paths

As with the convex freeform surface, this concave surface was defined in the form *z=f(x,y)*. Isoparametric slices in terms of *x* or *y* steps are equivalent to slices created with the surface-plane intersection method, when the plane is coincident with the *x* and *y* planes. The isoparametric tool path found using *x* slices and *y* slices is equivalent to the isocusp tool path found using surface plane intersection parallel to the *x* and *y* planes. These solutions will be presented as the isocusp solutions, with cutting direction parallel to the *x* and *y* planes respectively. The SDIC and isocusp tool paths are shown in Figure

4.32. Notice how the step-over between adjacent tool paths in the isocusp solution parallel to the x plane greatly increases as the cut direction approached the steepest path direction.

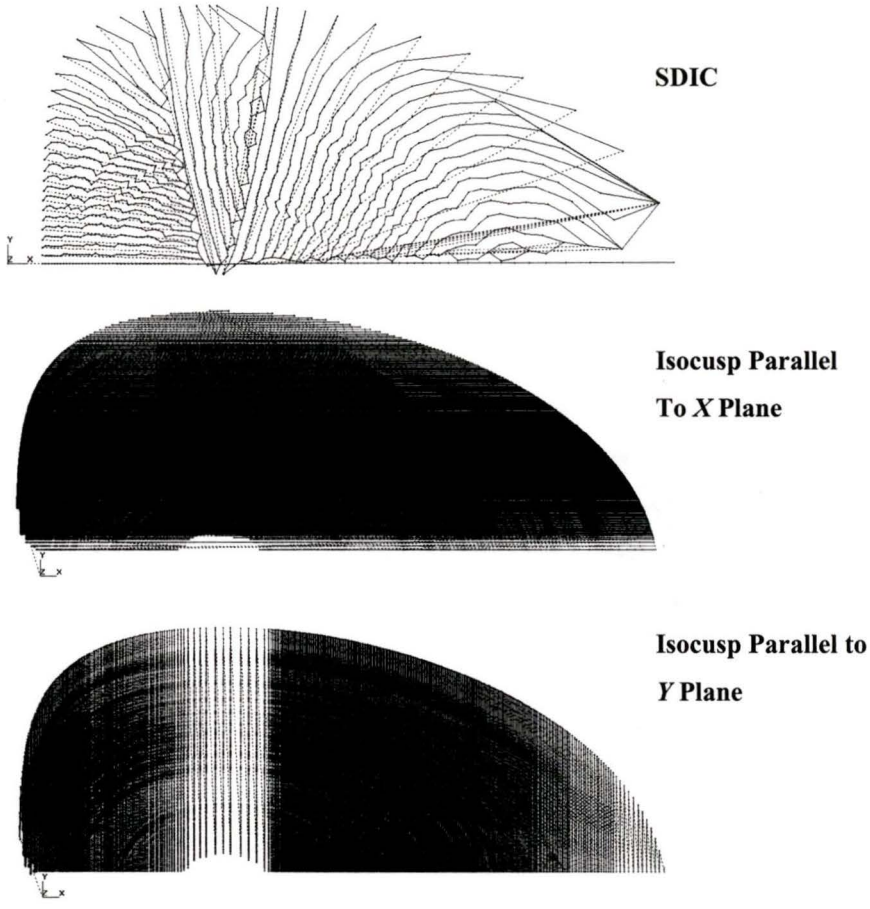

Figure 4.32 Freeform Concave Tool Paths: SDIC, Isocusp Parallel to X Plane, Isocsup Parallel to Y Plane

Freeform convex surfaces machined using these toolpaths are shown in Figure 4.29.

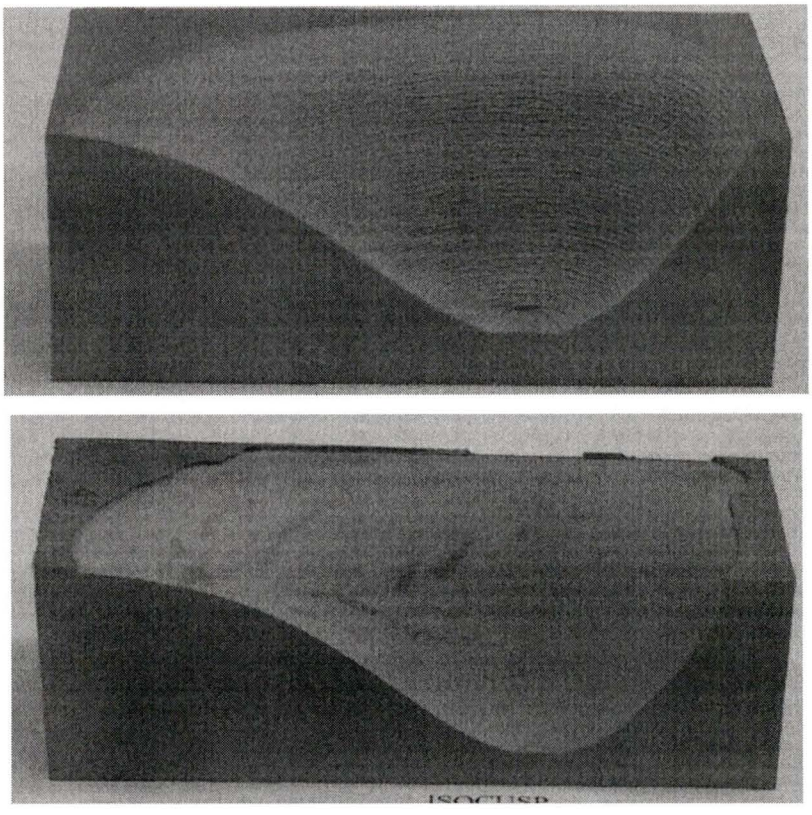

Figure 4.33 Machined Freeform Concave Surfaces (Top to Bottom): SDIC, Isocusp

The SDIC and isocusp tool path lengths are shown in Figure 4.34. The optimum SDIC tool path is 89.8% shorter than the isocusp tool path parallel to the y axis and 91.0% shorter than the isocusp tool path parallel to the x axis.

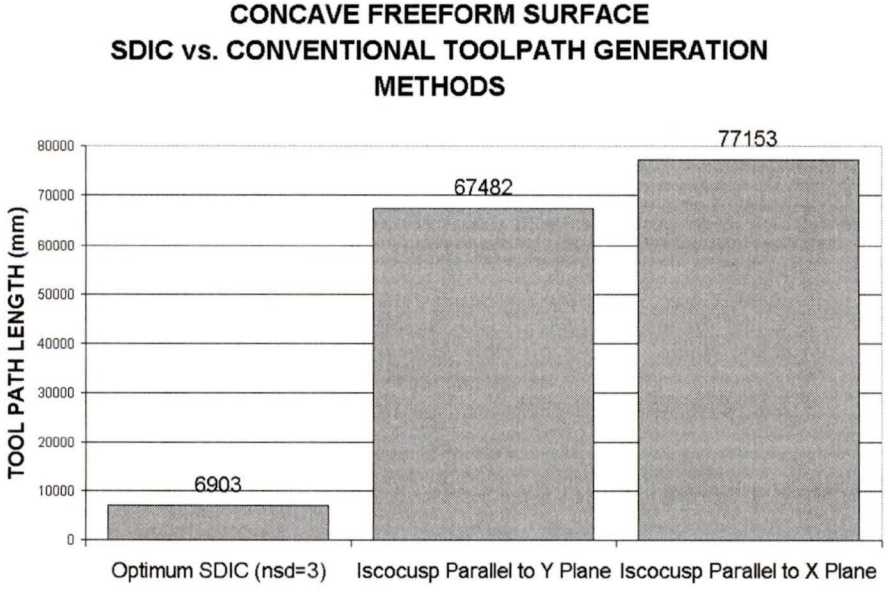

Figure 4.34 Concave Freeform Surface: Tool path Length Comparison

The large variation in tool path length between conventional tool path generation methods suggests that for a given surface, there are appropriate generation methods and cutting directions that should be used. For example, when isocusp machining a horizontal cylinder, the cutting direction should be specified parallel to the y plane, not the x plane, as shown in the tool path lengths for each direction.

4.9. Overall Tool Path Length Comparison

In order to accurately compare the SDIC tool path length to isocusp and isoparametric tool path lengths, the shortest alternative tool path is used. For example, for the horizontal cylinder the SDIC tool path length was compared to the isoparametric tool path length and not the isocusp path parallel to the x plane. The comparison of SDIC tool path lengths to the shortest alternative tool path length is shown in Figure 4.35. For all surfaces considered, the SDIC offers a reduction in tool path length over conventional tool path generation methods.

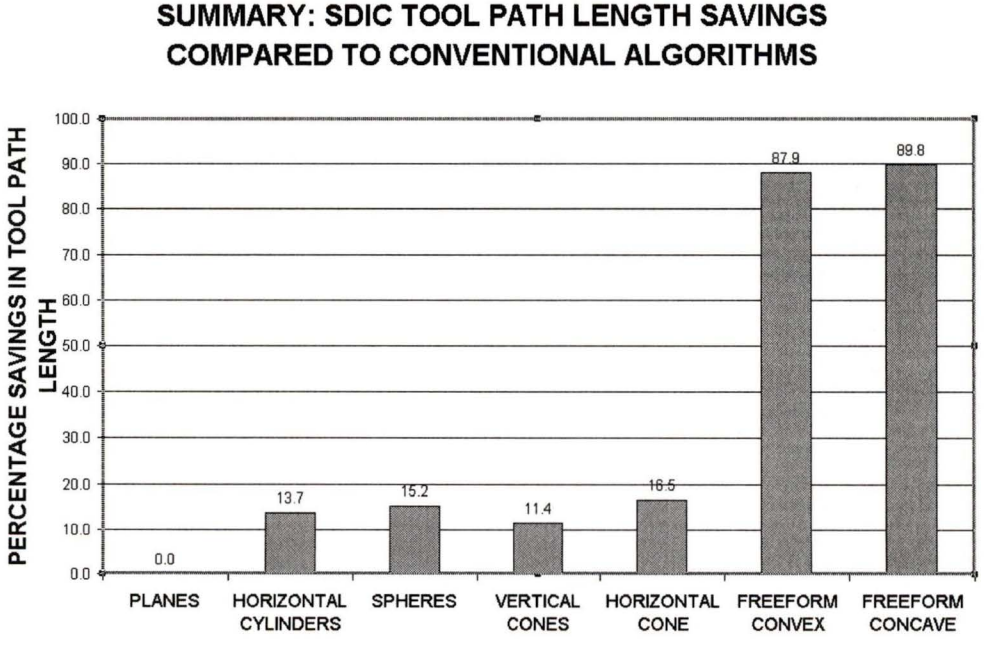

Figure 4.35 SDIC Savings

4.10. Calculation Time

For a given surface area, the time needed to calculate the SDIC tool path is directly dependent on the concentration of contour lines and the resolution of these contour lines representing the design surface. A greater concentration of nodes and contour lines improves the isocusp and steepest path approximations of the SDIC algorithm, as explained in Chapter 3.

For the surfaces machined in this section the existing SDIC algorithm is much slower than existing isocusp and isoparametric tool path generation methods. This is because of the iterative nature of the algorithm, approximating cusp heights and steepest directed paths at every node of every contour. By coding this algorithm in C rather than MATLAB the computation time needed cy of the SDIC algorithm could be greatly decreased. In specialized sculptured surface machining applications, this additional calculation time may be justified by significant reduction in tool path length.

CHAPTER 5 CONCLUSIONS

The effective cutting edge in sculptured surface machining is defined for end-mills and ball-mills. The relationship between effective cutting edge length, the angle of inclination, and the radius of curvature of the design surface is derived and presented. The effective cutting edge of ball-mills is compared to the effective cutting edge of end-mills over various angles of inclination. In general as the angle of inclination of the surface increases, the effective cutting edge length of an end-mill greatly increases, improving machining efficiency.

The effective cutting edge length is derived and displayed for planes, horizontal cylinders, spheres, vertical cones, and horizontal cones.

The principles of the SDIC algorithm and its implementation are explained in Chapter 3. Given a series of contour lines for a given sculptured surface, the algorithm generates the SDIC tool path based on the surface tolerance, end-mill dimensions, and the number of steepest directed paths. SDIC tool paths can be generated for either concave or convex surfaces.

SDIC tool paths were generated for planes, horizontal cylinders, spheres, vertical cones, horizontal cones, as well as convex and concave freeform surfaces. For every machining situation there is an optimum number of steepest directed paths which gives the shortest tool path length. By calculating the SDIC tool path for various numbers of steepest directed paths, the optimum number is found. The SDIC tool path gives substantial tool path length savings over tool paths generated using isocusp criteria or isoparametric criteria. Tool path length can be significantly reduced using the SDIC generation method. Gains using the SDIC method vary and are related to the angle of inclination of the surface being machined, as was demonstrated for horizontal cones with varying cone angles

At this stage the benefits of using the SDIC tool path generation method are in terms of reduced tool path length, which results in reduced machining time, reduced tool wear, reduced operator time, and reduced machine occupancy. Computation time associated with the existing SDIC method is greater than conventional isocusp and isoparametric methods.

These surfaces were machined from machining foam. Surfaces machined with the SDIC method were within the specified surface tolerance of 0.1mm.

5.1. Future Work

The focus of this research is to quantify the benefits of using the SDIC tool path generation method over conventional tool paths. There are many areas associated with existing SDIC tool path computation that could be improved upon.

In this research, the optimum number of steepest paths required to generate the shortest tool path length was found by trial and error. By examining the relationship between SDIC tool path length and the number of steepest directed paths over various surfaces, a better method of estimating the optimum number of steepest paths may be found.

For some sculptured surfaces, the generation of contour lines with sufficient resolution for SDIC tool path generation becomes an issue. These contour lines must contain sufficient nodes for an accurate approximation of isocusp step-over and steepest path between contours, as shown in Figure 3.5. This issue could be addressed by exploring methods of contour line generation from sculptured surfaces, and possibly introducing algorithms to generate additional nodes to increase the contour line resolution.

This SDIC algorithm can generate tool paths for either concave or convex surfaces, but not a concave/convex surface. These surfaces must be segmented into concave or convex surfaces for SDIC tool path generation. It may be possible to generate SDIC tool paths

for concave/convex surfaces by determining points of inflection between contour lines and adjusting cutter location calculations accordingly.

This SDIC algorithm is limited to concave or convex surfaces with a single summit (for convex surfaces) or pit (for concave surfaces). Multiple summit surfaces, as shown in Figure 5.1, cause a problem as contour lines diverge into multiple contour lines further along the surface. An algorithm is needed to detect multiple summits or pits, and to segment the surface into single summit surfaces by testing concavity/convexity of the surface.

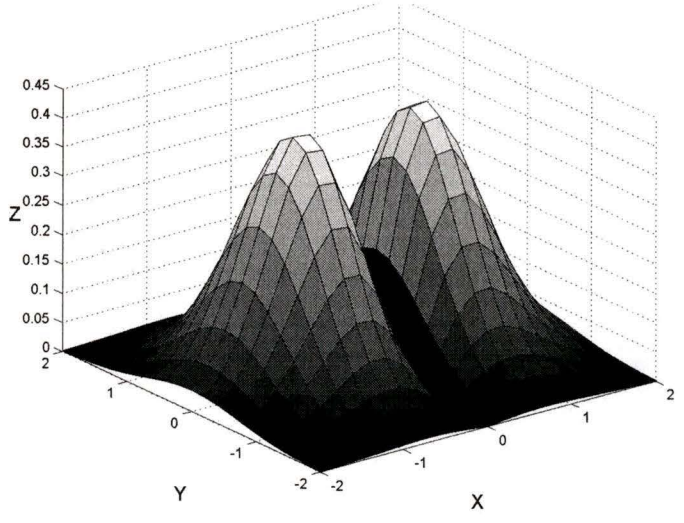

Figure 5.1 Multiple Summit Surface

REFERENCES

1. Bobrow, J.E., 1985, NC Machine Tool Path Generation from CSG Part Representations, *Computer-Aided Design*, 1985, Vol. 17, No. 2, pp. 69-76.

2. Chen, Y. D., Ni, J. and Wu, S. M., 1993, Real-time CNC Tool Path Generation of Machining IGES Surfaces, *Journal of Engineering for Industry*, Transactions. of the ASME **115**(4), pp. 480-486.

3. Chen, Zehong, 2002, *Optimal and Intelligent Multi-Axis CNC Tool Path Generation for Sculptured Part Machining*, PhD. Thesis, University of Victoria.

4. Chen, Z.C., Vickers, G.W., and Dong, Z., 2001, Integrated Steepest-Directed and Iso-Cusped Tool Path Generation for 3-Axis CNC Machining of Sculptured Parts, submitted to *Advanced Manufacturing Systems,* Transactions of ASME.

5. Chen, Z.C., Vickers, G.W., and Dong, Z., 2001, A New Principle of Tool Path Planning for Sculptured Surfaces - Steepest-Directed Tool Paths in 3-Axis CNC Machining, submitted to *Journal of Manufacturing Science and Engineering*, Transactions of ASME.

6. Chen, Z.C., Z. Dong and G.W. Vickers, 2001, Steepest-directed Tool Paths in 3-Axis CNC Machining – The Most Efficient Machining Scheme and Its Mathematical Proof, *Proceedings of ASME 2001 Design Engineering Technical Conferences and Computers and Information in Engineering Conference, DETC2001/CIE21301,* Pittsburgh, PA, September 9 –12.

7. Chen, Z.C., Dong, Z., and Vickers, G.W., 2002, A Study and Mathematical Proof on the Most Efficient Tool Feed Direction of Sculptured Surfaces in 3-Axis CNC Machining, submitted to *Journal of Integrated Manufacturing Systems.*

8. Elber, G. and Cohen, E., 1993, Tool Path Generation for Freeform Surface Models, *Second Symposium on Solid Modeling and Applications*, 419-428.

9. Finney, R.L., Thomas, G.B., 1994, *Calculus: Second Edition*, Addison Wesley Publishing Co.

10. Hahn, B.D., 1997, *Essential MATLAB for Scientists and Engineers,* John Wiley and Sons Inc.

11. Hermann, G., 1988, Algorithms for Real-Time Tool Path Generation, *Geometric Modeling for CAD Applications,* North-Holland, Amsterdam, pp. 295-305.

12. Huang, Y. and Oliver, J.H., 1994, Non-Constant parameter NC Tool Path Generation on Sculptured Surfaces, *International Journal of Advanced Manufacturing Technology*, Vol. 9, pp. 281-290.

13. Jensen, C.G. and Anderson, D.C., 1993, Accurate Tool Placement and Orientation for Finish Surface Machining, *Journal of Design and Manufacturing*, p.35.

14. Li, H., Z. Dong and G.W. Vickers, 1999, Optimal Tool Path Generation for 2 1/2 Milling of Dies and Molds, *Machining Impossible Shapes,* G.J. Olling, B.K. Choi and R.B. Jerard (Eds.), Kluwer Academic Publishers, pp. 272–278.

15. Maeng, H.Y., M. Ly and G.W. Vickers, 1996, Feature Based Machining of Curved Surfaces Using the Steepest Directed Tree Approach, *Journal of Manufacturing Systems*, Society of Manufacturing Engineers, Vol. 15, No. 6, pp. 379-389.

16. Suresh, K., Yang, D.C. H, 1994, Constant Scallop-Height Machining of Free Form Surfaces, *Trans. ASME Journal of Engineering for Industry*, Vol. 116, No. 5, pp. 253-259.

17. Vickers, G.W., Ly, M.H., Oetter, R.G., 1990, *Numerically Controlled Machine Tools*, Ellis Horwood Publishing Co.

VITA

Surname: Wenger Given Names: Paul Ashley

Place of Birth: Calgary, Alberta, Canada

Educational Institutions Attended:

University of Calgary, 1994 to 1999

University of Victoria, 2000 to 2002

Degrees Awarded:

BASc. Mechanical Engineering (with Internship Status), University of Calgary, 1999

Honours and Awards:

University of Victoria Fellowship Award, 2000 to 2001

BC Advanced Systems Institute Award, 2000

UNIVERSITY OF VICTORIA PARTIAL COPYRIGHT LICENSE

I hereby grant the right to lend my thesis to users of the University of Victoria Library, and to make single copies only for such users or in response to a request from the Library of any other university, or similar institution, on its behalf or for one of its users. I further agree that permission for extensive copying of this thesis for scholarly purposes may be granted by me or a member of the University designated by me. It is understood that copying or publication of this thesis for financial gain by the University of Victoria shall not be allowed without my written permission.

Title of Thesis:

Toolpath Planning Using the SDIC Method for Sculptured Surface Machining

Author [redacted]

Paul Ashley Wenger

December 20, 2002

[redacted]